

Energy system design under uncertainty

THÈSE N° 5559 (2012)

PRÉSENTÉE LE 30 NOVEMBRE 2012

À LA FACULTÉ DES SCIENCES ET TECHNIQUES DE L'INGÉNIEUR
LABORATOIRE D'ÉNERGÉTIQUE INDUSTRIELLE
PROGRAMME DOCTORAL EN ENERGIE

ÉCOLE POLYTECHNIQUE FÉDÉRALE DE LAUSANNE

POUR L'OBTENTION DU GRADE DE DOCTEUR ÈS SCIENCES

PAR

Matthias DUBUIS

acceptée sur proposition du jury:

Prof. F. Gallaire, président du jury
Dr F. Maréchal, directeur de thèse
Prof. A. Espuña, rapporteur
Dr A. A. Linninger, rapporteur
Prof. P. Xirouchakis, rapporteur



ÉCOLE POLYTECHNIQUE
FÉDÉRALE DE LAUSANNE

Suisse
2012

*Statistics are like bikinis.
What they reveal is suggestive, but what they conceal is vital.*
Aaron Levenstein

Remerciements

Je tiens à remercier François Maréchal pour son aide et son expérience en optimisation de procédés industriels, ainsi que pour la confiance qu'il m'a accordée dans la rédaction de ce document.

Je remercie également le Professeur Daniel Favrat pour avoir partagé une atmosphère autant conviviale que professionnelle au LENI.

Un grand merci au président du jury François Gallaire ainsi qu'aux membres du jury Antonio Espuña, Andreas Linninger et Paul Xirouchakis pour leur aide quant à l'amélioration et la finalisation de ce document.

Un doctorant ne serait rien sans financement, c'est pourquoi je remercie swisselectric et Alstom pour avoir rendu ces recherches possibles.

Je tiens à remercier l'ERCOFTAC pour le cours sur la propagation d'incertitudes donné à Munich en 2011. De telles passerelles entre domaines sont trop rares malgré tout ce qu'elles peuvent apporter.

Toute ma gratitude à Laurence Tock, qui m'a épaulé sur nos projets communs. Je te présente mes excuses les plus sincères pour toutes les fois où j'ai été trop absorbé par mes équations et pas assez par nos modèles.

Ma reconnaissance va également à Jonathan Demierre pour la relecture d'un chapitre aussi facile à lire qu'un manuel de montage d'armoire en suédois.

J'ai eu la chance de faire partie d'un laboratoire où la cohésion entre les doctorants compense largement les coups durs. Je tiens à remercier tous ceux que j'y ai croisés. Je n'en ferai pas la liste complète, mais je me permets de citer:

- Mes colocataires de bureau qui ont dû supporter mon système de rangement très... personnel: Zoé, Nicole, Helen-Büebeli, Nasibeh-Junior et Adriano.
- Le secrétariat: Brigitte, Suzanne, Faye, Irène et Sarah-Josette (désolé, j'ai pas pu m'en empêcher). Merci de votre patience, de vos efforts et pardon pour les heures remplies en retard. D'ailleurs... puisqu'on en parle, faut que j'aille vérifier...
- Samuel Henchoz par pure chauvinerie envers ses origines.
- Nicolas B., Nicolas D., Jonathan et Léda: Il y a des rencontres qui marquent.

Vous en faites partie. Merci pour votre amitié. Cette thèse n'aurait pas été possible sans vous.

- Un mot tout particulier pour Raffaele et Francesca: vous avez fait un immense travail en programmant un outil qui nous sert à tous encore aujourd'hui. Merci.
- Ainsi que tous les vieux: Antonin, Arata, Céline, Emanuele, Leonidas, Luc, Martin, Zach. Je me souviens encore de vos rires quand, alors que j'étais assistant, je jurais que jamais je ne ferai de thèse.
- J'ajouterais finalement les mécaniciens qui, malgré que je n'aie pas vraiment travaillé avec eux, m'ont beaucoup appris sur la soudure. Merci à Christophe, Jean-Pierre, Laurent, Martin, Nicolas et Romain.

Enfin, merci à tous ceux qui m'ont soutenu durant ces années. L'équipe de la Riviera, des Grisons, ma famille et Joelle qui m'a accompagné pendant tout ce temps.

Abstract

The current context leads energy system design to very demanding objectives, due to their variety. Indeed, despite an increasing energy demand, environment indicators are becoming always more important. So that for a given service, emission (and then associated consumption as well) is desired to decrease. Improving systems efficiencies is then a important step.

Such a problem is formulated as an optimization. It is based on numerical models. Every models differs by definition from reality. This difference can be translated into uncertainties. Usually, they are considered at their most probable value. However, their variation can lead to consequences between a performance decrease and plant inoperability. It is then critical to take into account the deviation due to uncertainties when optimizing an energy system.

The optimization problem will be described. It will introduce the description of functions and variables involved in energy system design. The formulation of the optimization under uncertainty will be developed, as well as mathematical methods for uncertainty propagation. Finally, an innovative method taking advantage of the high number of iterations due to the chosen solver will be described.

In this study, pinch analysis has been applied. Its limits related to uncertainties treatment will be presented.

Methods described here will be applied to an hybrid system of a fuel cell coupled with gas turbines. Results will be compared to a conventional optimization solutions. It will demonstrate that, despite sub-optimal objectives, the sensitivity of the system to uncertainties has been improved

Keywords: Optimization, stochastic, uncertainty, propagation, moments method, orthogonal polynomials, pinch analysis, energy system

Résumé

Le contexte actuel pousse la conception de systèmes énergétiques vers des objectifs exigeant par leur diversité. En effet, malgré une demande d'énergie grandissante, les critères environnementaux revêtent une importance croissante. Ainsi, pour un même service, la diminution des émissions, et donc de la consommation et recherche. L'amélioration des rendements de tout systèmes ayant trait à l'énergie est donc une étape essentielle.

Ce type de problème se présente sous la forme d'une optimisation. Ils reposent sur des modèles numériques. Hors, tout modèle comporte par définition un décalage avec la réalité. Ce décalage se traduit sous forme d'incertitudes. Dans bon nombre d'approches, elles sont considérées à leur valeur la plus probable. Cependant la variation de tels paramètres peut conduire à des conséquences allant d'une simple baisse de performance jusqu'à l'arrêt d'une installation. Il apparaît donc crucial de prendre en compte la variation due aux incertitudes lors de l'optimisation d'un système.

Une présentation du problème d'optimisation au sens mathématique sera faite. Elle permettra de décrire les fonctions et variables impliquées dans la conception de systèmes énergétiques. Puis la formulation du problème d'optimisation sous incertitudes sera exposées, ainsi que les différentes méthodes mathématiques permettant de les propager au travers du modèle. Finalement, une nouvelle méthode bénéficiant du nombres élevé d'itérations liés au solver choisi sera décrite.

Dans cette étude, l'analyse de pincement a été appliquée. Ses limites concernant le traitement des incertitudes seront détaillées.

Les méthodes présentées seront appliquées à un système de pile à combustible coupée à des turbine à gaz. Les résultats seront comparés à ceux d'une optimisation conventionnelle. Ils démontreront que malgré des objectifs optimaux à priori moins performant, la sensibilité du système aux incertitudes en a été améliorée.

Mots-clés: Optimisation, stochastique, incertitude, propagation, méthode des moments, polynômes orthogonaux, méthode du pincement, système énergétique

Contents

Abstract	iii
Résumé	v
Nomenclature	xi
1 Introduction	1
1.1 Motivation	1
1.2 Issues and objectives	6
1.3 Outline of the report	8
2 State of the Art and Innovation	11
2.1 Optimization Problem Formulation	11
2.1.1 Optimization problem	11
2.1.2 Typical Function in Energy System Design	15
2.1.3 Variables Classification	17
2.2 Optimization problem resolution	24
2.2.1 Chosen solver	24
2.2.2 Evolutionary algorithm	25
2.3 Optimization under Uncertainty	25
2.3.1 Uncertainty problem formulation	25
2.3.2 Uncertainty propagation	28
2.3.3 Proposition for second stage resolution	38
2.3.4 Stochastic programming	41
2.4 Other approaches	43
2.5 Conclusion	45
2.5.1 Methods comparison	45
2.5.2 Case studied	48
3 Model	49
3.1 Energy integration	49

3.1.1	Advantages and drawbacks	49
3.1.2	Composite curves	51
3.1.3	Uncertainties on heat streams	53
3.2	Fuel cell - gas turbine model	55
3.2.1	Fuel cell	57
3.2.2	Gas turbine	63
3.3	Conclusion	65
4	Optimization results	67
4.1	Hybrid fuel cell optimization	67
4.1.1	Fuel cell decision variables for standard optimization	68
4.1.2	Gas turbine decision variables for standard optimization	69
4.2	Pinch analysis	72
4.3	Conclusion	74
5	Stochastic programming results	77
5.1	Standard and stochastic optimization	77
5.2	Uncertainty representativity	78
5.3	Decision under uncertainty	85
5.4	Conclusion	97
6	Moments method results	99
6.1	Optimization convergence and number of iterations	99
6.2	Decision variables analysis	102
6.3	Variance analysis	106
6.4	Conclusion	111
7	Conclusion and future work	113
	Bibliography	117
A	Probability distribution function	125
A.1	Pearson IV	125
A.2	Beta distribution	126
A.3	Normal distribution	128
A.4	Uniform distribution	128
B	Stochastic programming: complementary results	131
C	Moments method: complementary results	135
	List of Tables	139

CONTENTS

ix

List of Figures

141

Curriculum Vitae

145

Nomenclature

Latin symbols

A	Cell area
D	Dependent variables space
d	Dependent variables
E_A	Activation energy
\dot{E}	Mechanical power
f_{CC}	Adjustment factor
F	Faraday constant
f	Objective function
fu	fuel utilisation
\dot{G}	Gibbs free energy
g	Inequality constraints
h	Equality constraints
I	Total current
i	Current density
\mathbb{L}_2	Set of square integrable functions
LHV	Lower heating value
L	Lagrangian
\dot{m}	Mass flow rate

n_{cells}	Total number of cells in the stack
n_{eval}	Number of function Evaluation
n_f	Number of objective function
\dot{n}	Molar flow rate
n_o	Number of operating variables
n_u	Number of uncertain variables
P	Pressure
\dot{Q}	Heat stream
R_e	Electrolyte ohmic resistance
R_i	Interconnect ohmic resistance
R	Ideal gas constant
R_{tot}	Total cell ohmic resistance
T	Temperature
U	Uncertain variables space
u	Vector of uncertain variables $u \in U$
x	All variables
x^*	Local optimum
x_s	State variables
y	Performances
z_d	Design decisions
Z	Decision variables space
z	Decision variables
z_o	Operating variables
z_v	Design variables

Greek symbols

δ	Dirac delta function
η	Butler Volmer overpotential
η_{diff}	Polarization losses
γ_1	Skewness
γ_2	Kurtosis
μ	Mean
σ	Standard deviation
σ_0	Conductance pre-exponential factor
σ_x	Conductance (x being a , c or e)
Θ	Parameters space
θ	Parameters
θ_c	Certain parameters
θ_u	Uncertain parameters
θ_{ulnp}	Long term non-periodic uncertain parameters
θ_{ulp}	Long term periodic uncertain parameters
θ_{ul}	Long term uncertain parameters
θ_{us}	Short term uncertain parameters
φ	Vapour fraction

Indices

a	Relative to anode
c	Relative to cathode
e	Relative to electrolyte

Acronyms

<i>cdf</i>	Cumulative Density Function
<i>DM</i>	Decision Maker
<i>EI</i>	Energy Integration
<i>FORM</i>	First order reliability method
<i>HEN</i>	Heat exchanger network
<i>HENS</i>	Heat Exchanger Network Synthesis
<i>HEX</i>	Heat Exchanger
<i>HLD</i>	Heat Load Distribution
<i>HRSG</i>	Heat recovery steam generator
<i>KKT</i>	Karush-Kuhn-Tucker
<i>LHS</i>	Latin Hypercube Sampling
<i>LP</i>	Linear programming
<i>MEA</i>	Monoethanolamine
<i>MER</i>	Minimum Energy Requirement
<i>MILP</i>	Mixed integer linear programming
<i>MINLP</i>	Mixed integer linear programming
<i>MOO</i>	Multi-Objective Optimization
<i>OCV</i>	Open current voltage
<i>pdf</i>	Probability Density Function
<i>PUO</i>	Physical Unit Operation
<i>SOFC</i>	Solid oxyde fuel cell
<i>SORM</i>	Second order reliability method
<i>STN</i>	Steam Network

Chapter 1

Introduction

Importance and influence of uncertainty in engineering will be outlined in the context of global warming perspective and focused on CO₂ emissions. Predictive aspect and uncertainties on present data leads to important variability of predictions. This underline the necessity of developing tools allowing engineers to take decisions considering uncertainties influence. Specifications and challenges for such methods will be described. Finally, the structure of this report will be summarized in the end of this chapter.

1.1 Motivation

In energy system design domain the main engineers' task is to design technologies providing several services or products based on given resources and subject to a number of constraints (equipment availability, cost of resources,...). This means to take decision based on results of models simulation and optimization. The consequence of taken decisions may have a great influence on economy, politics, environment, comfort of living. However, uncertainties may affect such procedures leading to wrong estimations and suboptimal decisions.

By example, figure 1.1 represents the different scenarios for the future global CO₂ emissions related to energy and industry [60]. They take several of factors into account such as global population, economic growth, technologies development and social tendency to global or local interaction. There is 4 families of scenarios:

family	economic growth	global population	technologies evolution	global/local
A1	rapid	peak at mid century	rapid	global
A2	slow	increasing	slow	local
B1	rapid	peak at mid century	rapid, clean and efficient	global
B2	intermediate	increase smaller than A2	less rapid than B1 and A1	local

Table 1.1: IPCC scenarios classification in 4 families

These families correspond to 6 groups, one group per family for *A2*, *B1* and *B2*, and 3 groups in *A1* which are:

- *A1FI* which is highly dependent to fossil fuels (comprising the high-coal and high-oil-and-gas scenarios).
- *A1T* which is predominantly non-fossil.
- *A1B* which is balanced between fossil and non-fossil.

The amount of CO_2 emissions at a given time varies depending on the assumptions and the uncertain parameters of the models. It appears clearly in figure 1.1 that, even if an average value can be found, it is hard for policymakers to evaluate the final emissions rates, due to predictive nature of the problem and to the number of factors. The two extreme cases being on one hand an optimistic interpretation, assuming a strong decrease of emissions, and on the other hand a pessimistic one, with an emissions rate ten times higher in 2100 than in 1990. Hence, interpretation of data by the decision maker (*DM*) becomes crucial and may influence a lot of decisions, like research funding, choice of energy conversion system at state level, support of private initiative for more efficient energy system, public transport development.

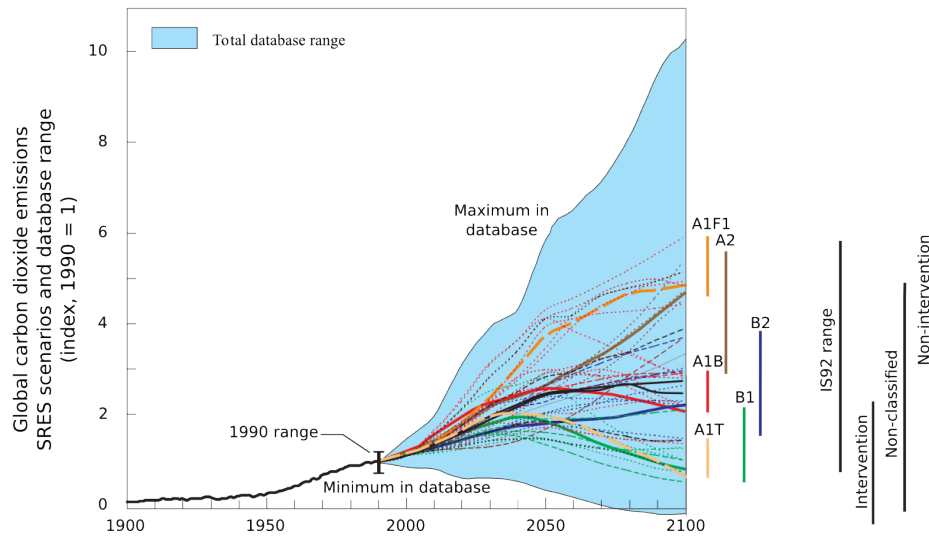


Figure 1.1: IPCC scenarios for CO_2 emissions from energy and industry area [60]

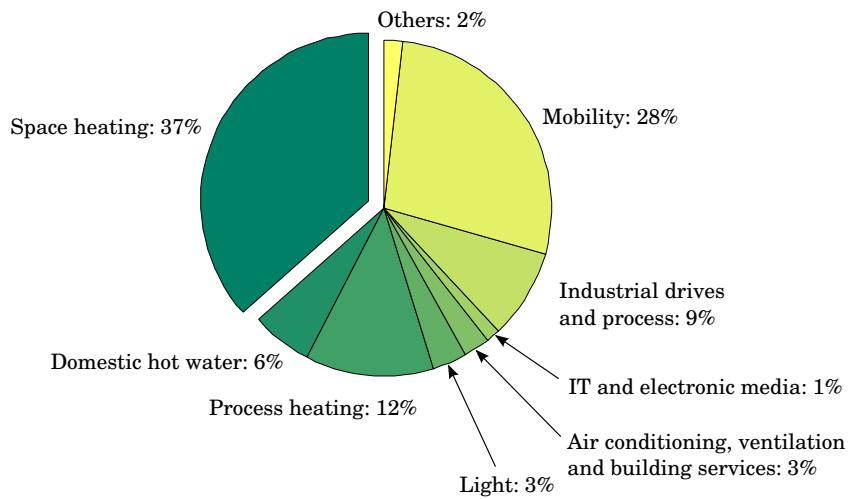


Figure 1.2: End-use energy consumption statistics for Switzerland (2010) [51]

One of the factors in table 1.1 in which engineers may play an important role is the technologies evolution. The following example shows the link between

uncertainty on CO_2 emissions and energy system design. As it can be seen in figure 1.2, 37 % of the consumed energy is used for space heating, this means 300.3 $PJ/year$ for Switzerland.

This shows the great need for efficient and well integrated heating system.

The second point of table 1.1 for which engineering can help decision-making is the trade off between global and local interactions, at least at energy system level. It has been demonstrated that replacing local boilers in buildings by a district heating may reduce CO_2 emissions [31]. This is due to the fact that on one hand space heating is mainly based on fossil fuels combustion (more than 75 %, see figure 1.3), and on the other hand Swiss electric mix is poor in carbon dioxide emission. Taking into account the presence of lakes in cities area that can be used as cold sources for heat pumps, all conditions are satisfied to build heating networks.

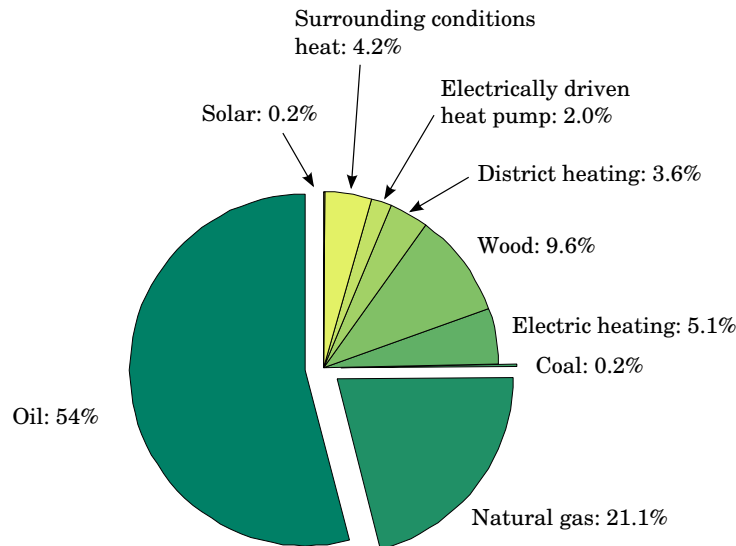


Figure 1.3: Energy sources for space heating of private households (2010) [51]

Despite obvious reason for considering a district heating, its installation is highly dependent on the building owner to accept being linked to the network. Refusal may be due to several reasons like the loss of autonomy, the fear of new technologies or simply a lack of trust in industrial services. Fortunately, most of them accept generally. This behaviour may be modeled as a binomial distribution. The one shown in figure 1.4 is based on 100 owners with a probability of 85 % for each of them to accept. If, for example, the DM accepts to build the energy system if at least 85 % of the buildings may be connected to the network, it means that there is in fact 50 % of chance to be achieved.

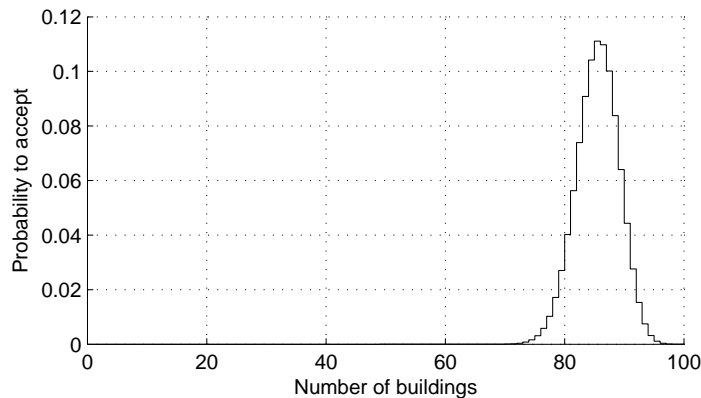


Figure 1.4: Binomial distribution for the district heating example

Adding to this, other uncertainties increase the problem complexity. They may be, non-exhaustively:

- The fuel and electricity cost
- The equipment constraints and performances
- The operating conditions (outdoor temperature, building needs varying with renovation,...)
- The eventual future building linking or renovation (implying changes in heating temperature)
- The uncertainties of the decision-making tool parameters

EPFL is based on a centralized heating system. It is a good example of well predicted context. Campus growth has been taking into account. Moreover, it is operating at low temperature allowing good exergetic efficiency. This is done by two networks: a medium temperature one design at 28 °C and low one at 26 °C. Finally higher temperature needs are fulfilled locally to ensure flexibility of the system.

In the same area, Lausanne district heating has been designed for 160 °C way out and 120 °C way in. Such high temperatures come from a bad estimation of future needs. Moreover, inability to adapt installation to actual requirement makes it inefficient during its whole lifetime.

Through such examples, it can be seen that uncertainties may lead to wrong decisions at any steps from the designer to the policymakers. It demonstrate the need for a systematic approach to design energy system under uncertainty in order to minimize CO_2 emissions as well as operating cost.

1.2 Issues and objectives

Through the example of section 1.1, Designing an energy system consists in making a decision based on a context by using numerical models. However, context as well as model may be subject to uncertainties.

- Energy systems are often strongly related to time dependent parameters. However, in a design procedure, dynamic simulation is often too computationally consuming and a static or quasi-static approach is considered. Variation in time are then used to build a probability distribution around a nominal value. This concerns for example some operating conditions like outdoor ambient temperature or energy prices.
- On another time scale, a lot of energy system imply predictive aspect, like technologies in development or used in a non-usual range. In such cases, an additional difficulty is to define a distribution since no information is available.
- Modeling is by definition an approximation of real phenomenon, what imply necessarily differences between model and reality which are translated in uncertainties on model parameters. Most of approaches constitute a trade off between accuracy and necessary computational means. By example, heat exchanger network area estimation through energy integration technique will not provide a result as detailed as a flowsheet simulation. However, its ability to be included into a great superstructure optimization and its computational efficiency make it very useful in complex systems design.
- Hardware is subject to uncertainty too. This includes energy technologies, measurement tools as well as regulation.
- At least but not last, human factor is a highly unpredictable element, as it has been shown in district heating example. A major difficulty is to model it, since it is difficult to measure (and statistics are subject to interpretation) and could be very complex in case of multi-agent system.

Usually, models are adapted to avoid managing uncertain variables in the design. For example heating system are treated as multi-period problem with a average outdoor temperature for each period. In some other cases, uncertainties are considered as not significant and the most probable value of uncertain parameters is used. An exception in determining the mean value concerns the case when state variables (i.e. the variable describing the thermodynamic state of the system) may be measured directly on site. Here, the uncertain parameters mean value shall be computed by data reconciliation technique [66]. To express the advantage of such

approach, let's define a set of measurement m_i , $i = 1; \dots; N_m$ of a variable x_j ; the mean is given by the average:

$$\tilde{m} = \frac{\sum_{i=1}^{N_m} m_i}{N_m} \quad (1.1)$$

However, this value may be biased. As an example, a badly calibrated instrument may lead to a wrong mean despite a small standard deviation. Such principles are illustrated by the scheme of figure 1.5. The assumption is that the perfect measurement is situated at the origin.

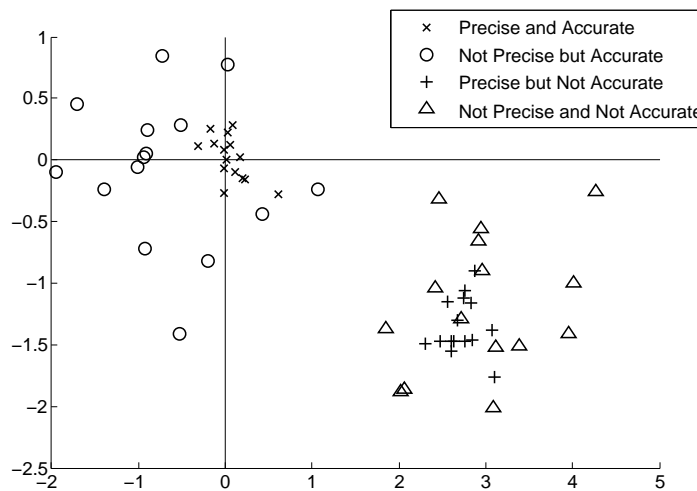


Figure 1.5: Scheme of the notion of precise/accurate measurement [44]

The final goal of data reconciliation is to evaluate accuracy (i.e. determining if measurements systematically biased) and spread (given by great variation in case of constant operation condition) and take measure to improve them.

Several methods ([2, 52]) may be used to detect errors taking into account related parameters. In this study, it will be assumed that such analysis has already been carried out and that the distribution of uncertain variables is known.

Hence, based on a set of uncertain variables and their related distributions, several questions related to their influence on energy system design raise:

- What is the standard deviation of system performances due to uncertain variables? Are the uncertain variables more influent than the decision variables, i.e. can the studied system be optimized or is it not enough well defined?

- What is the influence of uncertain variables on decision variables? Do they lead to similar decisions? Do all the decision variables have the same importance when taking into account uncertainties?
- What is the influence of uncertain variables on objectives? Shall uncertainties indicators be taken into account?
- How to express the notion of risk, reliability, flexibility, feasibility in the context of energy system design?
- How to propagate uncertainty through the model in an effective manner?

The purpose of this thesis is to answer these questions as far as computational means allow it, and provide methodology to the *DM*. Moreover, the techniques that will be used must have the following specifications [29]:

- It shall be exhaustive, covering the whole variables space.
- Accuracy is an important factor, since uncertainties related to numerical evaluations shall be decreased as much as possible
- Computational efficiency is crucial. Indeed, standard optimization consumes a lot of computational resources, so that uncertainties processing shall not imply too much more resources.
- By implementing it in a generic manner, proposed method may be used to any other problems or solver.

Finally the goal is to develop the methods that will be implemented in *OSMOSE* [13], a platform developed in LENI.

1.3 Outline of the report

The chapter 2 will compare the mathematical formulation of the problem, with the practice in energy system design. The conventional optimization problem will be presented, with an exhaustive description of its functions and variables. This will lead to a short description of different types of solver. Optimization under uncertainty problem will be defined, and different methods for uncertainty propagation will be detailed.

In the chapter 3 the system used as example in this study will be described. It consist in an innovative hybrid system composed by a fuel cell and two gas turbines. Moreover, the approach to solve this problem by energy integration will be commented as well as its consequence on uncertainty propagation.

The chapter 4 will show conventional optimization results. They will not be detailed since they can be found in literature. They will be compared with optimization under uncertainty results.

In the chapter 5, a new method for optimization of energy systems under uncertainty will be described. Its ability to explore the uncertain space will be demonstrated. Its results will be compared with standard optimization ones.

Finally, the chapter 6 will apply a method of uncertainty propagation on optimization. This method is valid as well for solver demanding not much iterations. Results will be compared to stochastic and standard optimization, and a detailed analysis of performance variance will be presented.

Chapter 2

State of the Art and Innovation

The aim of this chapter is to establish the theoretical concept of this thesis. The first section defines the energy system design mathematical formulation. The second section describes different optimization approaches and the one chosen. In the third section, optimization under uncertainty will be exposed from an analytical point of view on one hand and by comparing energy systems resolution methods on the other hand [18]. It has already been studied in several domains, like finance or continuum mechanics. Specificities of systems design problems will be described, leading to the choice of appropriate methods. Finally, they will be extended with innovative concepts. Other methods in use will be exposed and discussed. The review of the methods describe here is one of the main contributions of this work, since designing energy systems under uncertainty remains a mathematical challenge. Indeed, there is no established method up to now.

In this section, the state of the art will be jointly exposed with the problem formulation in order to simplify lecture.

2.1 Optimization Problem Formulation

2.1.1 Optimization problem

Energy system design is defined as an optimization problem. Usually, *DM* considers objectives as investment or operating cost, efficiency, environmental impact (through life cycle assessment methods) or simply the maximization of desired service or product.

A formalism has been developed [10, 12, 11] to translate system design into a mathematical formulation. Such generic approach offers the advantage that it may be applied to any system [86, 35, 37, 5] and with any solver.

Moreover, looking back at theoretical form of the problem remains important since it allows to study limits of numerical model as it will be described in this section. The most global formulation for an optimization problem is:

$$\min_z y = f(z) \quad (2.1)$$

With $f : \mathbb{R}^n \rightarrow \mathbb{R}$ called the objective function and $z \in \mathbb{R}^n$ the decision variables. The definition of optima for problem 2.1 are given by the optimality conditions. For z^* , a local minimum of f , the necessary optimality conditions is given by: The first order condition, for f differentiable in an open neighborhood of z^* ,

$$\nabla f(x^*) = \begin{pmatrix} \frac{\partial f(z)}{\partial z_1} \\ \vdots \\ \frac{\partial f(z)}{\partial z_n} \end{pmatrix} = 0 \quad (2.2)$$

And the second order condition, for f twice differentiable in an open neighborhood of z^* , $\nabla^2 f(x^*)$ is positive semidefinite, meaning:

$$\nabla^2 f(z^*) = \begin{pmatrix} \frac{\partial f(z)}{\partial z_1^2} & \cdots & \frac{\partial f(z)}{\partial z_1 \partial z_n} \\ \vdots & \ddots & \vdots \\ \frac{\partial f(z)}{\partial z_n \partial z_1} & \cdots & \frac{\partial f(z)}{\partial z_n^2} \end{pmatrix} \geq 0 \quad (2.3)$$

The sufficient optimality conditions is the same as equation 2.2 for the first order. For the second order, it stipulates that $\nabla^2 f(z^*)$ is positive definite:

$$\nabla^2 f(z^*) > 0 \quad (2.4)$$

So, the main difference between necessary and sufficient conditions is the case $\nabla^2 f(z^*) = 0$.

In energy system design, most of the problem are constrained so that they are formulated as:

$$\begin{aligned} \min_z y &= f(z) \\ \text{s.t. } h(z) &= 0 \\ g(z) &\leq 0 \end{aligned} \quad (2.5)$$

The function f is the objective function of the model. In others, it represents the performance indicator allowing to compare an energy system with another. A

multi-objective optimization may be used, especially to point up trade off between objectives. So, y may be a vector with $y \in \mathbb{R}^m$. In this study, $m \leq 4$, since greater number of objectives may be induces too much computing facility needs.

Together with the constraints h and g , they constitute the model, i.e. they are the set of mathematical equations representing the physical and economic behaviour of the model (thermo-chemical property of each streams, mechanical and thermal units specification, price of resources,...). Most of these problems are mixed integer. In case of a linear problem (LP), the equation 2.5 can be formulated as:

$$\begin{aligned} \min_t \quad & c^T z \\ \text{s.t.} \quad & h(z) = Az - b = 0 \\ & z \geq 0 \end{aligned} \tag{2.6}$$

In that case, there are three types of solutions:

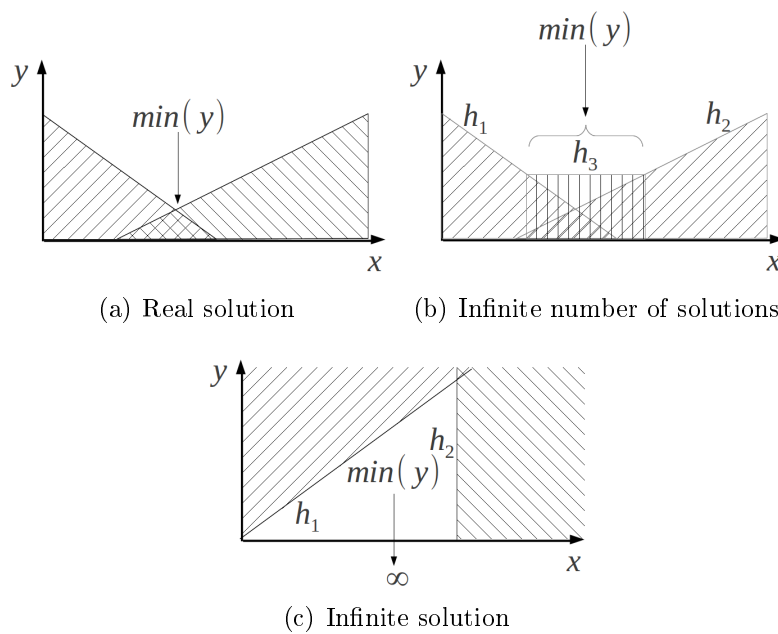


Figure 2.1: Linear problem

- (a) There is one real solution. It consist in a vertex formed by the intersection of several boundaries of the research domain.
- (b) There are an infinite number of solutions. Such case appears when the constraints form an edge or a surface orthogonal to the steepest descent.

- (c) There is one not real solution which is $\pm\infty$. In that case the search space is not bounded in the steepest descent direction.

A non-linear (*MINLP*) can have too many different forms to be described explicitly in a general expression.

The optimality conditions for problem 2.5 is determined by the Karush-Kuhn-Tucker (*KKT*) conditions. The Lagrangian L is defined as:

$$L(z, \lambda, \mu) = f(z) + \lambda^T h(z) + \mu^T g(z) \quad (2.7)$$

With $h : \mathbb{R}^n \rightarrow \mathbb{R}^p$ and $g : \mathbb{R}^n \rightarrow \mathbb{R}^q$. Moreover, h and g shall be continuously differentiable and linearly independent. There exists unique λ^* and μ^* so that:

$$\nabla_z L(z^*, \lambda^*, \mu^*) = 0 \quad (2.8)$$

$$\mu_j^* \geq 0, \quad j = 1, \dots, p \quad (2.9)$$

$$\mu_j^* g_j(z^*) = 0, \quad j = 1, \dots, p \quad (2.10)$$

Equation 2.10 is used to ensure that only active constraints will be considered in 2.8. As a reminder, a constraint $g(z) \geq 0$ is called active in z^* if $g(z) = 0$.

If f , h and g are twice differentiable:

$$\begin{aligned} C^T \nabla_{zz} L(z^*, \lambda^*, \mu^*) C &\geq 0, \quad \forall C \neq 0 \quad \text{so that} \\ C^T \nabla h_i(z^*) &= 0, \quad i = 1, \dots, m \\ C^T \nabla g_i(z^*) &= 0, \quad i = 1, \dots, p \end{aligned} \quad (2.11)$$

and if z^* is a strict local minimum,

$$C^T \nabla_{zz} L(z^*, \lambda^*, \mu^*) C > 0, \quad \forall z \neq 0 \quad (2.12)$$

Difference between a minimum and a strict minimum is that the optima z^* is unique in its neighborhood.

Verifying *KKT* conditions relies on derivative estimation. In case of explicit form for f , h and g , no problem shall be encountered. However in case of numerical models, what concerns most of cases in energy system design, several approach may be considered. First, numerical derivative may be used. But the computational cost they imply may be too high compared to the information they provide, i.e. the assurance to be at a local optima. Another possibility is the use of surrogate model, which may be built by gaussian quadrature [67], neural network [80] or any other interpolation technique [71], which will add a layer of uncertainty on the model. As well as in the first proposition the computational cost to train surrogate models during optimization is not worth enough. Indeed, most of numerical solvers have either a stopping-criteria or may be stopped once the user estimate that the

optimal solution is reached.

Hence, there is no analytical way to verify optimality of the solution. However, optimization can be carried out anyway since great improvements can be noticed. Moreover, previous considerations underline the importance on one hand of the optimization solver and on the other hand of the model used. Section 2.1.2 presents more in depth usual functions in energy system, especially used at LENI. Section 2.1.3 proposes a detailed classification of the related variables.

2.1.2 Typical Function in Energy System Design

In this study, the function f , g and h are included in the structure represented in figure 2.2. Such approach has been already applied at LENI in several different domains like fuel cells [56, 5], carbon capture [9], pulp and paper industry [66] and biomass conversion [30].

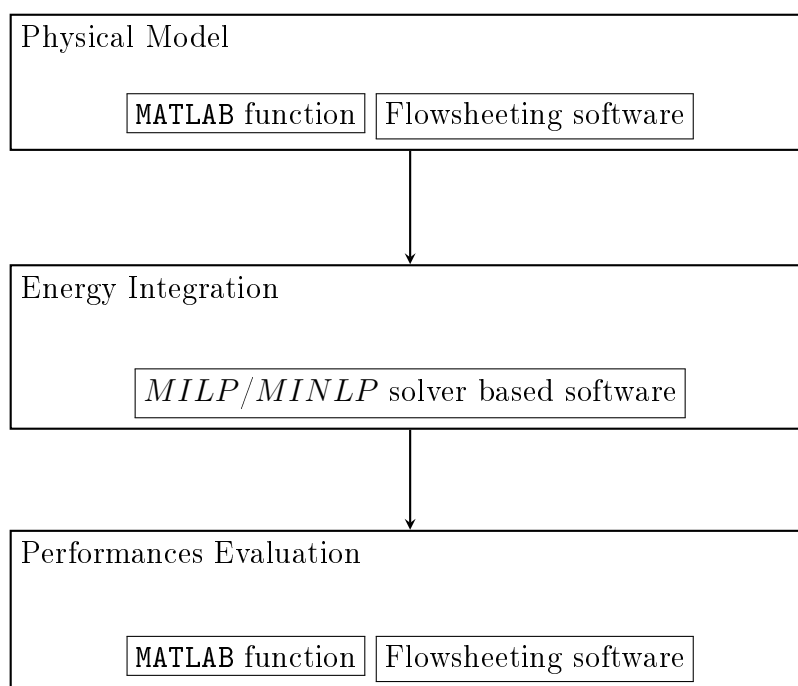


Figure 2.2: Resolution sequence

The model structure described in figure 2.3 is strongly related to the process design procedure. In energy system design, such approach has been studied and defined as an onion layer scheme [49, 55]. The principle is to start as close as possible of the process (chemical reaction) and to end by the heat recovering as

the most external layer. This way, the process can be designed and optimized first and then the utilities are treated.

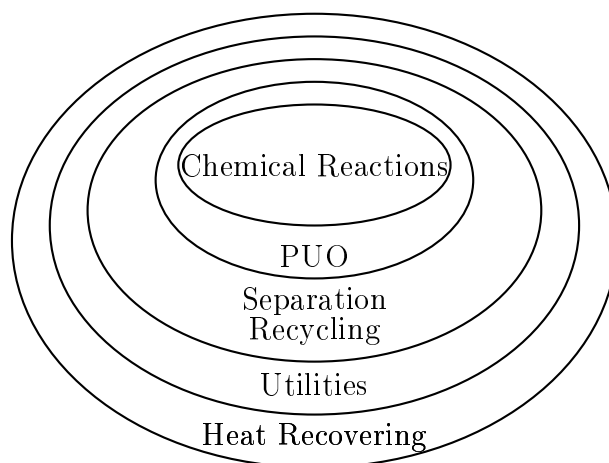


Figure 2.3: Onion representation

The physical model: It describes the thermodynamic state of the problem based on a set of input variables. Its role is to provide information to energy integration (mainly a list of hot and cold streams) and performances evaluation. It includes the chemical reactions, the physical unit operations, and eventual recycling or separation from figure 2.3.

A generic framework has been developed at LENI (OSMOSE), it uses MATLAB or flowsheeting software models. VALI¹ has been used in this study. This software can be used for modeling as well as for data reconciliation. It is a time and memory consuming task for several reasons. First, the model is solved based on an equation solver approach, implying several iterations to converge to the solution. Moreover, data transfer between flowsheeting software and the rest of the model is very demanding, since results files have to be written.

However every physical informations are calculated and can be accessed, whereas in a MATLAB model built by the *DM*, only important variables will be computed. Despite this drawback for computing performances, it offers the advantage of allowing to recover any value, and not only those chosen *a priori* by the *DM*.

The energy integration: The principle of energy integration (or pinch analysis) is to design and estimate a rational use of energy for a given system (provided by physical model). It consists in:

¹<http://www.belsim.com/>

- Determining the Minimum Energy Requirement (*MER*)
- Computing the necessary utilities to satisfy *MER*.
- Selection and sizing of common equipment used to fulfill energy needs (boiler, rankine cycle, heat pump, steam network,...).
- Design of heat exchanger network (*HEN*)
- And computation of all necessary information for the performance evaluation (energy consumed or delivered and *HEN* cost based on area)

It should be noticed that most of these elements are *MILP* problem and can be solved with a low computational cost. However, a special attention should be given on the *HEN*. Its cost and efficiency can be calculated in three steps ([62, 63, 64]), each of them providing a more detailed view than the previous one.

The first one is based on the *MER* [54] and provides a total heat exchanger area estimation and the pinch points location. It shall be noticed that only the ΔT_{min} is considered as decision variables at this level.

The second one is the Heat Load Distribution (*HLD* [27]), which is focused on determining which streams shall exchange together and what will be the heat loads and mass flows. This means that the streams involved in each heat exchange are identified, but that the physical options to connect them have still not been studied.

Those two previous problems are linear. However, the third step, the Heat Exchanger Network Synthesis (*HENS* [25]) is a *MINLP* problem, increasing greatly the computational cost. It solves the heat exchanger problem by providing a detailed superstructure.

Performances evaluation: It consists in ranking a solution based on thermodynamical, economical or environmental factors.

Of course, different resolution sequences may be chosen. However, in any case, complex superstructures remain resource consuming, what makes them the bottleneck of optimization. Such problems are *MINLP* problems and there is in most of cases no analytical formulation available. Hence the number of model evaluations is limited by computation means.

2.1.3 Variables Classification

This section details the variables related to energy system design. Indeed, the decision variables z in problem 2.1 is only one part of the variables involved in the problem. They can be classified in four types, the decisions variables z , the

parameters θ and the dependent variables d [1, 34, 36, 40, 26]. The description represented in figure 2.4 considers these contributions and goes one step further, describing possible uncertainties in an exhaustive manner:

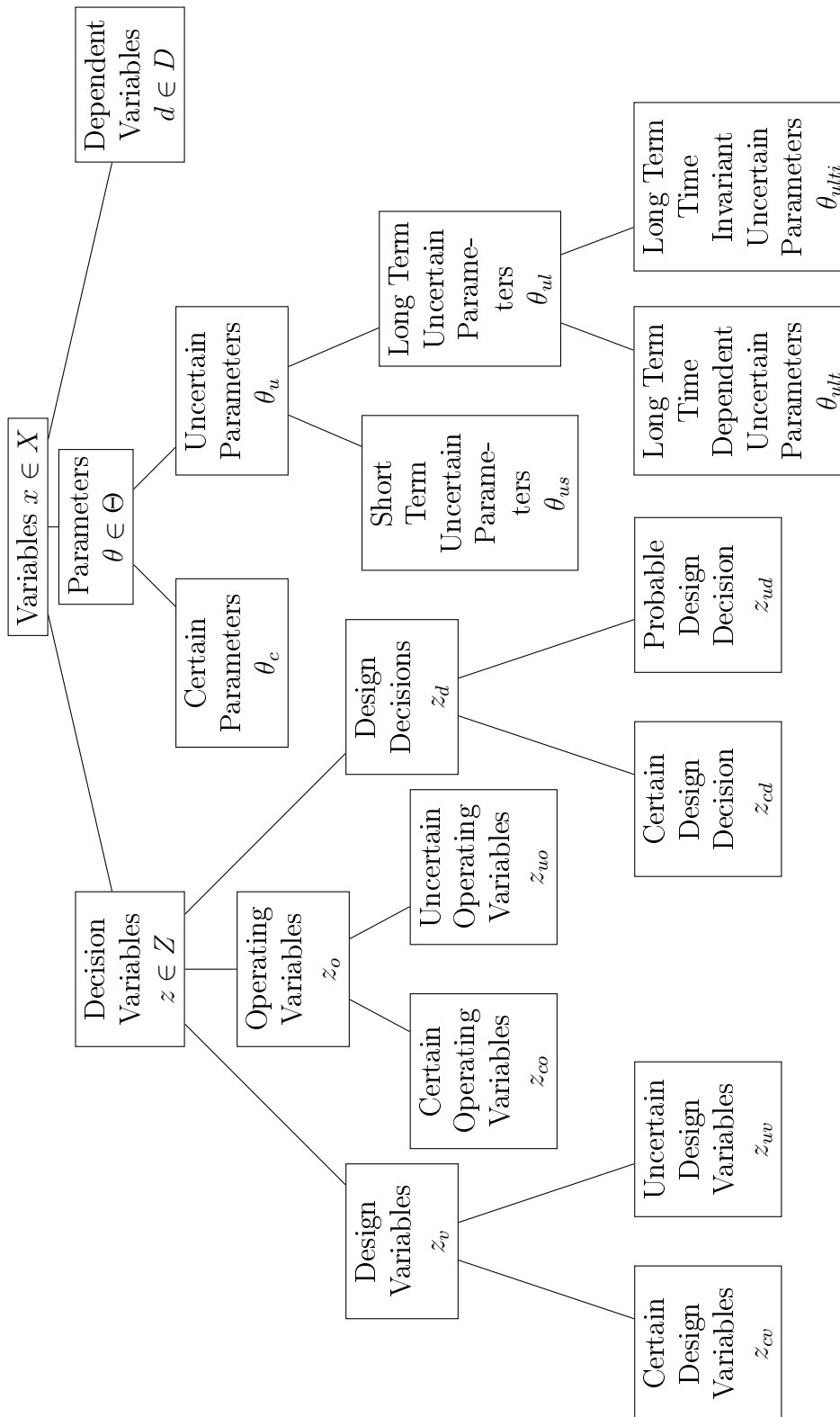


Figure 2.4: Variables classification

It should be noticed that the variables are classified here based on their role in the optimization problem. So, uncertainties are considered independently from their sources (model, measurements,...). They can be described as follows, x representing any variables of the problem:

- Decision variables z and their related space Z : the variables whose value will be adapted in order to minimize the objective function. The decision variable set results from the degree of freedom analysis. The decision variables may be separated into:
 - Design variables, z_v : continuous variables characterizing the design, for example size of equipments.
 - * Certain design variables z_{cv} : design variables that have no or almost no risk of failure. For example, a massflow controlled by a vane has a standard deviation so small compared to equipment efficiency that it can be considered certain.
 - * Uncertain design variables z_{uv} : design variables that may be different than the result of optimization. For example, the effective nominal power of a compressor may vary in a given range from the value specified in catalog. To distinguish desired value \bar{z}_{uv} from its deviation \tilde{z}_{uv} , z_{uv} is defined as $z_{uv} = \bar{z}_{uv} + \tilde{z}_{uv}$.
 - Operating variables, z_o : describe the operation of the plant such as pressures, temperatures, or flow rates. At the system level approach considered here, the details of automatic regulation is not modeled, since the model considers only steady-state or quasi-static behaviour. z_o is then the set point of measured values, whereas manipulated variables are considered as dependent variables. For example, z_o may be the temperature of a hot stream whereas the real manipulated variables is the cooling water flow rate.
 - * Every operating variables are uncertain in reality due to measurements errors and regulation system, or bad representativity of the measurement. A limit based on a maximum acceptable deviation should be defined between z_{co} and z_{uo} to establish their difference. However, since such statistics may be hard to evaluate without a detail transient model, resulting information and results should be used very carefully. As for design variables, $z_{uo} = \bar{z}_{uo} + \tilde{z}_{uo}$.
 - Design decisions, z_d : integer variables characterizing the design, indicating the selection of a technology for example.
 - * Certain design decisions z_{cd} are decisions that shall be taken without any *a priori* opinion of the *DM*. In other words all of them

are equally probable. This leads to a standard scenario approach.

- * Probable design decision z_{ud} includes decision related to a given probability. For example, in case of a district heating, this may be the probability of a household to accept to be connected to the network. In such cases, stochastic process [74] may be considered.
- Parameters, θ associated to space Θ : the models parameters are not variables *stricto sensu*. Their distinction is however necessary for the definition of uncertainty. They are divided into two categories:
 - The certain parameters θ_c , which can be considered as fixed or which variation can be neglected.
 - The uncertain parameters θ_u which are themselves classified into two types:
 - * The short term uncertainties θ_{us} are the parameters that will be known once the energy system will be built. As an example, the exact installation cost of a unit is known once it is bought.
 - * The long term uncertainties θ_{ul} , which will remain uncertain even during plant operation, as ambient temperature for example. They are themselves separated in two sets: the time dependent and invariant long term uncertainties.
 - The time dependent θ_{ult} are continuous and can be defined as uncertainties related to a duration. For example, for a heating system, the probability of having a given outlet temperature is strongly linked to the total time this temperature will happen during the year. In that case, it is a yearly period, but it depends on the uncertain parameter nature. The probability to be in maintenance may be considered on the whole lifetime for example.
 - The time invariant θ_{ulti} are discrete event variable. The probability of one equipment failure due to default is one example.
- Dependent variables, d from space D are resulting from the resolution of the equality constraints $h(z, \theta, d) = 0$ once the value of the decision variables is fixed. Then, problem 2.5 becomes:

$$\begin{aligned}
 \min_z \quad & y = f(z, \theta) \\
 \text{s.t.} \quad & h_1(z, \theta) = 0 \\
 & g(z, \theta) \leq 0
 \end{aligned} \tag{2.13}$$

Where h_1 is the equality constraints that are not related to dependent variables d . For notation issue, consider that from now $X = Z \cup \Theta$ and h is in fact h_1 .

Moreover, the space U gathering spaces of all uncertain variables $\tilde{z}_{uv}, \tilde{z}_{uo}, \theta_{us}, \theta_{ult}$ is defined. Its related variables $\vec{u} = [u_1, \dots, u_{n_u}]$ represents the vector of $z_{uv}, z_{uo}, \theta_{us}, \theta_{ult}$ ($n_u = n_{z_{uv}} + n_{z_{uo}} + n_{\theta_{us}} + n_{\theta_{ult}}$ being the number of uncertain variables). By opposition, the space $C = X - U$ includes all certain variables which will be generically called \vec{c} . It can be noticed that z_{ud} and z_{ulnp} is not included in \vec{u} . Indeed, discrete uncertain variables will be treated in a scenario approach, so that the method presented here focus on continuous random variables, i.e. on the resolution of one scenario.

“Uncertain variables” are in fact random variables from a mathematical point of view. They will be called “uncertain” in this study for a readability reason.

The role of these variables in the energy system design problem depends strongly on the development progress. Figure 2.5 shows above the time axis, the period while uncertain variables remain uncertain. Below time line is represented the period while decision variables can still be modified.

It is important to notice that the framework in this study appears at the beginning of the design procedure, so that a relevant preliminary design provides guidelines that can make following steps considerably easier. Moreover, at this level, there is a maximum number of degrees of freedom (z_v, z_d and z_o) available, and then more opportunity to improve performances.

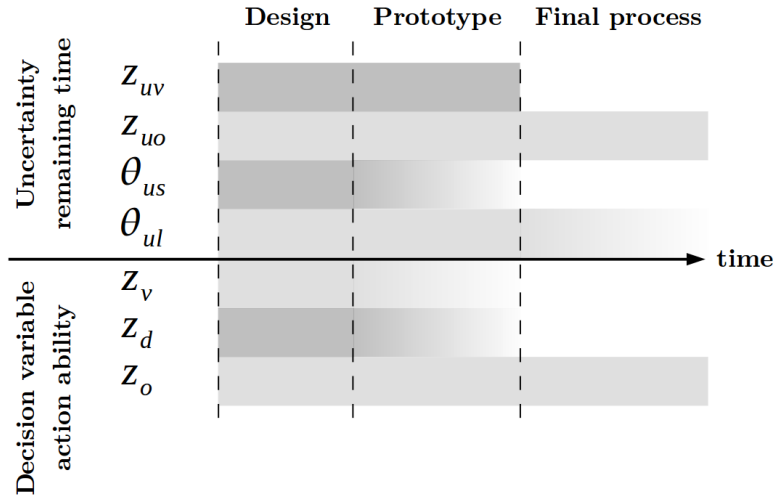


Figure 2.5: Influence of decision variables and uncertainties in time

Several gray area appears in shaded tons. Indeed:

- Short term uncertainties θ_{us} may become certain during prototype phase like an investment cost. By definition long term uncertainties θ_{ult} remain uncertain after system commissioning. However, they can become “less” uncertain. For example, average maintenance time can be deduced by a statistic analysis on previous years.
- Design decisions and variables may be fixed during prototype phase too. This depends on the possibility to rethink decisions already taken.

It should be noticed that in the approach proposed here, every operating variables z_o are assumed to be able to compensate the influence of any uncertain variables u to maintain $f(z_o, u) = y_{nominal}$. If one operating variables $z_{o,i}$ has in fact no influence on the objective submitted to uncertain variables u_j , operating strategy will consider other variables $z_{o,k}$. If $z_{o,i}$ may compensate u_j , it will be considered anyway, even if it is not the case in reality. A typical example is time scale issue: the thermostat of a residential building is supposed to regulate boiler fuel inlet to maintain house comfort temperature. However, it can not deal with rapid temperature variations (like window opening to ventilate). Such problem may be solved by using dynamic models. However, this study is restricted to static or quasi-static model.

Uncertain variables description can not be separated from their influence. They represent a risk that can be classified in three seriousness degrees (from the lightest consequence to the worst):

1. Performances may change due to unpredicted parameters. They can be improved (if an efficiency is better than what was forecasted for example), but most of time they are lowered. This is due to:
 - A non-adapted control strategy
 - A non-adapted design and a decrease of performances since equipments are used out of their nominal point
2. A soft constraint violation. Such constraint can be overridden but it induces penalty. For example if the colder hot stream of a process is colder than the cooling water in use, a refrigerating system shall be used, what is possible but increase investment and operating costs. Such behaviour describes the degree of flexibility of the system [1].
3. A hard constraint violation. It fixes the limit beyond which system can not be operated. It is the case of the previous example, it is illustrated in case that there is no possibility for buying a refrigerating system. This boundaries is the feasibility limit of the system [1].

From a mathematical point of view, case (1) and (2) are similar. For example, performances decrease can be compensated, most of time by an additional consumption of resources, what is a penalty. However, they will be considered different, since in case (2) superstructure is modified by adding new equipments. It must be noticed that all uncertain variables are considered independent. If it is not the case, other variables shall be found or the model shall be adapted. Indeed, some variables may be independent depending on the modeling scale. Such a condition is related to the joint probability formulation:

$$p(\vec{u}) = p([u_1, \dots, u_{n_u}]) = p(u_1 | \dots | u_{n_u}) \quad (2.14)$$

Which in case of Independence does not include covariance terms and is simply given by:

$$p(\vec{u}) = p(u_1) \cdot \dots \cdot (u_{n_u}) \quad (2.15)$$

2.2 Optimization problem resolution

2.2.1 Chosen solver

Based on equation 2.5, a great amount of optimization methods have been developed depending on the type of problem. Good overviews and perspective can be found in literature [10, 33]. They are classified in three types: gradient based, heuristic and mixed.

Gradient based methods are not the most recommended here since models considered in energy design can have a lot of local optima and discontinuities due to integer variables. A lot of starting points would then be necessary. Moreover, since most of energy problems are multi-objective, partial derivative estimation may increase greatly computational cost. Hence, the relevance of such methods depends highly on the studied problem (number of objectives, size of the superstructure, monotonicity of the model,..) [69].

A heuristic method based on an evolutionary algorithm has been chosen. It offers greater chances to reach global optimum and use of such algorithms is now wide spread. The one used in this study has been developed especially for energy system design [58, 53]. Clustering methods allow to conserve also non-optimal solutions until the end of optimization so as to compare them with final solutions. For example, if three technologies can provide the same service and that one of them is systematically worst than two others, the solver may maintain it alive to compare its best performances with the two options to be kept. It necessitates a lot of iterations what can be a disadvantage from computing time point of view but an advantage since stochastic methods developed here may need a lot of iteration to ensure the complete exploration of uncertainty space.

Of course some hybrid methods are more efficient as Sequential Approximate Optimization (SEQOPT)[50]. However, such an approach relies on surrogate models. Their error have to be quantified and compared to uncertainties taken into account. Heuristic models are based on deterministic models what makes study of uncertain variables easier despite they are more “brutal”. Finally, method for uncertainty processing developed here shall be generic and not depend on solver.

2.2.2 Evolutionary algorithm

In this section, evolutionary algorithm used here [58, 53] will be shortly described. Such algorithms are inspired by Darwin theory: “*Survival of the fittest*”. Fitness is given by the objective functions. The solver makes an initial population evolve to reach optima. Once the initial population is generated, the next generation are obtained by:

- Crossover: At least two parents are chosen to create a child based on their decision variables.
- Mutation: The decision variables of only one parent are slightly changed.
- Parents: The fittest parents may be maintained alive from one generation to another to ensure that created points from crossover and mutation shows a real improvement compared to previous generation.

The details on children creation and generation size criteria will not be given here. The two main parameters chosen by the user are the size of initial population and the maximal number of iterations.

2.3 Optimization under Uncertainty

2.3.1 Uncertainty problem formulation

Dealing with uncertainty has always been a great challenge in energy system design. However, computer science progress offer new possibilities in uncertainty processing. Number of examples can be found with different complexity levels. Linear problems [40, 12, 1] are easier to study. Indeed, as well as every monotonic functions [26], objectives or constraint variations are limited by uncertainty boundaries or activated constraints as represented in figure 2.6(a).

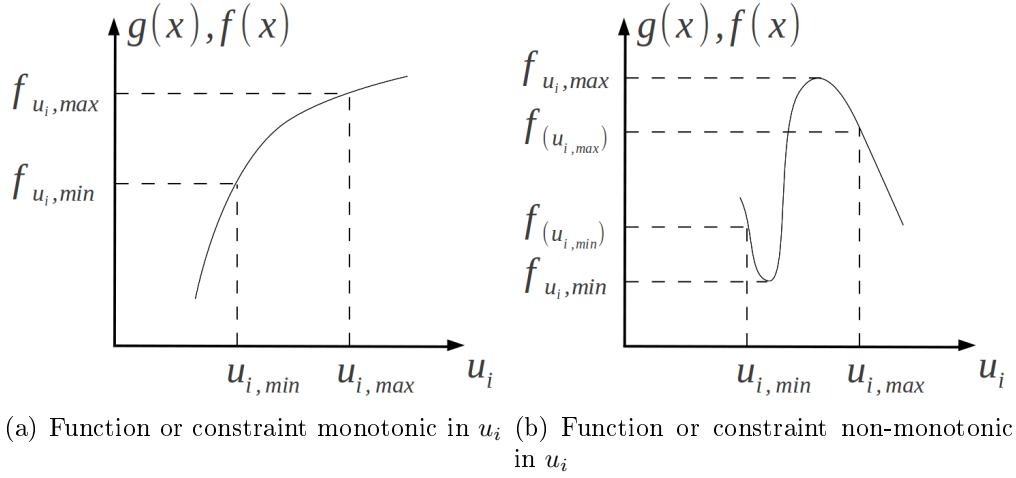


Figure 2.6: Monotonicity issue

Figure 2.6(b) shows a non-monotonic function. It is exaggerated to present both minimum and maximum out of u_i boundaries. In such cases, simulating the models for $u_{i,min}$ and $u_{i,max}$ do not allow to find $f_{u_i,min}$ and $f_{u_i,max}$. This situation is common in energy system. An example can be an uncertain demand for a load following facility. The efficiency is optimal in nominal conditions (standard demand d_{st}), but varies as soon as the produced power changes. In such case, the uncertain variables corresponding to the best efficiency is not at a boundary, so that $d_{min} < d_{st} < d_{max}$.

Quadratic formulation [72, 12] allows easy implementation too since convexity can be verified. A special case to notice is the availability of an analytical form of the functions and constraints, what allows exact derivative estimation and can improve model computing time [1, 26].

In addition to non-monotonicity and non-analytical models, this study focus on non-linear problems, with a great number of equations and variables and multi-objective problems. With respect to these conditions, this section first presents the mathematical formulation of energy system design under uncertainties. Then, numerical techniques to solve it will be described, as well as their limits.

General formulation with recourse: The principle in such approach is to decompose the problem in two layers. The design decisions and variables z_d and z_v are involved in the first-stage, whereas the operating variables z_o have a role in the second-stage. Such approach allows to consider the ability of operating variables to compensate uncertainties even during plant operation. Then, problem

2.5 becomes:

$$\underbrace{\min_{z_{cv}, \bar{z}_{uv}, z_d} \mathbf{E}_{\tilde{z}_{uv}, \tilde{z}_{uo}, \theta_u} \left(\underbrace{\min_{z_{co}, \bar{z}_{uo}} f(z, \theta) | g(z, \theta) \leq 0}_{(2)} \right)}_{(1)} \quad (2.16)$$

With $\mathbf{E}(x) = \mu_x$ being the expected value defined for discrete case: In other words, problem (1) and (2) can be formulated as:

- (2) For a given design and known uncertainties, find the best control strategy by searching optimal z_{co}, \bar{z}_{uo} .
- (1) Finding the best design given by $z_{cv}, \bar{z}_{uv}, z_d$, knowing that the system is able to gives the best possible performances for any uncertainty $\tilde{z}_{uv}, \tilde{z}_{uo}, \theta_u$.

In literature [40, 1, 70, 34], equation 2.16 may be called *two stages programming problem*. It is subject to:

$$\forall(\tilde{z}_{uv}, \tilde{z}_{uo}, \theta_u) \quad \exists(z_{cv}, \bar{z}_{uv}, z_d) | g(z, \theta) \leq 0 \quad (2.17)$$

Where equation 2.17 is known as the *feasibility constraint*. This key notion represents the hard constraints, or the limit of installation operability. Such problem may be called *reliability analysis* in other domains like continuum mechanics.

It should be noticed that feasibility constraint 2.17 does not have to be studied on the whole domain. Indeed, it can be demonstrated [39] that satisfying the most restrictive variables is sufficient, what leads to the problem 2.18 (for n_g constraints):

$$\max_{\tilde{z}_{uv}, \tilde{z}_{uo}, \theta_u} \min_{z_{co}, \bar{z}_{uo}} \max_{j \in [1, \dots, n_g]} g_j(z, \theta) \quad (2.18)$$

This expression remains hard to verify since usual models have no explicit formulation of constraints.

The problem 2.16 is known as infinite. Indeed, expected value relies on the whole uncertain variables space. Its discretization leads to the *multi-period* formulation. It should be noticed that even if the formulation is closed to the conventional multi-period problem used in energy systems, it does not necessarily reflect real duration. For n_s samples:

$$\min_{\vec{c}, z_{co}^1, \dots, z_{co}^{n_s}, \bar{z}_{uo}^1, \dots, \bar{z}_{uo}^{n_s}} \sum_{j=1}^{n_s} p_j f(\vec{c}, \vec{u}_j) \quad (2.19)$$

With c and u gathering respectively the certain and uncertain variables as defined in section 2.1.3. The goal of such formulation is to consider the second stage of equation 2.16. It computes the ability of the system to adapt to uncertain variables variation in order to:

- avoid to reach the feasibility limits, in other words to maintain the system operable
- keep the performances optimal. This is related to the variance of objective functions, and may be found in literature as *second moment analysis*.

This leads to *flexibility* definition. Despite there is several ways to expressed it in literature, the global sense remains the same. For $u_i \in [u_i - \delta, u_i + \delta]$, a flexibility index F could be given as [10]:

$$\begin{aligned}
 F &= \max \delta \\
 \text{s.t.} \quad & \max_{\tilde{z}_{uv}, \tilde{z}_{uo}, \theta_u} g(z, \theta) \leq 0 \\
 & \delta \geq 0 \in \mathbb{R}
 \end{aligned} \tag{2.20}$$

2.3.2 Uncertainty propagation

Principle in uncertainty propagation is to obtain a measure of uncertain variables effect on a performance y .

First level of propagation which is used in conventional design is based on mean value of uncertain variables. In best cases data reconciliation can be applied to determine μ_u .

Since all u_i are supposed independent:

$$p(\mu_u) = p(\mu_{u_1}) \cdot \dots \cdot p(\mu_{u_{n_u}}) \tag{2.21}$$

Such approach is relevant for the most probable case. However, occulting other possibilities means being not prepared in case they happen.

Three types of results [77] may be used when propagating uncertainties as expressed in figure 2.7.

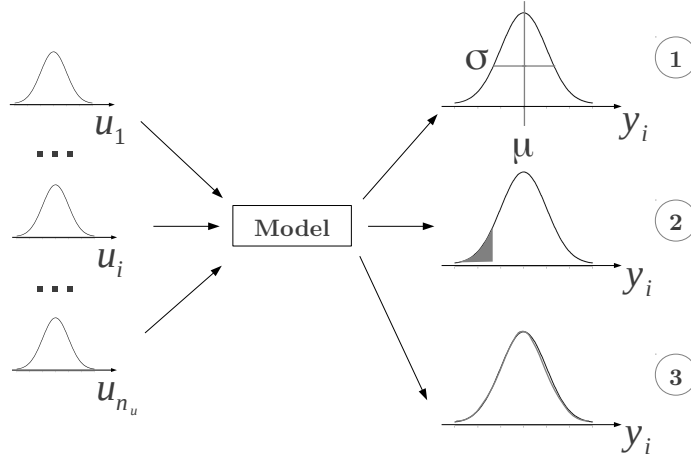


Figure 2.7: Uncertainty propagation output

1. Mean and variance gives information on function variability. Skewness may be useful in case of asymmetric *pdf*.
2. Quantile are used to measure probability of violating a constraint or probability for a solution to be better than another.
3. Finally, the probability density function itself is considered as the maximum information that may be obtained, allowing to compute moments as well as quantile.

Monte-Carlo simulation: First logical attempt to include uncertainty in energy system design is to use Monte-Carlo simulation. Its main advantage is that it totally relies on the deterministic model simulation. However, the number of necessary evaluations makes it a bad approach to be included in an optimization procedure for the problem treated here. For example, the mean usually converges as $1/\sqrt{n_{eval}}$ for one dimension [24]. Moreover, the number of function calls increases exponentially as a function of n_u , the number of uncertain variables. Some more efficient techniques have been developed to optimize the number of model evaluations and maintain a good representativeness of the uncertain space. Most common are Latin Hypercube Sampling (*LHS*) [43, 77], Hammersley [76, 87, 17] or Sobol [77] sequences.

Such approach is similar to scenario or multi-period approach (equation 2.19). The underlying principle is to discretize continuous uncertain space [38] and ensure feasibility of the solution [1].

Moreover, the question of non-injectivity should be underlined. Considering that

two uncertain variables can compensate their respective effect on objective functions, it means that two different sets of uncertain variables \vec{u}_{s1} and \vec{u}_{s2} can lead to the same performance y_1 as in figure 2.8.

This implies that the probability of y_1 to occur $p(y_1) \neq p(\vec{u}_{s1}) \neq p(\vec{u}_{s2})$. The probability $p(y_1)$ is actually given by all sets $\vec{u}_{si}|y_1$ leading to y_1 so that:

$$p(y_1) = \sum p(\vec{u}_{si}|y_1) \quad (2.22)$$

Where $\vec{u}_{si} = [u_1, \dots, u_{n_u}]$.

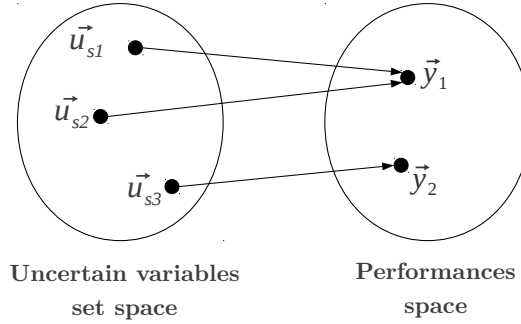


Figure 2.8: Non-injectivity problem representation

Which can be an infinite integral in case of continuous distribution. Hence, Monte-Carlo simulation does not allow an easy extrapolation of the objective distribution function. Complex methods as polynomial orthogonal may be used and will be discussed below. Another possibility is to consider kernel density estimation [69], but this method is non-parametric. On one hand, it is an advantage since it tolerates multi-modal distribution. On the other hand, its moments are difficult to compute, whereas they are necessary for optimization as performance indicators.

However, Monte-Carlo may be useful to study or validate solutions for one set of decision variables, but related conclusions shall be interpreted carefully. Estima-

tors are computed as follows (with n_{mte} , the sample size):

$$\begin{aligned}
 \tilde{\mu}_y &= \frac{\sum_{i=1}^{n_{mte}} y_i}{n_{mte}} \\
 \tilde{\sigma}_y &= \sqrt{\frac{\sum_{i=1}^{n_{mte}} (y_i - \tilde{\mu}_y)^2}{n_{mte} - 1}} \\
 \tilde{\gamma}_{1,y} &= \frac{\frac{1}{n} \sum_{i=1}^{n_{mte}} (y_i - \tilde{\mu}_y)^3}{\tilde{\sigma}_y^3} \\
 \tilde{\gamma}_{2,y} &= \frac{\frac{1}{n} \sum_{i=1}^{n_{mte}} (y_i - \tilde{\mu}_y)^4}{\tilde{\sigma}_y^4}
 \end{aligned} \tag{2.23}$$

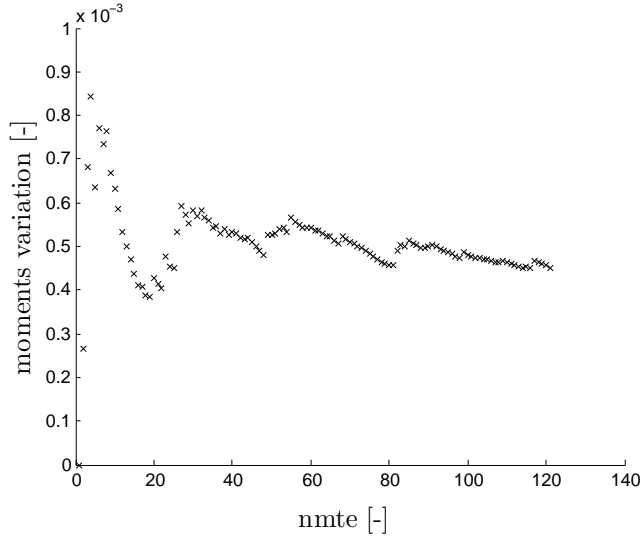


Figure 2.9: Convergence of Monte-Carlo simulation

Despite methods exist to pre-define sample size, here the stopping-criteria has been defined for a maximum deviation of the estimator between one iteration and another:

$$\max \left(\frac{(\tilde{\mu}_y|_i - \tilde{\mu}_y|_{i-1})}{\tilde{\mu}_y|_i}; \frac{\tilde{\sigma}_y|_i - \tilde{\sigma}_y|_{i-1}}{\tilde{\sigma}_y|_i}; \frac{\tilde{\gamma}_{1,y}|_i - \tilde{\gamma}_{1,y}|_{i-1}}{\tilde{\gamma}_{1,y}|_i}; \frac{\tilde{\gamma}_{2,y}|_i - \tilde{\gamma}_{2,y}|_{i-1}}{\tilde{\gamma}_{2,y}|_i} \right) < \varepsilon_{mte} \tag{2.24}$$

With $\varepsilon_{mte} = 0.01$ for example.

Figure 2.9 shows convergence for a model of fuel-cell coupled with a gas turbine [5, 23].

Orthogonal polynomials: Continuum mechanics differs from the present problem in the sense that it implies differential equations. However some approaches in uncertainty analysis may be relevant for this study.

An alternative to finite-element or finite-difference is spectral methods, which have a more local character. Principle is to find a Hilbertian basis (constituted by polynomials) to express $f(\vec{u})$. An analogy can be done by considering a geometric basis $B \in \mathbb{R}^3$:

$$B = \left[\begin{pmatrix} 1 \\ 0 \\ 0 \end{pmatrix}, \begin{pmatrix} 0 \\ 1 \\ 0 \end{pmatrix}, \begin{pmatrix} 0 \\ 0 \\ 1 \end{pmatrix} \right] \quad (2.25)$$

So, as well as the basis B , the hilbertian basis is normalized, orthogonal and allows to express any functions of \mathbb{L}_2 . As a reminder, \mathbb{L}_2 is all the functions F so that $\int_{\mathbb{R}} |F(x)|^2 dx < \infty$. Orthogonality is expressed from the fact that the multiplication of two vectors of the basis B is 0 unless one vector is multiplied by itself. For a Hilbertian basis it is expressed in the sense of its inner product:

$$\langle \psi_k(x), \psi_l(x) \rangle = \int_{-\infty}^{\infty} \psi_k(x), \psi_l(x) w(x) dx = \delta_{kl} \quad (2.26)$$

Where $\psi_k(x), \psi_l(x)$ are two members of the basis, $w(x)$ is the appropriate weighting function and δ_{kl} the Kronecker symbol.

Details of polynomial chaos expansion will not be exposed here, since the goal is to study their suitability for energy system design problems.

So the expansion of $y = f(\vec{u})$ is:

$$y = \sum_{\vec{\alpha} \in \mathbb{N}^{n_u}} c_{\vec{\alpha}} \Psi_{\vec{\alpha}}(\vec{u}) \quad (2.27)$$

The principle is to expand y , considering a Hilbertian basis α_i associated with each uncertain variable u_i . The notation $\vec{\alpha}$ is not totally correct, since it does not describe exactly a vector, but all the possible combination between the elements of each basis α_i . It can be summarized by considering a sum of truncated series and an error term ε .

$$y = \sum_{j=0}^m c_j \Psi_j(\vec{u}) + \varepsilon_{m+1} \quad (2.28)$$

Where m is the number of possible combinations between the elements of the n_u Hilbertian basis.

Assuming that the coefficients c_j are known, it becomes possible to compute desired values related to y distribution. The *pdf* itself can be extrapolated by Monte-Carlo simulation associated with kernel smoothing techniques [77]. This requires a lot of iterations, but is possible, since polynomial chaos expansion deliver an analytical form of y .

the statistical moments may be computed as:

$$\begin{aligned}
\mu_{y,PC} &= c_0 \\
\sigma_{y,PC}^2 &= \sum_{j=1}^m c_j^2 \\
\gamma_{1y,PC} &= \frac{1}{\sigma_{y,PC}^3} \sum_{i=1}^m \sum_{j=1}^m \sum_{k=1}^m d_{ijk} c_i c_j c_k \\
\gamma_{2y,PC} &= \frac{1}{\sigma_{y,PC}^4} \sum_{i=1}^m \sum_{j=1}^m \sum_{k=1}^m \sum_{l=1}^m d_{ijkl} c_i c_j c_k c_l
\end{aligned} \tag{2.29}$$

Where $d_{ijk} = \mathbf{E} [\Psi_i(\vec{u}) \Psi_j(\vec{u}) \Psi_k(\vec{u})]$, respectively $d_{ijkl} = \mathbf{E} [\Psi_i(\vec{u}) \Psi_j(\vec{u}) \Psi_k(\vec{u}) \Psi_l(\vec{u})]$, which can be computed analytically [78] as a function of i, j, k and l for kurtosis in case of Hermite expansion.

Hence, the issue is to find an efficient manner to compute coefficients c_j of equation 2.28. Two approaches are used in continuum mechanics:

- The *Galerkin* or *intrusive* approach, which will not be considered here since its formulation is specific to each case. So, this method does not fit the objective of this study to deliver a generic algorithm.
- The *Non-intrusive* approach, which is based on a series of call of the deterministic model, and that will be considered here. It can be itself divided in two types of methods:
 - The projection methods. Their starting point is the fact that:

$$c_{\vec{\alpha}} = \mathbf{E} [y \Psi_{\vec{\alpha}}(\vec{u})] \tag{2.30}$$

This mean can be computed in an empirical manner by simulation or by using Gaussian quadrature to compute the integral of the expected value. Both of these methods necessitate a great amount of calls to the model to converge to an accurate solution.

- The regression methods. It consists in minimizing the mean square error ε_{m+1} of equation 2.28:

$$\min_{c_j, j=1, \dots, m} \mathbf{E} [y - c_j \Psi_j(\vec{u})] \tag{2.31}$$

Here again, the expected value may be solved by simulation or Gaussian quadrature.

The bottleneck of this approach is the number of model evaluations. In simulation methods, it is related to Monte-Carlo simulation, or any more efficient sampling methods. In Gaussian quadrature, it is related to the number of collocation points. The relevance of such approach is then determined by the advances in sampling techniques. One of them, which has not been investigated in this study but would deserve attention is sparse grid [6, 84]. It is based on Smolyak algorithm [73], which allows to avoid the *curse of dimensionality*, i.e. the number of knots growing exponentially with the number of dimensions.

It shall be noticed that the weighting function in equation 2.26 is linked with uncertain variables *pdf*. Indeed, in case $w(x) = p(x)$, the orthogonality formulation is similar to moment definition. It is possible to consider a mix of several types of polynomials [85] if the uncertain variables do not have all the same distribution, as described in table 2.1.

Distribution	Polynomials
Normal	Hermite
Gamma	Laguerre
Uniform	Legendre
Beta	Jacobi

Table 2.1: Distribution and related orthogonal polynomials

However, the convergence of the expansion will be deteriorated, so that a higher order (implying more iterations) will have to be considered.

Moments method: Such approach is widely used in continuum mechanics [46, 57] and starts being used in aerodynamics [45] and is also known as perturbation method. The principle of moments methods is to extrapolate performances *pdf* from their partial derivative in u_i . Concretely it means estimating mean μ and standard deviation σ (even skewness γ and kurtosis β). However, due to non-injectivity they can not be calculated directly. Moments method is based on Taylor expansion series of objectives.

For a constant set of certain variables $\vec{c} = cst$ second order Taylor expansion in $\vec{u} = \mu$ is expressed as:

$$y = f(\vec{u}) \cong f(\vec{u})_{\mu} + \sum_{i=1}^{n_u} \left(\frac{\partial f(\vec{u})}{\partial u_i} \right)_{\mu} \cdot (u_i - \mu_{u_i}) + \frac{1}{2} \sum_{i,j=1}^{n_u} \left(\frac{\partial^2 f(\vec{u})}{\partial u_i \partial u_j} \right)_{\mu} \cdot (u_i - \mu_{u_i}) \cdot (u_j - \mu_{u_j}) \quad (2.32)$$

Where subscript μ means “evaluated in $\mathbf{E}(\vec{u})$ ”. Moreover, to simplify notation, $f(\vec{u})$ will be written as y for equation 2.33 and 2.34. Mean and standard deviation are expressed as:

$$\begin{aligned}\mu_y &= \underbrace{y_\mu}_{1^{st} \text{ order}} + \underbrace{\frac{1}{2} \sum_{i=1}^{n_u} \left(\frac{\partial^2 y}{\partial u_i^2} \right)_\mu \cdot \sigma_{u_i}^2}_{2^{nd} \text{ order}} \\ \sigma_y^2 &= \underbrace{\sum_{i=1}^{n_u} \left(\frac{\partial y}{\partial u_i} \right)_\mu^2 \cdot \sigma_{u_i}^2}_{1^{st} \text{ order}} + \underbrace{y_\mu^2 + \sum_{i=1}^{n_u} \left(y \frac{\partial^2 y}{\partial u_i^2} \right)_\mu \cdot \sigma_{u_i}^2 + \sum_{i=1}^{n_u} \left(\frac{\partial y}{\partial u_i} \cdot \frac{\partial^2 y}{\partial u_i^2} \right)_\mu \cdot \gamma_{u_i}}_{2^{nd} \text{ order}} - \mu_y^2\end{aligned}\quad (2.33)$$

Such approach has already been used in energy system design [50]. However third moment (skewness) may give useful information on *pdf* asymmetry. It is expressed as:

$$\begin{aligned}\gamma_{1y} &= y_\mu^3 + \frac{3}{2} \sum_{i=1}^{n_u} \left[2y \left(\frac{\partial y}{\partial u_i} \right)^2 + y^2 \frac{\partial^2 y}{\partial u_i^2} \right]_\mu \cdot \sigma_{u_i}^2 \\ &+ \sum_{i=1}^{n_u} \left[2y \left(\frac{\partial y}{\partial u_i} \right)^3 + 3y \frac{\partial y}{\partial u_i} \cdot \frac{\partial^2 y}{\partial u_i^2} \right]_\mu \cdot \gamma_{u_i} - \mu_y^3 - 3\mu_y \cdot \sigma_y^2\end{aligned}\quad (2.34)$$

Formulation for kurtosis of a Taylor series expansion is difficult to determine, so that only first order will be considered [88]:

$$\gamma_{2y} = \left(\frac{\partial y}{\partial u_i} \right)_\mu^4 \cdot \gamma_{2u_i}\quad (2.35)$$

As a reminder, numerical derivative (central) is given in equation 2.36.

$$\begin{aligned}\frac{\partial y}{\partial u_i} &= f'(u_i) = \lim_{h \rightarrow 0} \frac{f(u_i + h/2) - f(u_i - h/2)}{h} \\ \frac{\partial^2 y}{\partial u_i^2} &= f''(u_i) = \lim_{h \rightarrow 0} \frac{f(u_i + h) - 2f(u_i) + f(u_i - h)}{h^2}\end{aligned}\quad (2.36)$$

Despite such estimation is better for $h \rightarrow 0$, it should be determined carefully. Indeed, software used for modeling are based on a given precision. In particular, flowsheeting and energy integration software results are strongly related to their

convergence, what leads to different values for the same input parameters. For example, VALI allows a precision up to $e = 10^{-9}$. This means that the closer h will be to e , the less stable will be the derivative estimation. In the present case, a margin of two order of magnitude has been considered since 10^{-7} is still wide enough compared to objective order.

Pearson system: Results of propagation methods may be post processed to obtain an analytical distribution function of the performances. Table 2.2 summarizes the results of the methods described previously:

Method	Result
Monte-Carlo	Samples of uncertain variables and corresponding performances
	Moments estimators of the performances by simple post-processing
Orthogonal polynomials	Polynomial interpolation of model response to uncertain variables
	Moments interpolation
	<i>pdf</i> of performances providing supplementary model evaluations and post-processing
Moments method	Extrapolated moments

Table 2.2: Propagation methods results

It can be observed that all of them allow to compute moments. It gives information on dispersion and asymetry of the *pdf*. However, an analytical formulation of the probability density function of y may be useful, to compute quantile for example.

Several methods allow to do this [3]. Johnson systems associates quantiles to well known distributions [47]. Hence it do not fit here since quantiles are not available for every propagation methods. Generalized lambda distribution is a simple and flexible approach, but Pearson systems [48, 65] will be considered since they are well known and have already been applicated in other fiels [45]. Principle is to define a standard distribution based on the four first moments. Despite such approach is not recent [65], it is still relevant and used in aerodynamics area [45] for example. It consists in a map as the one represented in figure 2.10.

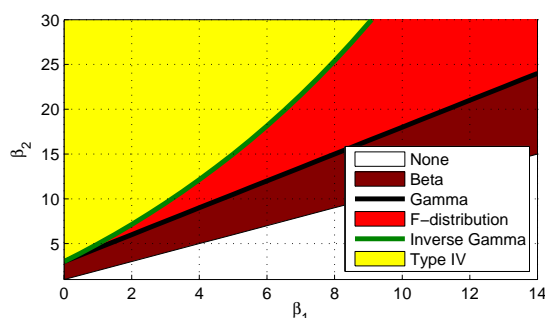


Figure 2.10: Pearson system

In figure 2.10, β_1 and β_2 are given by:

$$\begin{aligned}\beta_1 &= \gamma_1^2 \\ \beta_2 &= \gamma_2 + 3\end{aligned}\tag{2.37}$$

It must be noticed that all the possible zones are not represented in 2.10. So, Pearson's system can lead to the following six types of distributions:

- I: Beta distribution
- II: Symmetric Beta distribution
- III: Gamma distribution
- IV: 4th type is not a standard distribution and won't be described here (see appendix A.1)
- V: Inverse gamma distribution
- VI: F-distribution

Without describing such approach in depth, this method consists in solving the differential equation (with $p(u)$ the density):

$$\frac{p'(u)}{p(u)} = -\frac{x+a}{c_0 + c_1u + c_2^2}\tag{2.38}$$

Values of a , c_0 , c_1 and c_2 depend on β_1 and β_2 . Their results give the type of distribution (and the related parameters).

At this stage, it is then possible to extrapolate density function of y based on the uncertain variables as represented in figure 2.11.

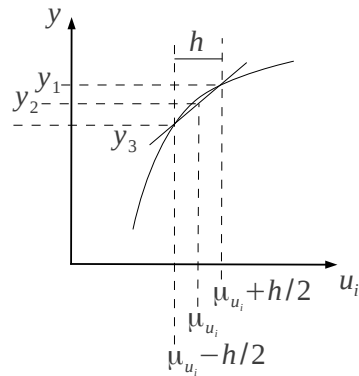


Figure 2.11: Propagation by moments method

However, this does not take into account flexibility, i.e. the second stage of problem 2.16. Next section gives a proposition to solve it.

2.3.3 Proposition for second stage resolution

The energy system differs from other fields like continuum mechanics due to their ability to adapt to uncertain conditions, at least partially, even after the plant installation.

First issue is the fact that no dynamic model is available, so that regulators and their related transfer functions are not considered.

Moreover, designing an optimal control under uncertainty for a given process costs a lot in terms of computational resource. This is mainly due to the fact that such method implies a sampling to define scenarios and then solve a multi-period problem [61]. The combination between the manipulated variables, the measured variables (z_o) and the different uncertainties leads to a great number of periods, despite usage of efficient sampling techniques like *LHS* [59].

The goal here is then to find an estimation of flexibility of the system without going into the details of control optimization.

Figure 2.12 and 2.13 shows schematically the effect uncertainties on objective function with and without operating strategy.

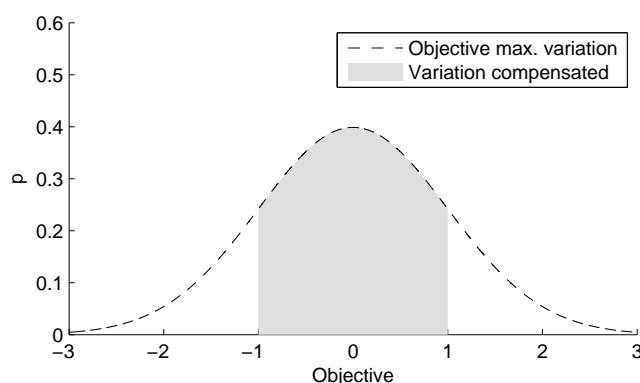


Figure 2.12: Normal distribution and potential compensated area

In figure 2.12 the colored area defines objective variations that can be compensated by an appropriate control of the system. This limits is defined by the operable range of operating variables $[z_{o1}, z_{o2}]$. It should be noticed that this range is not the same that $[z_{o,min}, z_{o,max}]$, the limits considered for optimization. Indeed, first case is the variation tolerated for a built installation, whereas second one is the panel of possibilities proposed on the market, what implies $[z_{o1}, z_{o2}] \in [z_{o,min}, z_{o,max}]$. Hence, z_o may compensate uncertainties influence on objective as long as $z_{o1} < z_o < z_{o2}$, as represented in figure 2.13.

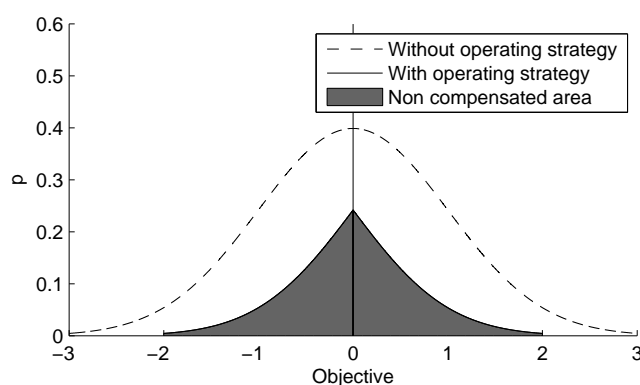


Figure 2.13: Variance decrease effect

The compensated area has become a partial Dirac delta function $\delta \cdot A_{comp}$. Its area A_{comp} is the same as the one of the light gray one in figure 2.12 and is given by the cumulative distribution function. The dark gray area in figure 2.13 is the

case when operating variables regulation is not sufficient to compensate objective variation. Its area A_{left} is such that $A_{comp} + A_{left} = 1$.

2.3.3.1 Second stage for moments method

A first attempt to evaluate operating variable adapting to uncertainties has been to take part of the $2n_u + 1$ model evaluations of moments method. Principle is to generate three sets of operating decision variables per uncertain variables as explained in figure 2.14. This allows the optimizer to consider different operating variables depending on uncertainties values. Critical points of this approach are:

- The h parameter in equation 2.36 is critical. Indeed, it shall be small enough to represent well enough the derivative, but big enough to notice a significant difference in operating decision variables.
- The advantage of this method is that no more function evaluation is needed than partial derivative estimation. However, it implies $3 \cdot n_u$ times more decision variables, hence a greater computer resource consumption during optimization. It is hard to deduce the number supplementary iterations when using heuristic algorithm, so that this number will be found by experiment.

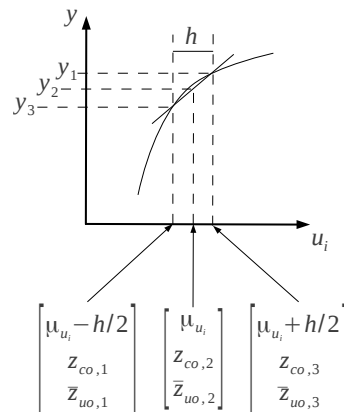


Figure 2.14: Propagation by moments method including flexibility

This method did not succeed for several reasons:

- It multiplied by 3 the number of operating decision variables, and the search space as well. The number of model evaluations per iteration do not increase. However, the number of iterations for the optimization to converge becomes too high.

- Any operating variable is not necessarily influent on any uncertain variables. Hence some optimal value may be search by the solver for $z_{co,1}, z_{co,3}, \bar{z}_{uo,1}$ and $\bar{z}_{uo,1}$ in figure 2.14 whereas there is no solution. This may be changed by allowing the solver to manage the list of operating variables z_o to take into account for uncertainty u_i . However, this has not been further studied.

2.3.4 Stochastic programming

A new way in optimizing an energy system design under uncertainty is proposed [19]. It takes advantage of the evolutionary algorithm property of demanding a lot of iterations. Despite its accuracy is not proved mathematically, it will be shown that such approach can lead to changes in final solutions.

The principle is summerized in figure 2.15. At each model evaluation, uncertain variables are drawn based on their probability law.

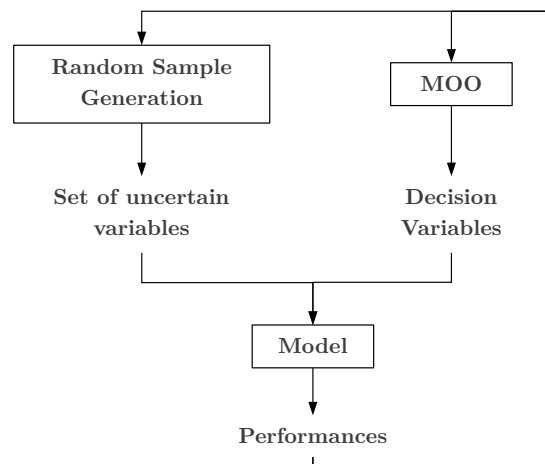


Figure 2.15: Stochastic programming optimization

Three results shall be obtained as represented in figure 2.16. This example is based on an analytical test case (Himmelbau) used in the development of the solver itself [53].

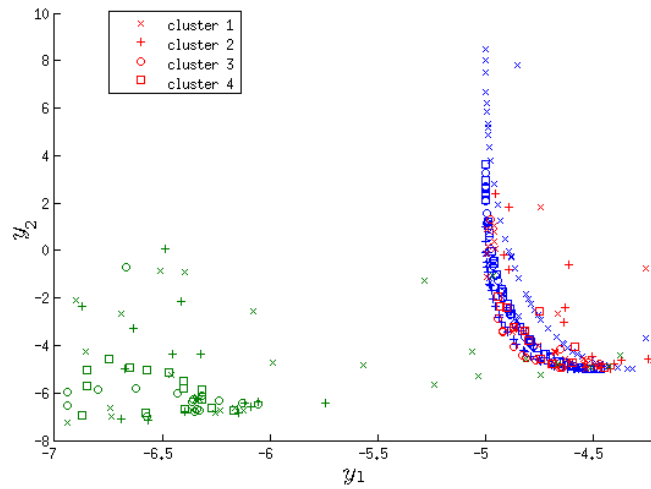


Figure 2.16: Stochastic optimization results

The blue Pareto front results from a conventional optimization. It is the limit of the feasible domain, considering each uncertain variables u_i at their most probable value (the *mode*) \hat{p}_{u_i} . Green points are obtained from algorithm in figure 2.15. They present better performances, since some uncertain variables draw may allow to improve objective function and then to go further than the limit given by the blue points. These points can be recomputed, considering uncertain variables at their mode \hat{p}_{u_i} instead of the value they had during the optimization, leading to red points.

In that case, as it can be seen in figure 2.16, cluster 2 is the most affected by uncertainties. Despite this approach can not quantify influence of uncertainties on the objectives, it allows to study the influence of uncertainties on decision variables. Its main interest is that it does not necessitate more model evaluations than conventional optimization.

As a reminder, the mode may be different than the mean μ_{u_i} . This two estimators are the same for symmetric definition like normal or uniform, but their difference appear important in the following example. The efficiency of an equipment is decreasing over its lifetime (for any reason, like structure weakening or wear). This can be modeled by an exponential distribution as a function of time, as the one in figure 2.17.

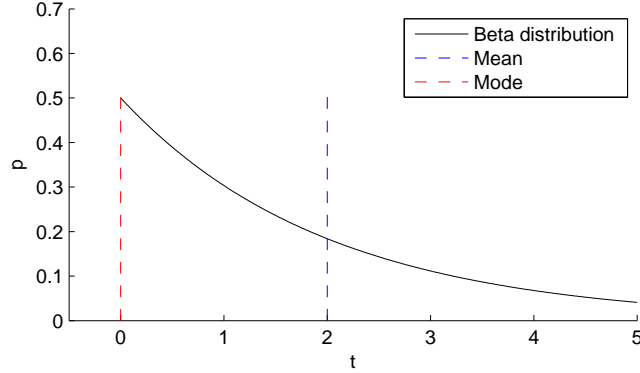


Figure 2.17: Difference between mean and mode

Most of pre-design are based on new equipment performances. However, this means that the older the equipment will be, the further it will be from original design. Designing a system considering the mean of an uncertain variable may allow to ensure higher average performances on the whole life time, despite lower performances right after the installation.

2.4 Other approaches

The following section describes briefly other methods which have not been investigated here.

FORM/SORM: This states for first/second order reliability methods [16] are used to study constraints violation. In other words, reliability is translated in a measure of non-failure probability. Here, decision variables z are considered as constant, so that the constraint $g(u) < 0$ is only function of the uncertain parameters ($u = u_1, \dots, u_{n_u}$). This defines:

$$\begin{cases} g(u) < 0 & \text{Success} \\ g(u) = 0 & \text{Limit state} \\ g(u) > 0 & \text{Failure} \end{cases} \quad (2.39)$$

Considering a joint probability distribution $p(u)$, reliability is given by:

$$R = \int_{u|g(u)<0} p(u) du \quad (2.40)$$

First step in this method is to project g in a standard normal space using isoprobabilistic transforms [68]. Thus, u becomes \dot{u} and g, \dot{g} . The normalized space

is characterized by the fact that the mean values of any \dot{u}_i is 0 with a variance $\sigma_{\dot{u}_i} = 1$. Assuming that mean value is not in the failure domain (i.e. $g(\mu_u) < 0$), the most significant point of the constraint is the closest to the origin u^* as represented in figure 2.18. Methods to find this point can be found in literature [16]. The size of the vector between origin and u^* is β . It is designed by the reliability index. *FORM* assumes a linear constraint (normal to \bar{u}^*) whereas *SORM* is based on a quadratic one.

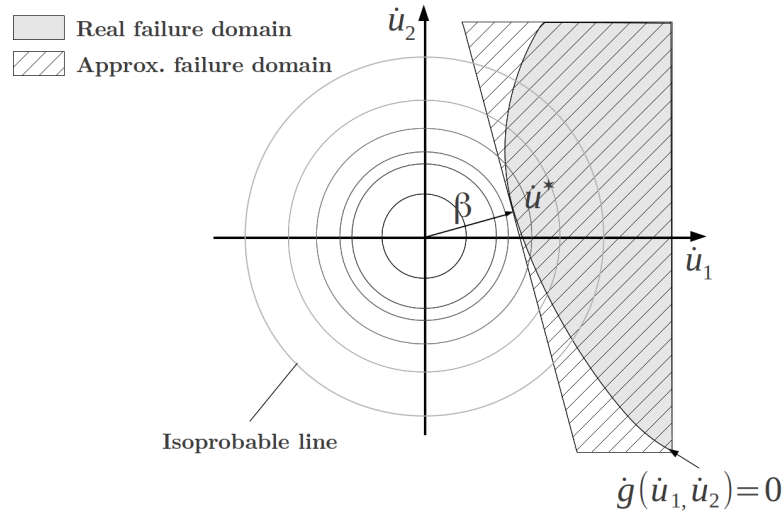


Figure 2.18: FORM principle

Despite such approach necessitates one optimization (to find β) at each model evaluation and that $g(u)$ shall be redefined for each set of decision variables, it remains more efficient than Monte-Carlo [77].

However, it has not been further investigated in the present study since Pearson system allows to recover an analytical expression for the distribution function. Moreover, modelisation proposed here offers the advantage to compute constraints value as well as objective functions. So that uncertainty propagation can be applied on $g(x)$, and reliability can be defined by quantile:

$$R = \int_{\min(g(x))}^0 p(g(x)) dx \quad (2.41)$$

Which is represented in the gray area in figure 2.19.

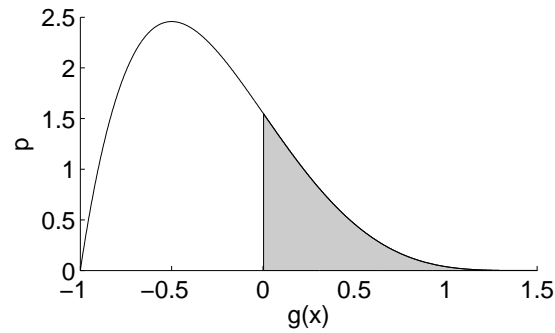


Figure 2.19: Reliability defined by quantile

Fuzzy programming [8]: This approach focus too on reliability. Its main characteristic is that it tolerates constraints violation, linking it to a membership function which is typically (for a constraint $g(x) < c$):

$$m(x) = \begin{cases} 1 & \text{if } g(x) \leq c \\ 1 - \frac{g(x) - c}{\Delta c} & \text{if } g(x) \in [c, c + \Delta c] \\ 0 & \text{if } g(x) > c \end{cases} \quad (2.42)$$

Maximizing $m(x)$ should then be added to other objectives. However, this has not been considered here. Indeed, in energy system design, cost related to overridden constraints is generally already taken into account in objective function, unless it concerns hard constraints. As an example, a boiler may be activated or not depending on ability of hot streams of the systems to fulfill heat needs of the cold streams. Investment and operating cost of this boiler gives more useful information than a membership function, which is not linked with concrete consequences.

2.5 Conclusion

2.5.1 Methods comparison

The energy system design problem as been established as an optimization problem. Its mathematical formulation has been described and detailed. The models that lie behind the functions of the mathematical formulation have been exposed. In LENI, they consist in a sequence of several softwares. This is one of the bottleneck of the optimization since it consumes a lot of computational resource for great superstructure simulation.

Functions definition can not be dissociated from the related variables description.

A classification has been presented, in relationship with the development stage in which they are crucial or not. In future work, this classification should be enriched by linking uncertain variables with operating variables able to compensate, i.e. working in the same time scale.

Techniques for optimization problems resolution have been briefly described since there is already good reviews in literature. In the proposed approaches, heuristic methods have been chosen. One of their main advantage is that they rely only on the deterministic model, avoiding to introduce uncertainties due to a surrogate model. Moreover, a software and a related syntax has been developed at LENI, based on a evolutionary algorithm.

Optimization under uncertainty formulation has been exposed. The two stages programming problem has been detailed with the key notions of feasibility and flexibility. Hence, the issue of considering the ability of the system to adapt has been emphasized. However, the type of treated problems has demonstrated the difficulty to use approach like multi-period for example. Advanced mathematical methods to propagate uncertainties have been studied and compared. They allows to solve the first stage of the “two stages programming problem”. Three methods have been proposed:

- Monte-Carlo simulation
- Orthogonal polynomials
- Moments methods

Monte-Carlo simulation imply a number of calls to the model increasing exponentially with the number of uncertain variables. So, they are too consuming to take place in an optimization procedure. However they remain useful to assess results of other methods for one set of decision variables, or one point of the Pareto curve. Orthogonal polynomials may be a good alternative, but estimating the coefficient for polynomial chaos expansion is computationally expensive with simulation method (collocation methods may be compared to Monte-Carlo simulation) or gaussian quadrature. Smolyak algorithm may make this type of propagation competitive. However, this is hard to evaluate since the number of model evaluations necessary to expand the model with orthogonal polynomials is highly case related.

Moments methods are based on derivative evaluations, increasing the number of evaluation to $2n_u + 1$. This approach will be applied here. Moreover a new method has been proposed to include the second stage in the derivative estimation.

A stochastic programming has been defined allowing to optimize a system taking into account its uncertain variables without additional iterations. However, this method concerns only the heuristic solvers demanding a lot of iterations, like most

of the heuristic approach.

These methods can be compared based on several criteria:

- Propagation: Method allows to propagate objectives *pdf* at each model evaluation. This may be done by propagating moments and applying pearson system. Stochastic programming do not deliver objectives *pdf* at each model simulation, but it may allow this through statistics on the whole optimization procedure.
- Solver: Propagation method works for any optimization solving method. From a theoretical point of view, Monte-Carlo may work with any solver. However, the fact that it needs a high number of samples makes it not suit for most of the solver and models.
- Constraints: Obtained results respects constraints of the model. Orthogonal polynomials and moment methods allows to verify it only if of an explicit form of the constraint is available.
- Deterministic: Results rely only on model simulation.

Advantages and drawbacks of each method are summarized in table 2.3.

Methods	Propagation	Solver	Constraint	Deterministic
Monte-Carlo	yes	~	yes	yes
Orthogonal polynomials	yes	yes	~	no
Moments	yes	yes	~	no
Stochastic	~	no	yes	yes

Table 2.3: Uncertainty propagation methods

Finally FORM/SORM and fuzzy programming have been described since they are widespread in uncertainties management. They focus on constraint violation. They have not been further explored in this thesis since propagation methods presented here allows to retrieve analytical expressions for the *pdf*, making this two approaches less efficient.

2.5.2 Case studied

Section 2 outlines exhaustives approaches for energy system design under uncertainty. However, one case studied can not gather all the issues discussed here. Two methods will be applied:

- The stochastic programming since it has been developed in this thesis, so that its results still need to be assessed.
- The moments method since it demands only a small number of model evaluation ($2n_u + 1$) to propagate uncertainties. For high number of uncertain variables, orthogonal polynomials may be relevant, but they rely on sampling methods, which competitiveness is hard to evaluate a priori.

An innovative hybrid fuel cell system [23] has been chosen as application case. It is described in depth in section 3. It includes the following types of variables with respect to figure 2.4:

- Considered decision variables are design variables z_v and operating variables z_o , both being certain. Design decision z_d may have been used to define if a technology shall be considered or not. Instead of this, characteristic massflows have been used as design variables.
- Uncertain variables are short term uncertain parameters θ_{us} and long term, time dependent long term uncertain parameters θ_{ult}

This is sufficient since the variables involved in the problem influence the results interpretation but not the method choice.

Chapter 3

Model

Methods presented in chapter 2 will be applied on a solid oxide fuel cell coupled with gas turbines [20]. Such model is a technological challenge and may offer great efficiency. The key role of energy integration will be discussed, highlighting its advantage and limits when facing problems subject to uncertainties. Finally the model itself will be described as well as its decision and uncertain variables.

3.1 Energy integration

3.1.1 Advantages and drawbacks

The resolution sequence considered in this study has been presented in figure 2.2. It must be noticed that the method developed here is based on energy systems, but does not depend on the model itself. The decomposition in three steps (physical model, energy integration and performance evaluation) is a choice that may be discussed, but methods exposed in chapter 2 are independent of the model resolution approach under condition of a differentiable objective function. Unlike flowsheeting and performance implementation which are well known, a short reminder on the energy integration (*EI*) is presented here. The main purpose of *EI* is to define a rational use of utilities to fulfill heating and cooling demand by determining possible heat exchanges. They may have been defined directly in the the flowsheeting software in order to bypass the second step of the resolution sequence. Both approaches can be justified with the following arguments [32]:

Flowsheeting:

Advantages:

- Each heat exchanger of the network is modeled and simulated. So, detailed information can be obtained without requiring internal optimization, as in

the case of *HLD* or *HENS*.

- It allows part load simulation, considering changes on performances for a designed heat exchanger (*HEX*).
- Each *HEX* can be considered separately, allowing different types of heat exchangers.

Drawbacks:

- Proposed heat exchanger network relies on assumption made by the decision maker. Hence, such a configuration is specific and hard to optimize by hand, even for one process configuration.
- Due to previous point, *HEN* can not be adapted to the process in a generic manner. It is then hard to optimize a process, since heat exchanger network performances (mainly cost and efficiency) are computed for a fixed (and not optimized) design.

One option could be to optimize it simultaneously with the rest of the system. However, increasing the number of integer variables enlarges the complexity of the problem.

Energy Integration:

Advantages:

- It allows to balance heat recovery and electricity production. For example steam network (*STN*) design shall be given by trade off between the purchase price of hot utilities and the sale price of electricity.
- It gives a global view of the process through pinch analysis (to avoid heat exchange across the pinch point for example).
- Performances are adapted to any configuration of the superstructure, allowing optimization solver to take into account *HEN*.

Drawbacks:

- *HEN* network is design after targeting. In other words, energy integration has to be computed after flowsheeting and *MER* definition. A simultaneous approach would allow to earn computing resources, specially since *HENS* is non-linear.

- Energy integration fits only for steady state operation. Moments methods evaluates function $f(u)$ for $u_i - h/2$ and $u_i + h/2$. So, energy integration will consider a different HEN for $f(u_i - h/2)$ and $f(u_i + h/2)$, while the same one shall be considered, but in different operating conditions. This issue is a complicated problem which will be discussed further in section 3.1.3.

3.1.2 Composite curves

Bases of pinch analysis will be briefly exposed here to facilitate reading the results. Input of this method is a list of all streams of the process to be studied. Each heat exchange is modeled in the flowsheeting software as represented in figure 3.1. Only one of the two material streams is defined, so that energy integration is free to find an optimal way to fulfill heating or cooling needs.

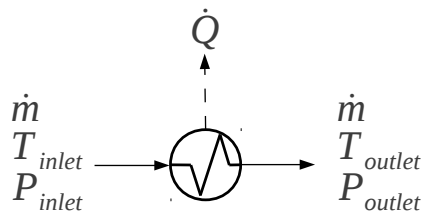
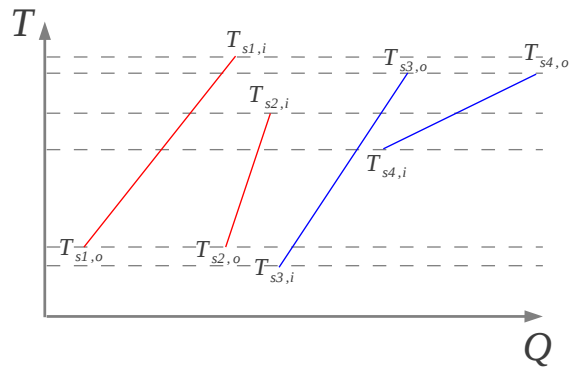


Figure 3.1: Heat exchange definition

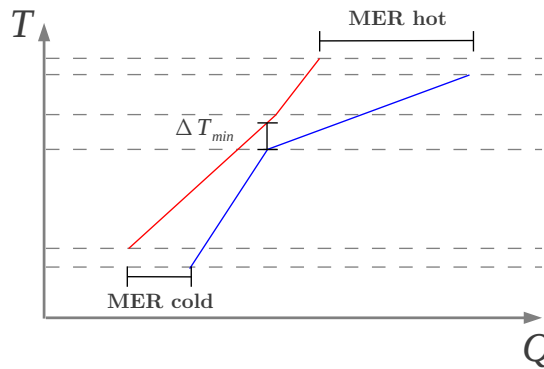
Streams are separated into two groups:

- Hot streams, which need to be cooled (in red in figure 3.2).
- Cold streams which need to be heated (in blue in figure 3.2).

They are characterized by their inlet and outlet temperatures and their heat load. Constant specific heat (c_p) is assumed. The example in figure 3.2(a) shows four streams, two hot and two cold ones. It should be noticed that they can be placed anywhere on the horizontal axis, since their heat load is given by an enthalpy difference, which is independent of the considered reference.



(a) Streams



(b) Composite curves

Figure 3.2: Composite curves construction

To obtain composite curve of figure 3.2(b), several steps are necessary.

1. Considering either hot or cold streams, the heat load of each streams is cumulated in each temperature range.
2. A $\Delta T_{min}/2$ is defined for each stream. So that ΔT_{min} in figure 3.2(b) is the sum of $\Delta T_{min,hot}/2$ and $\Delta T_{min,cold}/2$, for the hot and cold streams involved in the pinch. If ΔT_{min} of the system is bigger than the assigned value, the cold stream will have to be translated to the right (or the left for hot streams).
3. Based on the value of ΔT_{min} , the minimum energy requirement can be determined (for hot and cold utility). This energy is the minimum energy necessary for the process to be operated assuming that all thermodynami-

cally possible heat exchange are considered. In other words, it describes the case where most of the internal heat exchanges of the process are achieved.

Such a graphical approach is very useful since it allows to identify quickly what are the critical streams by locating the pinch points.

3.1.3 Uncertainties on heat streams

Pinch analysis can provide more or less detailed information on the system heat exchanges. As a reminder of section 2.1.2, the steps to design a heat exchanger network are:

- Determining the *MER* and computation of the necessary utilities to satisfy it.
- Heat load distribution to define streams involved in each heat exchange.
- Heat exchanger network synthesis to design the heat exchanger network.

One condition for applying moments method is that the objective function $f(u)$ shall be continuous and differentiable.

Several objectives like heat exchanger area or total investment cost can be computed by *HENS* and *HLD*. However, these methods are not continuous. This is due to the integer variables, for example, the minimum number of streams connections or restriction on heat exchanges [7]. Methods for flexible heat exchanger network have been developed [79, 22], but they are mainly based on scenario approach. Thus, they are difficult to use to propagate a continuous distribution function unless propagation is performed for each scenario, what takes too much computing time.

So, minimum energy requirement will be considered in this study. Assuming that it is possible to build an ideal, totally flexible heat exchanger network, *MER* becomes a good indicator of thermodynamic performance of the system. However, it should be analyzed carefully.

Figure 3.3 shows the influence of $T_{s4,i}$ variations, while all other heat loads and temperatures are kept constant (with the value they had in figure 3.2(b)). It shows the direct linear relationship between uncertainties and *MER*.

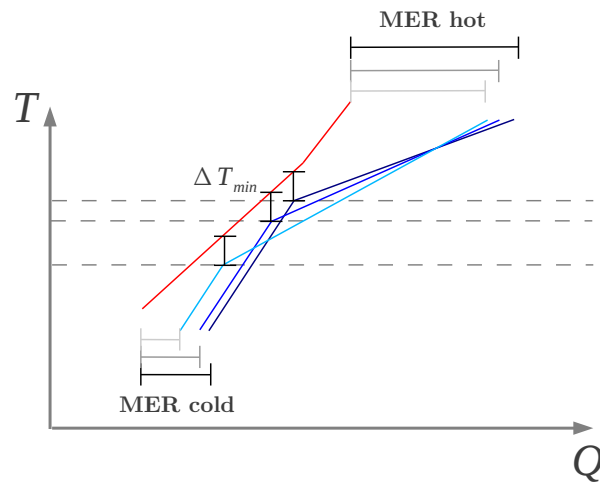


Figure 3.3: Composite curve under uncertain temperature

This is valid as well for ΔT_{min} , heat loads, and temperature variations under the conditions that pinch do not switch to other streams (figure 3.4).

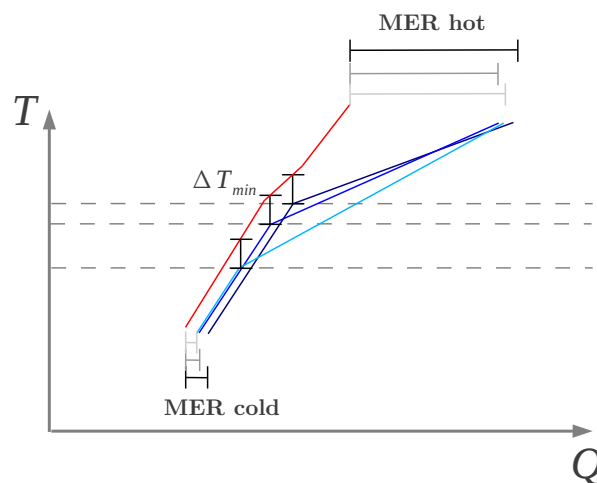


Figure 3.4: Influence of pinch

In such conditions, the function $MER = m(u)$ may become at least not differentiable, and even not monotonic.

In conclusion, MER is an indicator that can be propagated by moments methods

despite their changes due to the system uncertainties under the following conditions:

- There is no pinch point activation or deactivation due to the uncertain conditions in the neighborhood of the the studied solution.
- Activated pinch points always involve the same streams.

3.2 Fuel cell - gas turbine model

The system considered here is an innovative concept of fuel cell coupled with a gas turbine [23] as represented in figure 3.5. Such combination has already been studied [4, 5, 50]. However, pressurizing fuel cell is a crucial issue. The main interest of this system is that gas turbine system is compatible with fuel cell working at atmospheric pressure. Moreover, simulation allows to forecast better performances than other published results [23].

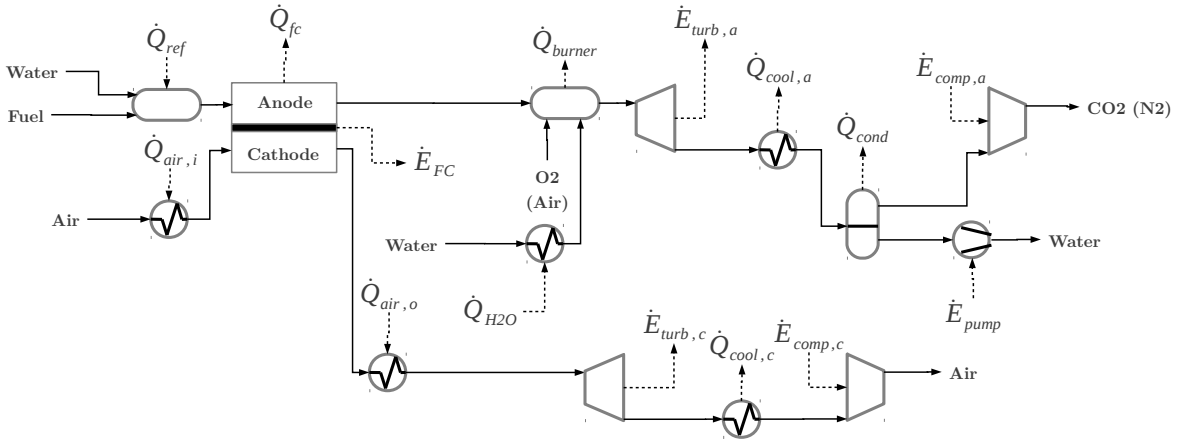


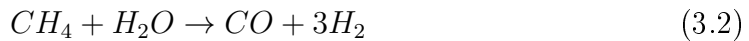
Figure 3.5: Global superstructure

Fuel is processed in the reformer by shift and steam reforming reactions.

Shift (-41 [kJ/mol]):



Steam reforming (+206 [kJ/mol]):



The resulting syngas composition is given by the reforming temperature, fixing the balance between the shift (exothermic) and the steam reforming (endothermic). The fuel cell considered is a solid oxide fuel cell (*SOF*C). One of its main characteristics is its high operating temperature. The cathode and anode outlet are injected into an inverted Brayton cycle, so that working fluid is expanded to sub atmospheric pressure before being compressed.

In the present case, pure oxygen has been considered for the post-combustion. It has been taken into account in the efficiency based on cryogenic air separation with a consumption of $\dot{E}_{O_2} = 1080 [kJ/kg_{O_2}]$ [41].

A constant power of 10 [kW] has been fixed for the total system, air and fuel flow rates being adapted to satisfy this condition.

Section 3.2.1 and 3.2.2 describe more in detail the fuel cell and gas turbine models. Decision and uncertain variables will be listed as well. Two uncertain variables concern both part of the system. They are the $\Delta T_{min}/2$ for liquid water (low) and for all other streams (high).

In system integration, $\Delta T_{min}/2$ shall be optimized to gives the best compromise between heat exchanger cost and utility needs [28]. However, in the present case, cost have not been estimated. Indeed, such system is still at the conception stage so that there is no relevant cost estimation available. Hence, $\Delta T_{min}/2$ has not been optimized but fix at the mean value given in table 3.1. It should be noticed that two different values have been considered. $\Delta T_{min,high}$ is used for heat exchange involving water condensation or evaporation, $\Delta T_{min,low}$ being considered for any other stream.

However non-constant c_p , uncertainty on heat transfer coefficient and all approximation related to a 1D steady state model leads to assuming an uncertain $\Delta T_{min}/2$. Its distribution and parameters are hard to quantify, since they are highly dependent on the studied case. Values assumed here are given in table 3.1.

Variable	Minimum	Mean	Maximum	Distribution
$\Delta T_{min,low}/2$	2	3	4	Uniform
$\Delta T_{min,high}/2$	3	5	7	Uniform

Table 3.1: $\Delta T_{min}/2$ distribution and parameters

The objectives used for optimization are:

- The efficiency ε given by:

$$\varepsilon = \frac{(\dot{m}_{ng,FC} + \dot{m}_{ng,boiler}) \cdot LHV_{ng} + \dot{E}_{O_2}}{\dot{E}_{FC} + \dot{E}_a + \dot{E}_c} \quad (3.3)$$

With $\dot{m}_{ng,FC}$ and $\dot{m}_{ng,boiler}$ the natural gas flow rate in the fuel cell and the possible additional boiler, LHV_{ng} the natural gas lower heating value and \dot{E}_{FC} the electricity production of fuel cell, respectively \dot{E}_a and \dot{E}_c for the anodic and cathodic inverted Brayton cycle.

- The anodic pressure ratio π_a . The cathodic one has not been chosen since it is less influent. Moreover, due to sub atmospheric conditions, high π_a reflect system complexity. Finally, they also imply greater volume and then so that pressure ratio is also an indication for investment cost.

3.2.1 Fuel cell

The figure 3.6 shows a scheme of fuel cell. This study is based on planar cells, but tubular design may be found. Oxygen (or air) enters in the cathode. Fuel is injected in the anode. *SOFCS* are usually fed with H_2 and CO , however, other fuels (like CH_4) may be used indirectly, by adding first a fuel processing step. So residual fuel, H_2 , CO , water and carbon dioxide may be found at the fuel cell inlet. Both electrode are electronically conductive, whereas electrolyte is an ion conductive membrane. It results from this that chemical potential difference between anode and cathode drives oxygen ion through the electrolyte. This behaviour is a great advantage of fuel cell since it allows to convert chemical energy into electrical energy without passing by thermal and mechanical energy.

Size of each layer in figure 3.6 are not scaled since thickness of each component may vary depending on the element chosen as mechanical support (leading to so-called anode- cathode- or electrolyte-supported fuel cell). Interconnect design is a great challenge which goal is to optimize oxidant and fuel distribution and avoid pollutant deposition.

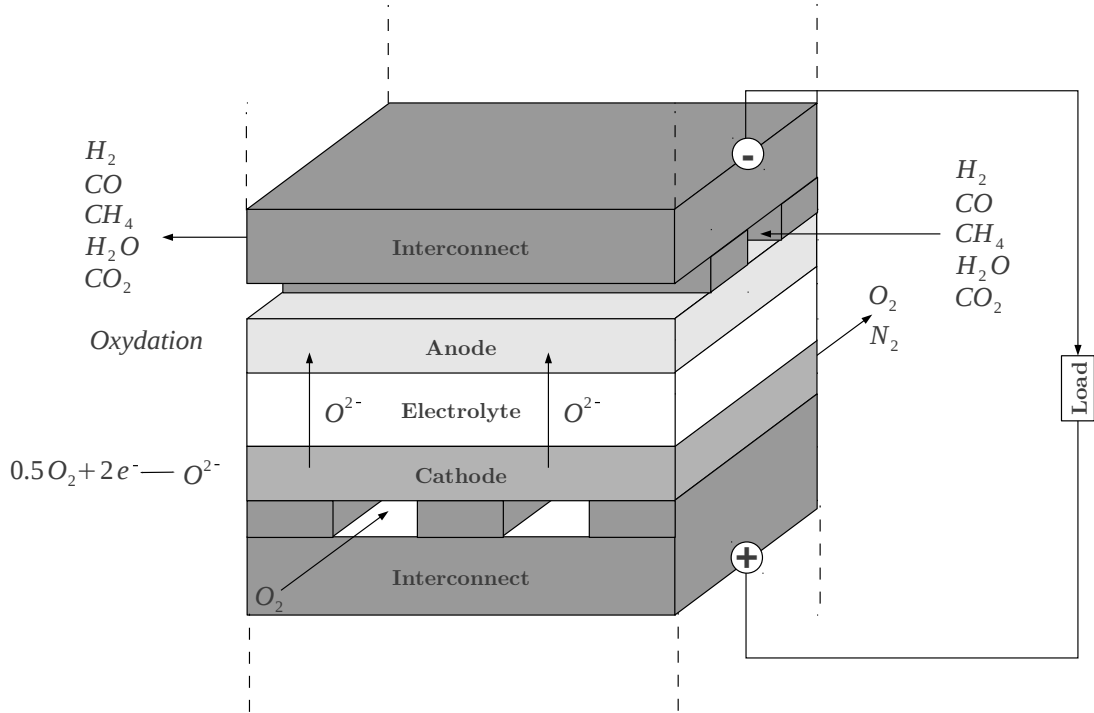


Figure 3.6: Fuel cell scheme

Such cells are mounted in series to form a stack so that the number of cells influence the tension, not the current.

Model used for the fuel cell has been developed in [82]. The power produced by the fuel cell is:

$$\begin{aligned} \dot{E}_{FC} &= -\Delta\dot{G}_{tot} - R_{tot}I^2 - (\eta_a + \eta_c + \eta_{diff,a} + \eta_{diff,c})n_{cells}I \\ I &= i \cdot A = \frac{\dot{n}_{O_2,membrane}4F}{n_{cells}} \end{aligned} \quad (3.4)$$

Where I is the current, i the current density, A the cell area, n_{cells} the number of cells, $\dot{n}_{O_2,membrane}$ the amount of pair of oxygen ion passing through the electrolyte and F the Faraday constant. In the current case, area is considered constant (200 [cm²]) whereas the number of cells is adapted to define the optimal design. It has been treated as a continuous variable. It may have been relevant to consider a fix number of cells and a varying area, but it would not have been possible to compare the results with previous work [23].

The available Gibbs free energy is given by:

$$\Delta\dot{G}_{tot} = (\dot{G}_{c,out} + \dot{G}_{a,out}) - (\dot{G}_{c,in} + \dot{G}_{a,in}) \quad (3.5)$$

The losses are induced by resistance (electric and ionic), and by kinetics of the reaction. They are separated in two groups: the ohmic losses (proportional to I^2) and non-ohmic losses proportional to I . This is the reason why fuel cells are not operated at 100 [%] of fuel utilization. Indeed, in such conditions (with high current density), ohmic losses become too important. The ohmic losses R_{tot} is composed by the interconnect and electrolyte resistive loss:

$$\begin{aligned} R_{tot} &= R_i + R_e \\ R_i &= n_{cells} \cdot \frac{R_{i,a} + R_{i,c}}{A} \\ R_e &= f_{CC} n_{cells} \cdot \frac{L_e}{\sigma_e A} \\ \sigma_e &= \sigma_{0,e} e^{\left(-\frac{E_{A,e}}{R \cdot T_{FC}} \right)} \end{aligned} \quad (3.6)$$

With $E_{A,e}$ the electrolyte activation energy, T_{FC} the fuel cell temperature and f_{CC} being an adjustment factor. Butler Volmer overpotentials η_a and η_c can be found by solving the equation 3.7:

$$\begin{aligned} i &= i_{0,c} \cdot \left(e^{\left(\frac{\eta_c}{2 \cdot R \cdot T_{FC}} \right)} - e^{-\left(\frac{\eta_c}{2 \cdot R \cdot T_{FC}} \right)} \right) \\ i &= i_{0,a} \cdot \left(e^{\left(\frac{\eta_a}{R \cdot T_{FC}} \right)} - e^{-\left(\frac{\eta_a}{R \cdot T_{FC}} \right)} \right) \end{aligned} \quad (3.7)$$

Where:

$$\begin{aligned} i_{0,c} &= \frac{\sigma_c 2 \cdot R \cdot T_{FC}}{F} \\ \sigma_c &= \sigma_{0,c} e^{\left(-\frac{E_{A,c}}{R \cdot T_{FC}} \right)} \end{aligned} \quad (3.8)$$

Respectively:

$$i_{0,a} = \frac{\sigma_a 2 \cdot R \cdot T_{FC}}{3F} - \left(\frac{E_{A,a}}{R \cdot T_{FC}} \right) \quad (3.9)$$

$$\sigma_a = \sigma_{0,a} e$$

Polarization losses $\eta_{diff,a}$ and $\eta_{diff,c}$ is given by:

$$\eta_{diff,a} = - \frac{R \cdot T_{FC}}{2F} \cdot \log(1 - fu)$$

$$\eta_{diff,c} = - \frac{R \cdot T_{FC}}{2F} \cdot \log\left(1 - \frac{fu}{\lambda}\right) \quad (3.10)$$

Considered decision variables for the fuel cell are:

Variable	Minimum	Maximum	Unit
$\xi_{H_2O,c}$	0.7	3.5	[-]
T_{ref}	973.15	1073.15	[K]
T_{FC}	973.15	1073.15	[K]
λ	2	10	[-]
fu	0.7	0.8	[-]
i	0.3	0.5	[A/cm ²]

Table 3.2: Fuel cell decision variables

With:

- $\xi_{H_2O,c}$ being the steam to carbon ratio in the reformer.
- T_{ref} the reformer temperature.
- $\lambda = \frac{\dot{n}_{in,c,O_2}}{\dot{n}_{in,c,O_2} - \dot{n}_{out,c,O_2}}$ defining the air usage of the fuel cell.
- $fu = \frac{\dot{n}_{fuel,FC,in} - \dot{n}_{fuel,FC,out}}{\dot{n}_{fuel,FC,in}}$ the fuel utilization.

Based on this model, uncertain variables considered are the activation energy E_A , the conductance proportional factor σ_0 , and the interconnect resistive losses $R_{i,a}$

and $R_{i,c}$. They have been calibrated on data provided by SOFCpower¹. It is a company manufacturing high temperature cells for *SOFC*. They perform tests on 500 clusters of 6 cells each. For each cluster, average tension has been measured for 3 different fuel utilization. These statistics have not been carried out especially for this study, so that every measurements have been taken in the same conditions (see table 3.3). A better approach would be to consider a design of experiment approach [14], allowing to determine each uncertain variable influence.

It should be noticed that fuel cells performance is highly depending on their design. However, models used here are not enough detailed to include cell geometry and have been fitted on other cells. So, despite average performance differs between statistics and the present model, the purpose here is to adjust model's variance to measurements variance. This is done by successive Monte-Carlo simulation, changing boundary of each uncertain variables until the same order of magnitude can be reached.

Variable	Value	Unit
T_{FC}	1023.15	[K]
Fuel composition	0.6 H_2 0.4 N_2	[–] [–]
Fuel flow rate	1.5	[Nl/min]
Cathodic air flow rate	15	[Nl/min]

Table 3.3: Fuel cell test conditions

Fuel cells are characterized by their current-tension curve (figure 3.7). The three fuel utilization and corresponding current are:

- *OCV*, or open current voltage.
- 60 % fuel utilization, meaning 0.43 [A/cm^2]
- 75 % fuel utilization, meaning 0.54 [A/cm^2]

The box plot in figure 3.7 represent the following values. The red line is the median. The blue box defines the 25 % and 75 % boundary. Black segments shows extreme values, and red cross are the outliers.

¹<http://www.sofcpower.com/>

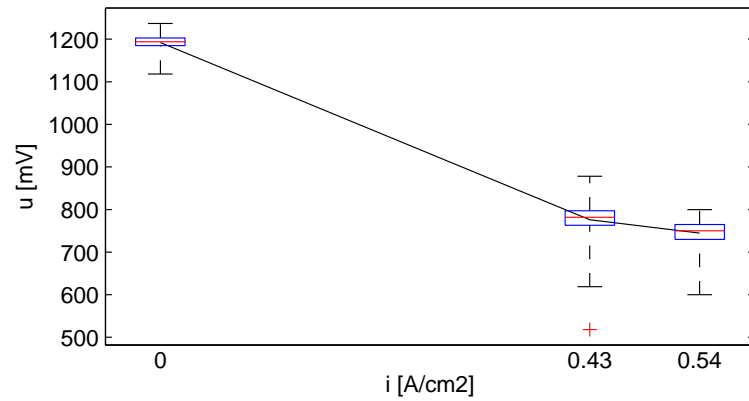


Figure 3.7: Statistics on *SOFC* characterization

It can be noticed that statistics for 60 and 75 [%] fuel utilization are similar. *OCV* has not been considered due to model instability close to *fu* boundaries. Figure 3.8 shows an histogram of the first case statistics. Its asymmetry appears clearly.

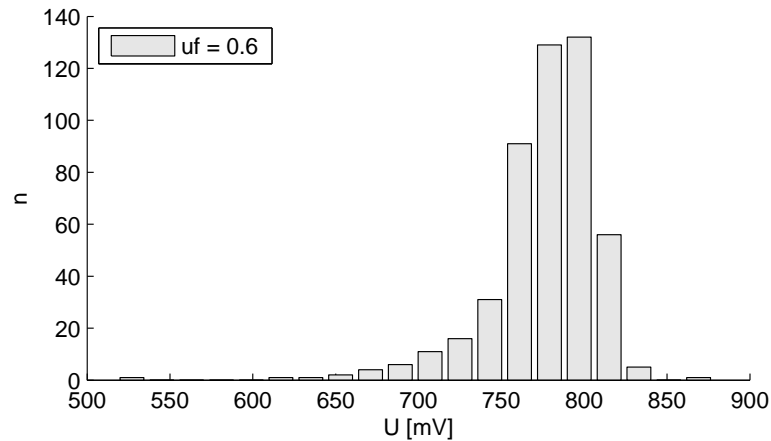


Figure 3.8: Current-Tension statistics for 60 % fuel utilization

Table 3.4 compares statistics estimators of *SOFC* power data and Monte-Carlo simulation on studied models.

Parameter	Experimental data	Modeled uncertainties
Variance σ^2	2317	2284
Lower deviation $\mu - U_{min}$	258	170
Upper deviation U_{max}	101	75

Table 3.4: Statistics comparison

So that probability distribution considered for each uncertain variables is given in table 3.5 and 3.6.

Variable	Units	Minimum	Mode	Maximum	a	b
$E_{A,c}$	[J/mol]	82988	$1.012 \cdot 10^5$	$1.082 \cdot 10^5$	6	2.9444
$\sigma_{0,c}$	[S/cm]	7.2472	8.602	9.5482	6	4.4921
$E_{A,a}$	[J/mol]	94340	$1.06 \cdot 10^5$	$1.227 \cdot 10^5$	2	2.4318
$\sigma_{0,a}$	[S/cm]	$3.6483 \cdot 10^5$	$4.3303 \cdot 10^5$	$4.8066 \cdot 10^5$	6	4.4921
$E_{A,e}$	[J/mol]	70786	79535	92062	2	2.4318
$\sigma_{0,e}$	[S/cm]	313.69	372.33	413.29	6	4.4921
$R_{i,a}$	[Ω]	0.0178	0.02	0.02315	2	2.4318
$R_{i,c}$	[Ω]	0.0267	0.03	0.034725	2	2.4318

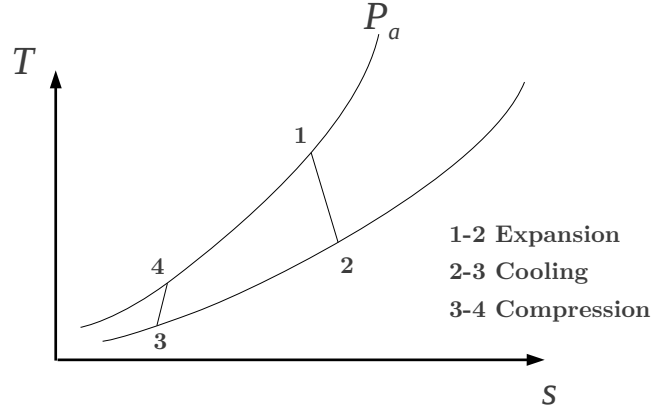
Table 3.5: Fuel cell uncertain variables (beta distribution, a and b parameters)

Variable	Minimum	Maximum
f_{cc}	3	5

Table 3.6: Fuel cell uncertain variable (uniform distribution)

3.2.2 Gas turbine

For hybrid systems, fuel cell is usually operated at high pressure by compressing air and fuel inlet in order to burn and expand hot exhaust gases [5, 19]. Here, an inverted Brayton cycle has been considered [81]. In this configuration, fuel cell is operated at atmospheric conditions as in a standalone case. Difference lies in the fact that the outlet stream of the burner is directly expanded to sub-atmospheric pressure, cooled and compressed afterwards.

Figure 3.9: $T - s$ diagram of an inverted Brayton cycle

The model includes two cycles, expanding anode and cathode outlet. In the first case, heat is provided by burning the residual fuel in a post-combustion. Anodic turbine inlet temperature is limited to 1573 [K] (assumed ceramic turbine tolerance). To achieve this, an optional heat exchanger is considered to avoid turbine damaging. In the second case, depleted air is heated before being expanded, energy integration determining if hot utility is necessary. Table 3.7 shows decision variables for the gas turbine part of the model.

Variable	Minimum	Maximum	Unit
$T_{in,turb,c}$	1073.15	1573.15	[K]
$T_{in,burner,H_2O}$	374.15	973.15	[K]
$T_{in,comp,a}$	298.15	343.15	[K]
$T_{in,comp,c}$	298.15	343.15	[K]
π_a	2.5	10	[-]
π_c	2.5	10	[-]
$\xi_{H_2O/a,out}$	0	2	[-]

Table 3.7: Anodic and cathodic gas turbine

With:

- $\xi_{H_2O/a,out} = \frac{\dot{M}_{H_2O,in,burner}}{\dot{M}_{a,out}}$ defining the amount of water injected in the burner.

Here, turbomachinery efficiency have been considered uncertain. Same efficiency have been considered for turbine and compressor, for the anodic cycle as well as the cathodic one.

Variable	Minimum	Mode	Maximum	a	b
$\varepsilon_T, \varepsilon_C$	0.79	0.85	0.86	6	1.83

Table 3.8: Gas turbines uncertain variables (beta distribution, a and b parameters)

3.3 Conclusion

The resolution sequence used in this study has been detailed in chapter 2. Here, a particular attention has been paid on energy integration.

First, its advantage and drawbacks has been discussed and compared with a flow-sheeting approach. Energy integration has been chosen here since it is well adapted to an optimization solver needing a lot of iterations. Indeed, it allows to estimate heat exchanges in an efficient manner without simulating the network in depth.

Then, main issues about energy integration under uncertain streams and ΔT_{min} has been exposed. It shows that it is difficult to propagate uncertainties through heat load distribution or heat exchanger network synthesis. It would be possible by considering a scenario approach, but this would highly increase the computational resource needed. However, MER remains relevant in such method, considering that it is piecewise differentiable. Hence, the solutions of the Pareto curve close to pinch activation may not be considered but uncertainties can be propagated in all other cases.

The application case used here is a solid oxide fuel cell coupled with gas turbines. The proposed configuration is an innovative system allowing to operate fuel cells at atmospheric pressure with a directly integrated gas turbine. The fuel cell model has been built based on experimental data.

Boundaries for decision variables as well as probability density function for uncertain variables have been described.

Chapter 4

Optimization results

The standard optimization results will be presented here. They will be compared in chapter 5 and 6 to stochastic programming and moments method. So only the useful results will be commented here. Further informations can be found in [23].

4.1 Hybrid fuel cell optimization

Results presented in this section have already been published in [23]. However, optimization have been reconducted for several reasons. First one is to ensure reproducibility of the results. Indeed, due to some small differences concerning model assumptions and decision variables range, results may slightly differ, remaining in the same order of magnitude. Secondly, the main optimization results are presented here to be compared with stochastic programming and moments method results.

Objectives considered for the fuel cell optimization are the system first law efficiency ε and the anodic pressure ratio π_a . Among all the issues related to the development of such technology, dealing with sub-atmospheric pressure between turbine and compressor is a great challenge, for anodic as well as for cathodic side. Anodic has been chosen since it is more decisive with respect to pinch analysis as it will be described in this chapter. It should be noticed that it is a decision variable.

Results are presented in figure 4.1 as a Pareto front. System efficiency (based on lower heating value) varies from 82.5 to 83.4 [%] and π_a between 2.5 and 4.8 [—].

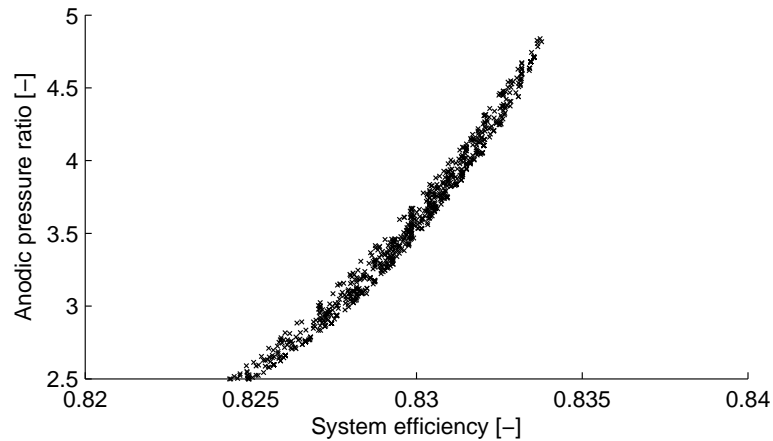


Figure 4.1: Optimal Pareto front for *SOFC* model

4.1.1 Fuel cell decision variables for standard optimization

Fuel utilization is optimal for 0.8 [-] whereas current density is maintained at its minimum limits: $0.3 [A/cm^2]$. Fuel cell temperature is also optimal for its upper boundary, at $1073 [K]$. Steam to carbon ratio is increasing from 1.29 to 1.34 [-].

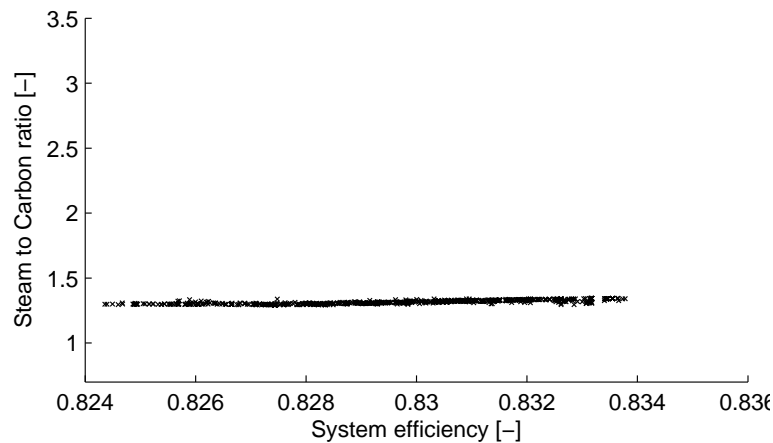


Figure 4.2: Steam to carbon ratio

This is due to the fact that π_a increasing. A higher H_2 content in fuel imply greater flow rate through the turbine. in addition, more water is condensed between anodic turbine and compressor, what takes part of the fact that pumping

water consumes less energy. So, compressor consumption increases less than it would have been for a constant steam to carbon ratio.

Steam reforming temperature is decreasing from 1073 [K] to 1068 [K].

Air factor is decreasing as well from 3.30 to 2.94 [-], since hydrogen combustion requires less oxygen.

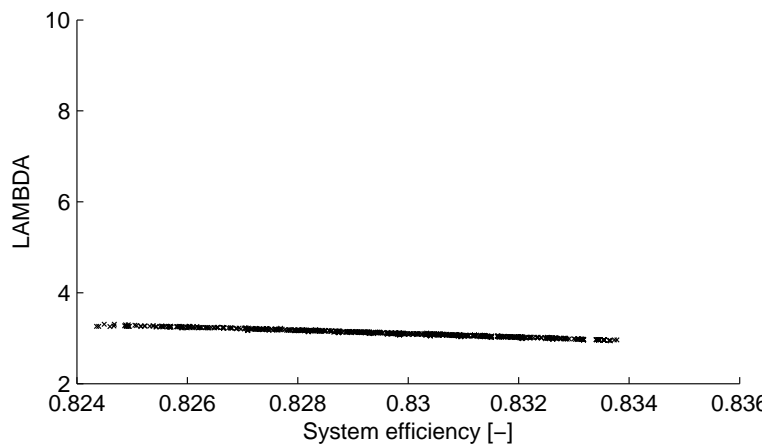


Figure 4.3: Air factor λ

4.1.2 Gas turbine decision variables for standard optimization

A small increase can be increase can be observed for π_c from 3 to 3.1 [-].

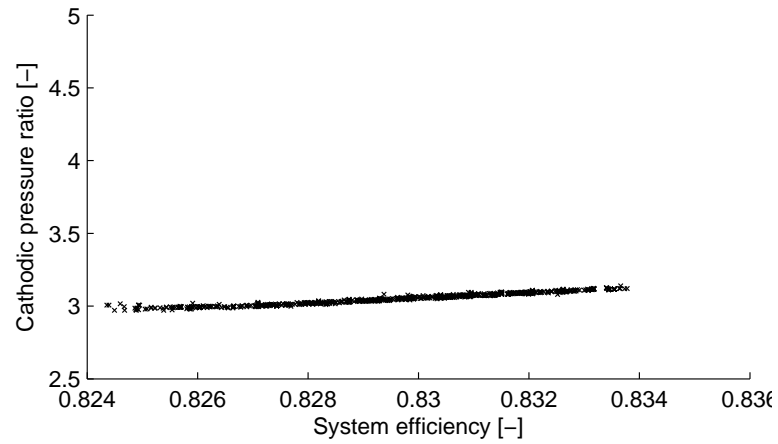


Figure 4.4: Optimal cathodic pressure ratio

However, decrease of cathodic turbine inlet temperature from 1307 to 1311 [K] together with the decrease of air factor justify decrease in cathodic compressor and turbine specific power (respectively from 17 [%] to 15.5 [%] and from 40 [%] to 36 [%]).

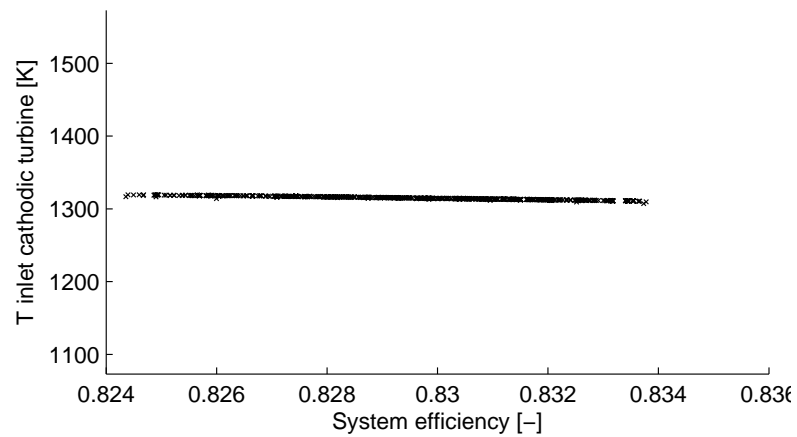


Figure 4.5: Cathodic turbine inlet temperature

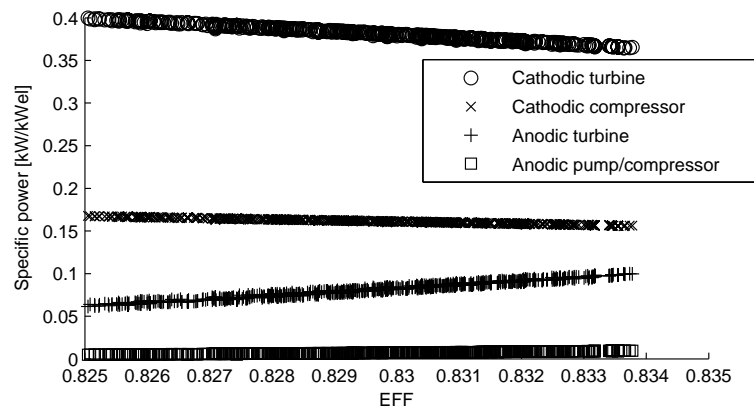


Figure 4.6: Gas turbines and compressors specific power

Both of the anodic and cathodic compressors inlet temperatures are constant at 299 [K].

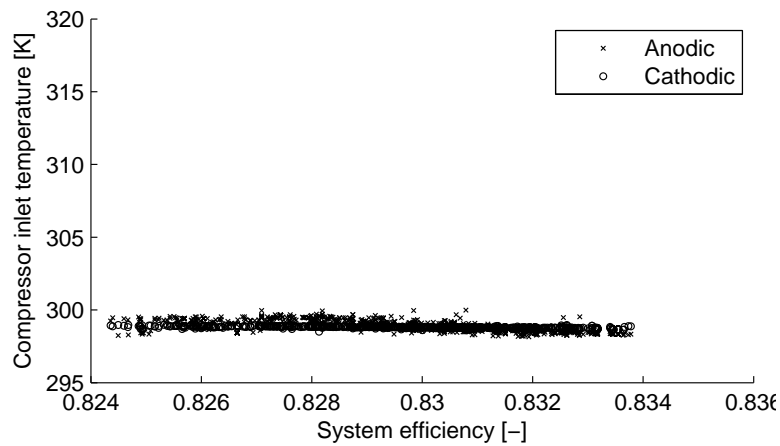


Figure 4.7: Anodic and cathodic compressors inlet temperature

Finally, it can be observed that water excess is a solution that never appears in the optimal Pareto curve. Optimal solution won't be more detailed here since more informations can be found in [23].

4.2 Pinch analysis

The point *A* in figure 4.8 will be studied here more in detail. It is characterized by an efficiency of 83.0 [%] and a pressure ratio of 3.50 [-].

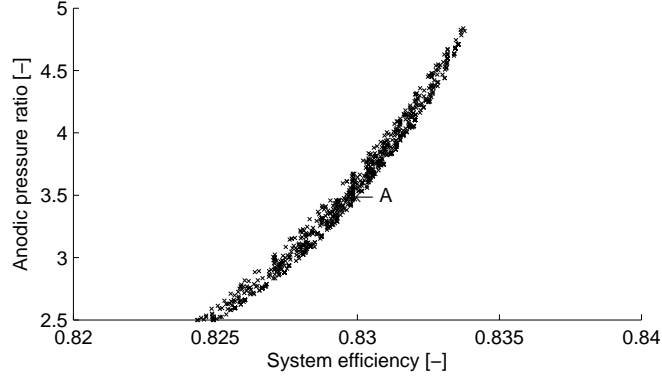


Figure 4.8: Sankey diagram

Its corresponding decision variables are given in 4.1.

Variable	Value	Unit
$\xi_{H_2O,c}$	1.31	[-]
T_{ref}	1070	[K]
T_{FC}	1073	[K]
λ	3.1	[-]
fu	0.8	[-]
i	0.3	[A/cm ²]
$T_{in,turb,c}$	1314	[K]
$T_{in,burner,H_2O}$	—	[K]
$T_{in,comp,a}$	299	[K]
$T_{in,comp,c}$	299	[K]
π_a	3.5	[-]
π_c	3	[-]
$\xi_{H_2O/a,out}$	0	[-]

Table 4.1: Fuel cell decision variables for point *A* in figure 4.8

One of the reason for such good efficiency of the system presented here is almost thermally self sufficient (what may already be achieved for *SOFC* in a stand alone

usage [83]). As it can be seen in Sankey diagram presented in figure 4.9, the order of magnitude of the hot utility is 0.1 [%] of the total energy consumption. This diagram has been computed based on decision variables presented in figure 4.1.

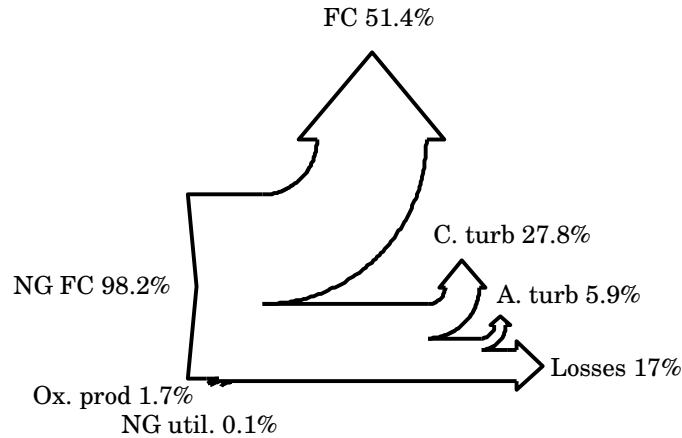


Figure 4.9: Sankey diagram

This means that heat sources (mainly reforming, fuel cell itself and post-combustion) covers a great amount of heat needs as it can be seen in figure 4.10.

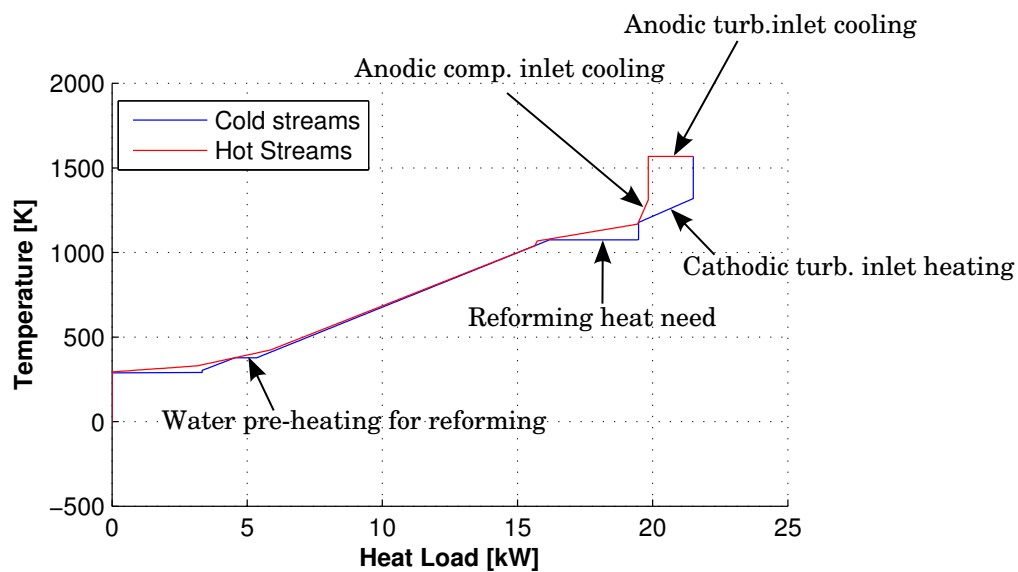


Figure 4.10: Composite curve (corrected temperatures)

Four pinch points can be noticed:

- A first one is due to the heat sink of the cathodic inverted Brayton cycle. It is limited by the heat stream provided by cooling of exhaust gases before anodic compressor.
- A second pinch is related to the plateau of the assumed perfectly auto-thermal reforming.
- The third pinch is just below the second one and is created by the cathodic compressor inlet cooling.
- The fourth pinch occurring at the lowest temperature is due to the evaporation of water during the pre-heating before the reforming.

This observation can be extended to every optimal solutions. Figure 4.11 shows the hot utilities specific power $\dot{Q}_{hot,spec}$ for each point of the Pareto front.

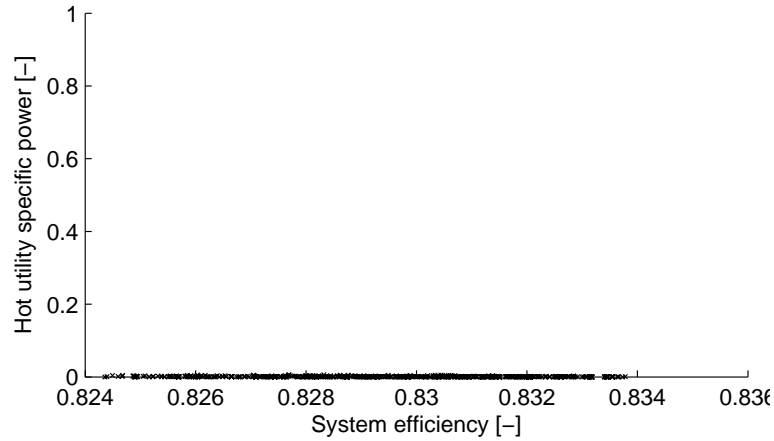


Figure 4.11: Hot utilities specific power for the whole Pareto front

It can be seen that $0 < \dot{Q}_{hot,spec} < 0.05$. This means that optimal solution are defined by the limit of pinch activation without additional heat supply. It should be noticed that in the next chapters, this optimization will be called *standard* optimization.

4.3 Conclusion

The optimization of the model presented in chapter 3 has been performed, using an evolutionary algorithm. It leads to an efficiency varying from 82.5 to 83.4 [%] and pressure ratio π_a between 2.5 and 4.8 [-]. The results for decision variables

have been briefly explained. It has been demonstrated that optimization leads to activation of four pinch points, maximizing heat recovery and avoiding hot utilities need.

Chapter 5

Stochastic programming results

The results of stochastic programming will be presented here. Its Pareto front will be compared to standard optimization results.

The representativity of uncertain variables samples will be demonstrated. The link with two stages programming and variables classification will be established.

Decision variables optimal results will be exposed. One pinch points will be chosen and its streams variation due to uncertain parameters will be detailed.

Finally, the concept of optimality of stochastic or standard approach will be discussed with respect to mean and mode value of uncertain variables.

5.1 Standard and stochastic optimization

The optimization results are reported in figure 5.1. The blue points are the Pareto obtained by standard optimization (uncertain variables considered at their mode), as shown in figure 4.1. It is the limit of the feasible domain for fixed uncertain variables.

Green points are the results of stochastic programming. The uncertain variables have the value they had during optimization procedure. This values are those randomly generated following the algorithm described in figure 2.15. This explains why some green points present better performances than blue Pareto curve. Indeed, depending on the generated set of uncertain variables, the limit of the feasible can be pushed further. For example, if the value drawn for a turbine efficiency is better than its mode, the total system efficiency may reach higher value than the blue limit.

Finally, all green points have been recomputed considering same decision variables, but using uncertain variables at their mode, which is the one considered during standard optimization. This results is given in red in figure 5.1. In opposition to green points, it can be observed that they are all contains backward the blue

points. If it were not the case, it would have meant that standard optimization has not converged and that some additional generations are needed.

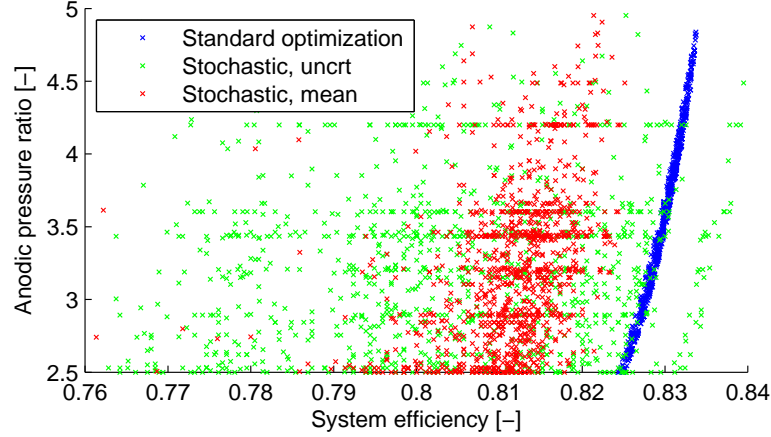


Figure 5.1: Pareto for standard, stochastic with uncertain variables and stochastic with uncertainties at the mode

In standard optimization of section 4, $6 \cdot 10^4$ model evaluations have been used. It appears that $2 \cdot 10^4$ would have been sufficient since no significant improvement of the Pareto curve can be observed for the last generations. For stochastic optimization, $7 \cdot 10^4$ iterations have been considered. Optimization convergence can not be estimated by Pareto curve progression in that case due to uncertain variables effect. However, it will be demonstrated in the next section that it is a sufficient number of model evaluations to explore the whole uncertain variables space.

5.2 Uncertainty representativity

Heuristic optimization algorithm have more chance than gradient based one to find global optima, but the price to pay is a great number of function evaluation. However, this may become an advantage for the stochastic programming approach described in section 2.3.4. But the assumption of a sufficient number of individuals shall be verified so that representativity of the uncertainties space is ensured. Indeed, the total population size is choose by the user since there is no stopping criteria [53].

It must be noticed that the total number of individuals gathering all generations n_{ind} differs from the number of uncertain variables sample n_{us} . This is due to the

fact that some parents from one generation may be kept alive in the next generation. In such cases, uncertain variables generated initially for the parents are not redrawn. This is mainly related to traceability and reproducibility reason. In this example, the cumulation of every generation represent a total population of 85211 individuals, but only 65625 are uniques.

In the following figures, the cumulative distribution function of the original distribution is represented in solid line. The crosses are the cumulative statistics of uncertain variables randomly drawn during optimization, with respect to equation 5.1. For a sample $u_1, \dots, u_{n_{us}}$

$$c(u_i) = \frac{\sum_{i=1}^i u_i}{\sum_{i=1}^{n_{us}} u_i} \quad (5.1)$$

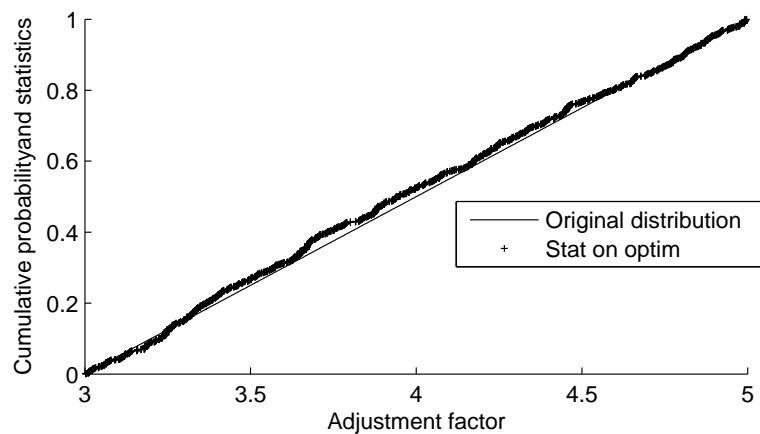


Figure 5.2: Adjustment factor *cdf* and statistics

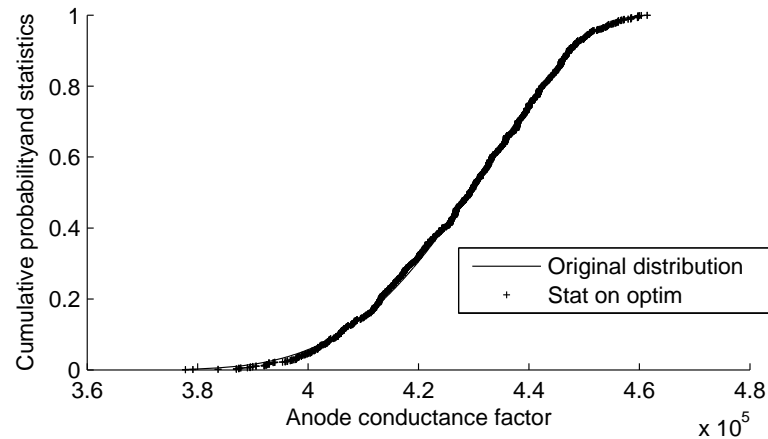


Figure 5.3: Anodic conductance factor *cdf* and statistics

As it can be seen in figure 5.2 and 5.3, statistics fits with the theoretical *cdf*, independently of the type of distribution (respectively uniform and beta in these cases). The cathode activation energy $E_{a,c}$, cathode conductance factor $\sigma_{0,c}$, the electrolyte conductance factor $\sigma_{0,2}$ and high and low $\Delta T_{min}/2$ are well represented too (results are given in appendix B).

Selection procedure of the solver (described in section 2.2.2) plays a critical role. Due to random behaviour of the stochastic programming approach, it may happen that a set of uncertain variables leading to bad performances is compensated by an appropriate set of decision variables. For example, if uncertain variables lead to a good efficiency for fuel cell, but a bad efficiency for the gas turbines, this may be compensated by increasing the fuel utilization. In such cases, individual is kept “alive“. But uncertain variables leading to sub optimal objectives for any decision variables will be systematically “killed”.

For example, the anodic activation energy $E_{a,a}$ selection will be detailed. Figures 5.4 shows a comparison between theoretical cumulative distribution function and the statistics on alive individuals based on equation 5.1.

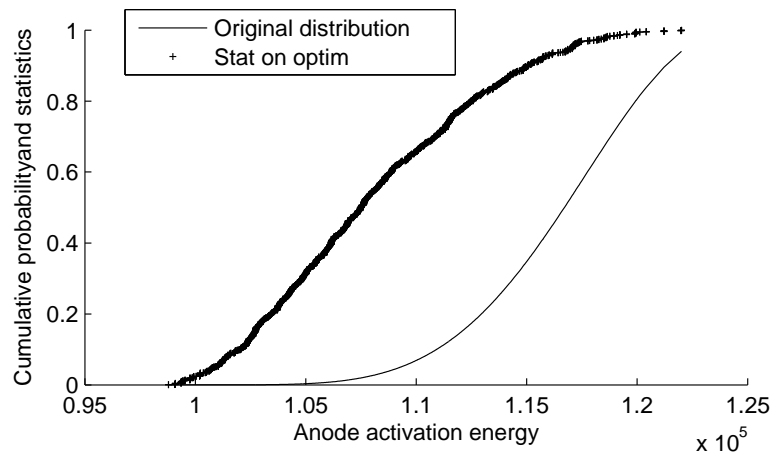


Figure 5.4: Anodic activation energy theoretical *cdf* and statistics on alive population

It can be seen that statistics is biased. Figure 5.5 shows the theoretical probability distribution function with the minimum and maximum alive individuals.

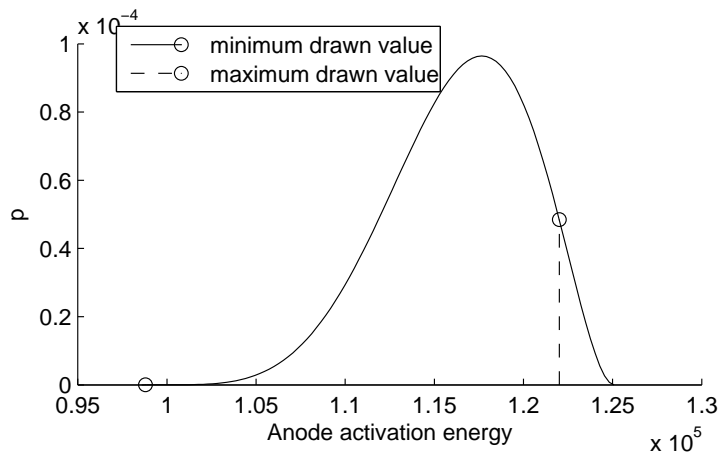


Figure 5.5: Maximum and minimum drawn and alive values

It can be seen that activation energy higher than $1.22 \cdot 10^5$ [*J/mol*] do not allow performance good enough. It shall be expressed as physical characteristics as maximum grain size, homogeneity, cell geometric design, but this is beyond the scope of this study.

At this step, it is important to consider conclusion in three different spaces:

- The objectives space: The decision maker can fix a maximum tolerated performances deviation by adjusting selection parameters of the solver. Indeed, the *DM* may choose to stop system operation in case of too low performances.
- The uncertain variables space: The more influent uncertain variables will be identified, and their extreme values with respect to the lowest performances accepted by the decision maker. One of the advantage of this approach, is that it fits for non-monotonic objectives function $f(u)$.
- The decision variables space: As a result from the previous point, the optimal decision variables do not take into account “killed” values for uncertain variables. This is due to the fact that decision variables shall be optimal only for the acceptable performances deviation, since the system will not be operated in other cases.

Other uncertain variables concerned are the electrolyte activation energy $E_{A,e}$, both anodic and cathodic interconnect resistance $R_{i,a}$ and $R_{i,c}$ and the efficiency of the turbomachinery ε_T and ε_C (figure 5.7,5.8, 5.9, 5.10 and 5.11). There may be multiple reasons why this parameters are concerned and not others. For $E_{A,a}$, its wide range induce the highest variation of efficiency (as well as $E_{A,e}$). Figure 5.6 shows a sensitivity analysis on anodic activation energy.

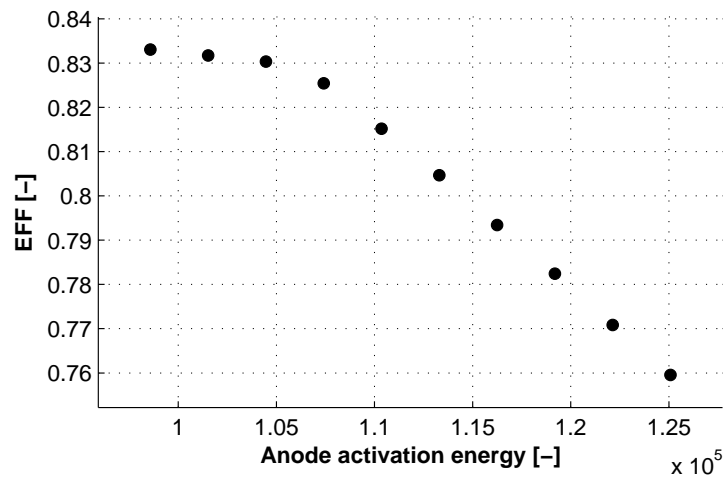


Figure 5.6: Sensitivity analysis on anode activation energy

It has been computed with all other uncertain variables at their mode, and the decision variables given in table 4.1.

Another important factor is the independence of uncertain variables. Indeed, the more dependent they are, the more chance there is that other drawn variables compensate their effect on performances. Table 5.1 summarize the maximum and minimum drawn values for each uncertain variables.

Variable	Minimum drawn	Maximum drawn	Units
$E_{A,c}$	88310	$1.0762 \cdot 10^5$	[J/mol]
$\sigma_{0,c}$	7.4644	9.1707	[S/cm]
$E_{A,a}$	98789	$1.2201 \cdot 10^5$	[J/mol]
$\sigma_{0,a}$	$3.7781e + 05$	$4.6142e + 05$	[S/cm]
$E_{A,e}$	74104	92590	[J/mol]
$\sigma_{0,e}$	321.4	395.35	[S/cm]
$R_{i,a}$	0.01867	0.022861	[Ω]
$R_{i,c}$	0.027951	0.034557	[Ω]
f_{CC}	3.003	4.9967	[—]
ε_T	0.81162	0.85964	[—]
ε_C	0.80818	0.85955	[—]
$\Delta T_{min}/2_1$	2.0012	3.9977	[K]
$\Delta T_{min}/2_2$	3.0026	6.9902	[K]

Table 5.1: Boundaries of drawn uncertain variables

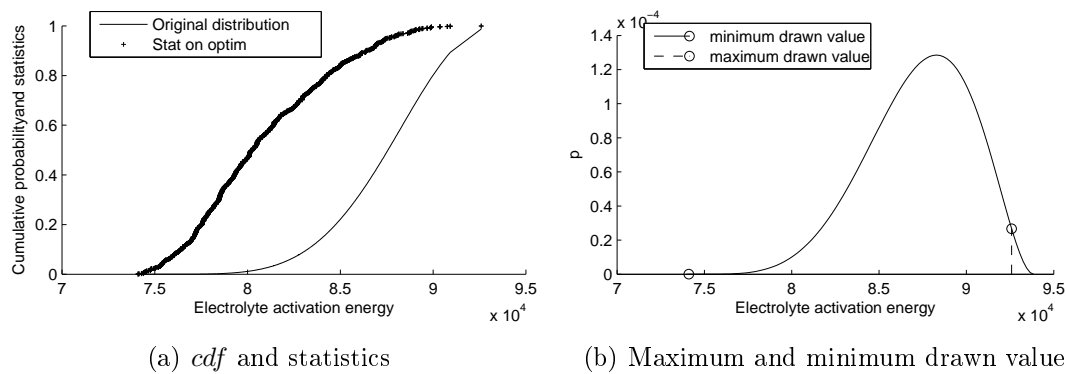


Figure 5.7: Electrolyte activation energy

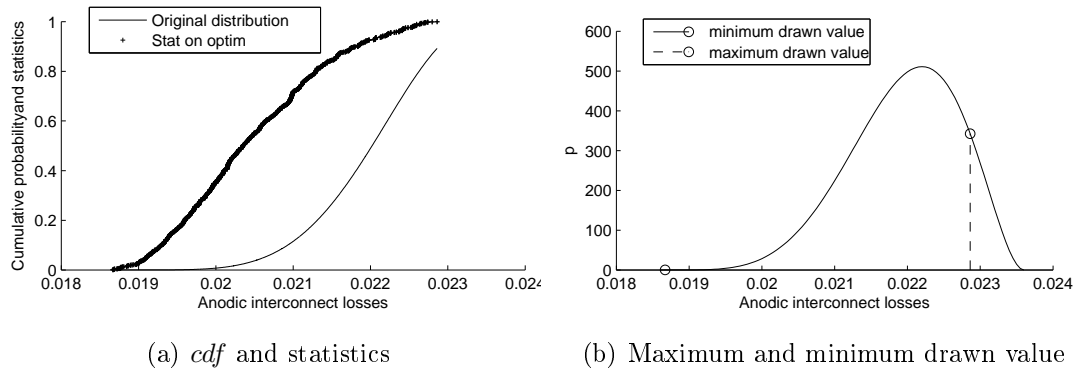


Figure 5.8: Anodic interconnect losses

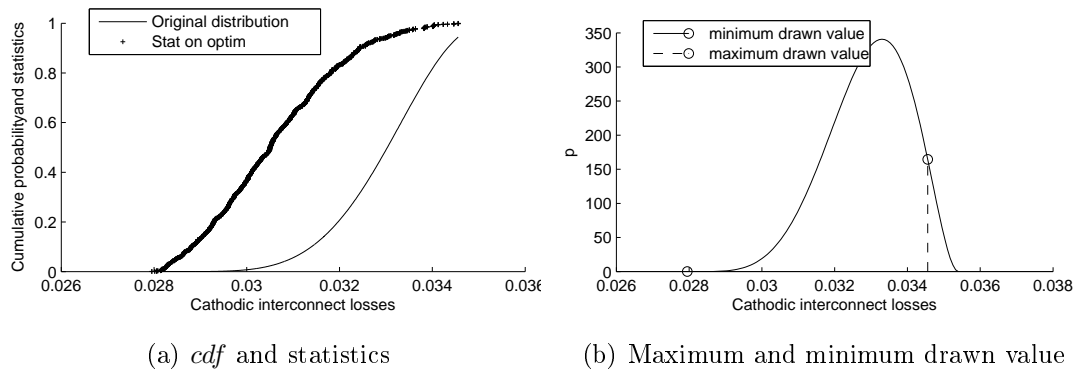


Figure 5.9: Cathodic interconnect losses

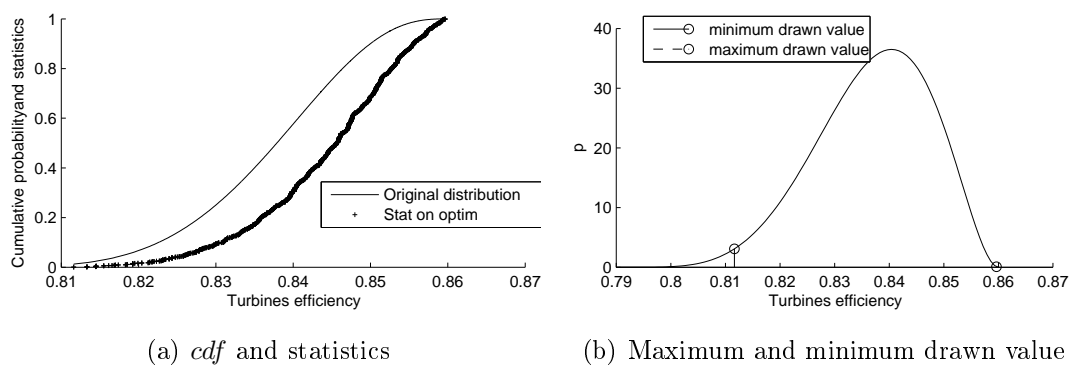


Figure 5.10: Anodic and cathodic gas turbines efficiency

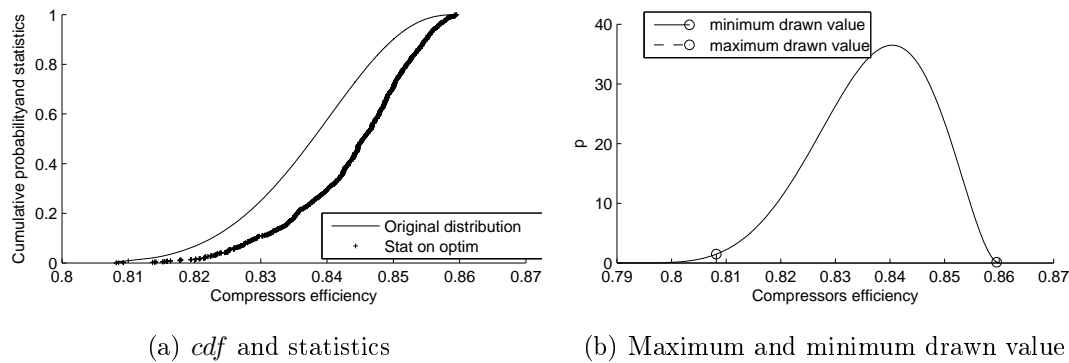


Figure 5.11: Anodic and cathodic gas compressors efficiency

5.3 Decision under uncertainty

As described in figure 4.10, four pinch points can be observed in the results of standard optimization. Here, the higher temperature pinch point will be studied here more in detail. It has been chosen since it implies less streams than the others, so that they can be easily identified. It is schematically represented in figure 5.12. It must be noticed that, to improve readability, this composite curve is not scaled.

First, the heat loads of this streams will be assumed constant. Dotted lines represent the value of the stream during the standard optimization, respecting the color code of blue for cold streams and red for hot streams. The streams resulting from the stochastic optimization are drawn in full lines. Each temperature is indicated as T_i/T_j , T_i being temperature from the stochastic optimization (actually their most probable value), T_j from the standard one. The temperature difference $\Delta T_{min,0}$ is the one considered during standard optimization, which is 10 [K].

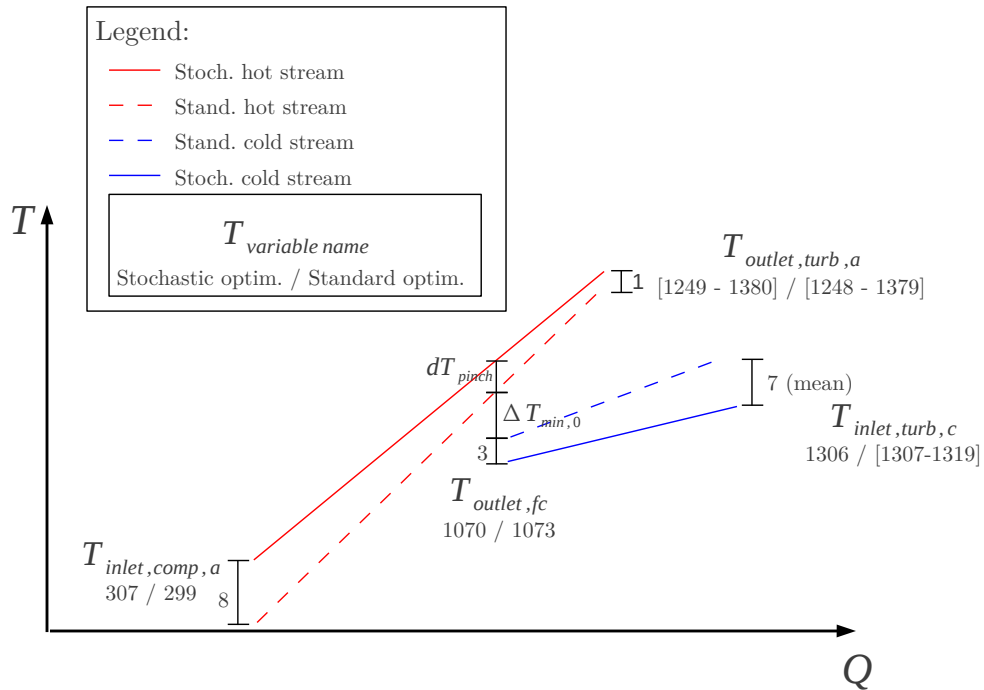


Figure 5.12: Uncertainties on streams involved in high temperature pinch

The fuel cell outlet temperature appears to be 3 [K] lower in stochastic optimization. On the hot side, the temperature difference between stochastic and standard case dT_{pinch} can be estimated at around 1.4 [K]. The total margin of stochastic streams is then $1.4 + 3 = 4.4$ [K]. As a reminder, uncertainty have been considered on $\Delta T_{min}/2$ and it may have a maximum variation of 4 [K]. So, for same heat loads, the limit of pinch point activation will be respected for any temperature variation. However, it will be seen that heat loads change implying that this pinch point may be activated in stochastic solution. But this demonstrates that system is able to adapt to temperature changes.

It can be noticed that the margin is higher for the cold stream. This can be explained by the fact that the anodic turbine inlet temperature is limited at 1573 [K]. Moreover, anodic turbine pressure ratio is not subject to uncertainty. So the only uncertain variables affecting $T_{out,turb,a}$ is the anodic turbine efficiency. On the contrary the outlet temperature of the fuel cell $T_{out,fc}$ suffer from all the fuel cell uncertainties.

It can be noticed that the cathodic turbine inlet temperature is asymmetric, with a tendency to be lower than its mean (1306 [K]). It is modeled by a Pearson IV distribution. Its mean is constant for any objectives unlike the standard optimization,

where it vary from 1307 to 1319 [K]

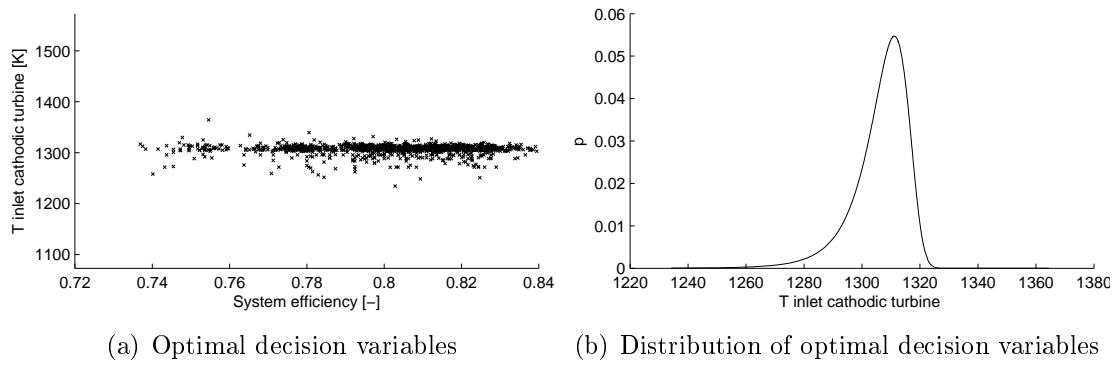


Figure 5.13: Cathodic turbine inlet temperature statistic

$T_{out,turb,a}$ is the only temperature in figure 5.12 varying in both case (stochastic and standard). This is due to constant values for $T_{in,turb,a}$ and to the fact that it is strongly related to π_a , as it can be seen in figure 5.14. This result has been recomputed with the uncertain variables fixed at the value they had during stochastic optimization.

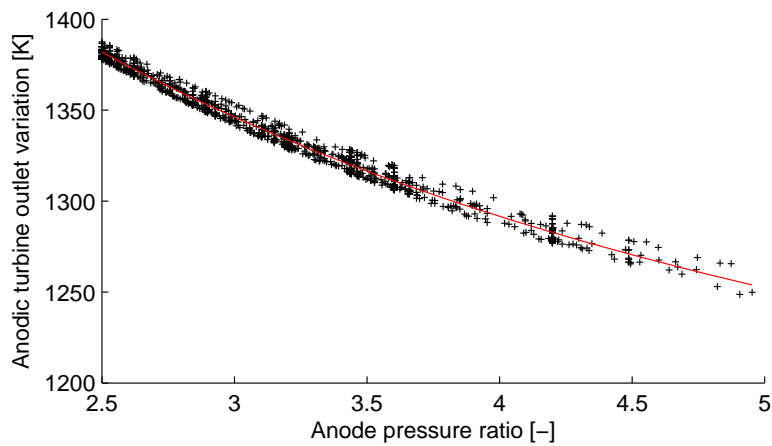


Figure 5.14: Anodic turbine outlet temperature variation

It is fitted by an exponential function $T(\pi_a)$ in red in figure 5.14:

$$\begin{aligned}
 T(\pi_a) &= a \cdot e^{(b\pi_a)} + c \cdot e^{(d\pi_a)} \\
 a &= 434.2 \\
 b &= -0.4936 \\
 c &= 1297 \\
 d &= -0.01298
 \end{aligned}
 \tag{5.2}$$

Comparing this function with the results of standard optimization (figure 5.15), a temperature difference of 1 [K] can be computed.

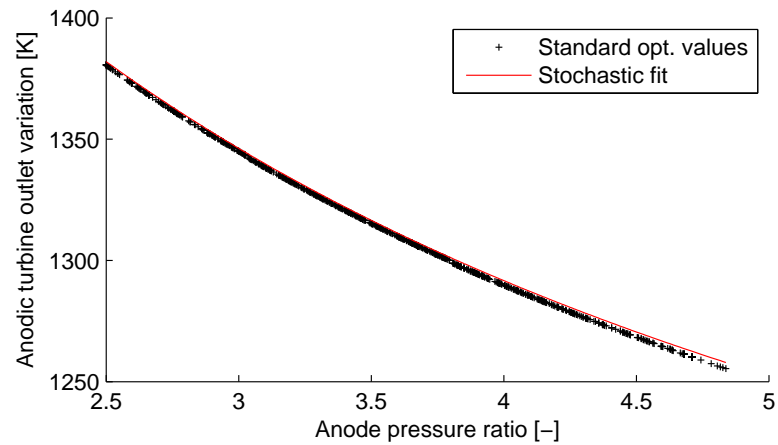


Figure 5.15: Anodic compressor outlet temperature variation: Stochastic/standard optimization results

The second temperature of the hot stream, $T_{in,comp,a}$ has less influence on the high temperature pinch point since this stream has a great heat load and that pinch occur at the hot end. Is is symmetrically distributed by a Pearson IV as well and its mean is 307 [K].

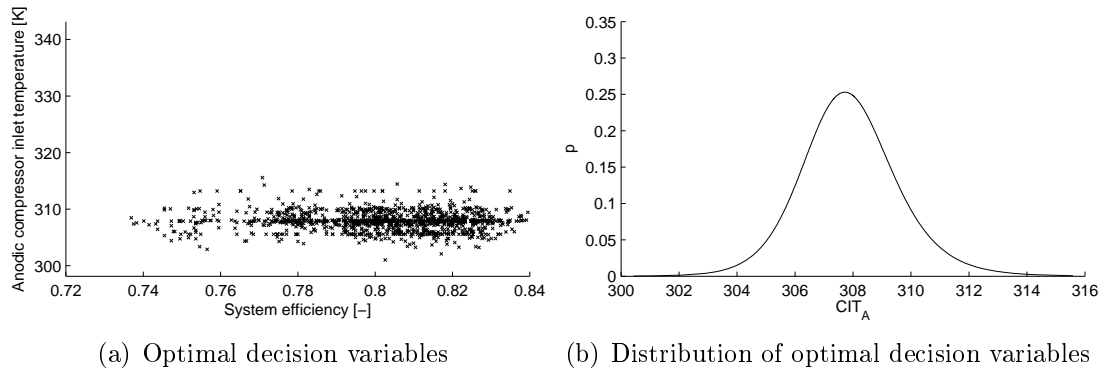


Figure 5.16: Anodic compressor inlet temperature statistic

Other decision variables will not be studied in detail, since the method has been demonstrated on the high temperature pinch point. Fuel cell most probable temperature is 1070 [K]. It is modeled by a beta distribution. Its skewness shows a great asymmetry, implying greater chance to be lower than its mode. This may be related to previous discussion on the higher temperature pinch point, which show a preference for lower temperature at the fuel cell outlet.

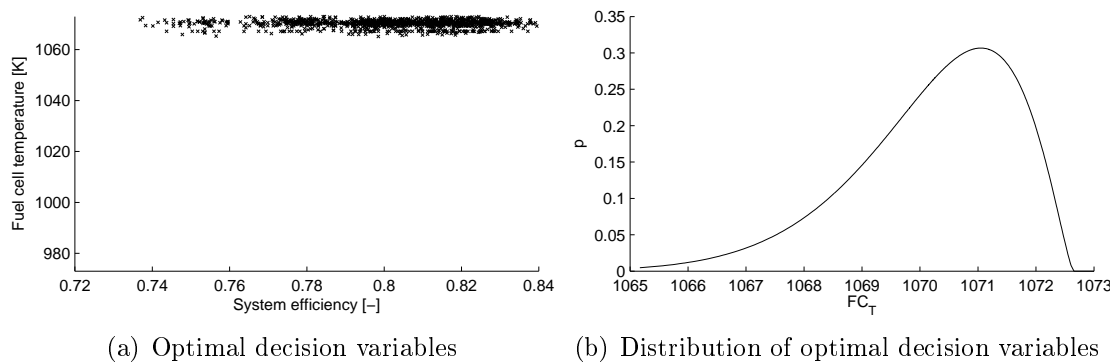


Figure 5.17: Fuel cell temperature statistic

As for standard optimization, cathodic compressor inlet temperature has the same mean value as the anodic one, that is to say 307 [K]. Pearson IV is considered here as well. It is clearly asymmetric.

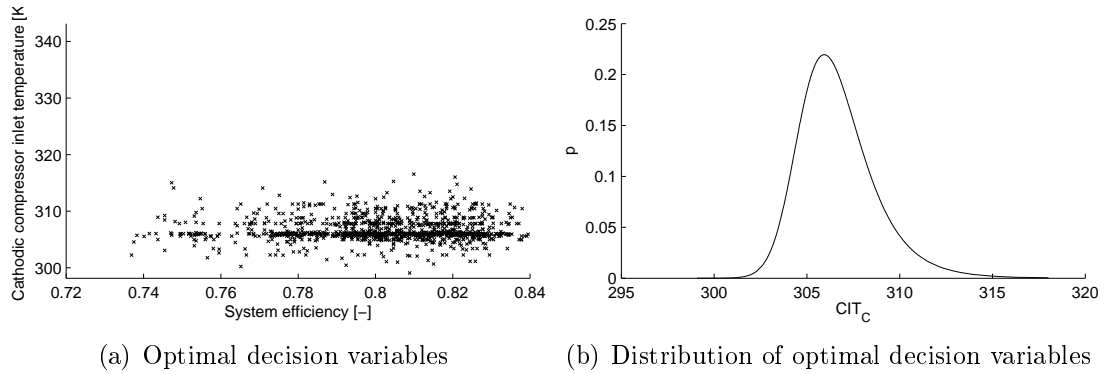


Figure 5.18: Cathodic compressor inlet temperature statistic

The cathodic pressure ratio appears to be constant as well at 2.85 [-].

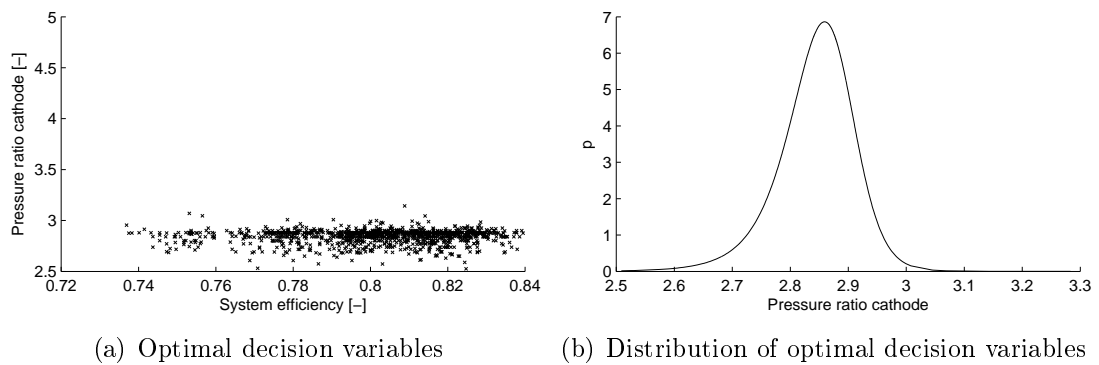


Figure 5.19: Cathodic pressure ratio statistic

Fuel utilization most probable value is 0.8 [-] as in the standard optimization. Since it is the higher boundary, it has only more chance to be lower. It is modeled by a beta distribution.

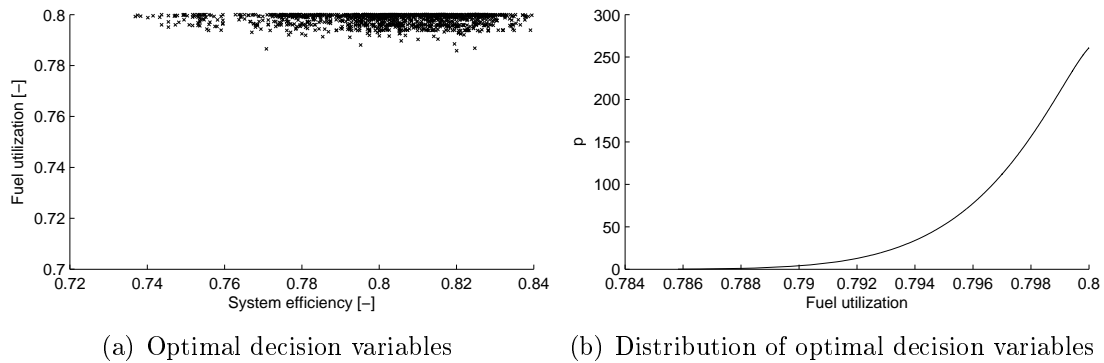


Figure 5.20: Fuel utilization statistic

Current density mean slightly increase compared to standard optimization, but it remains clearly asymmetric as fu . It shows that both variables adapt jointly to find the best value on the iv curve. It is modeled as well by a beta distribution

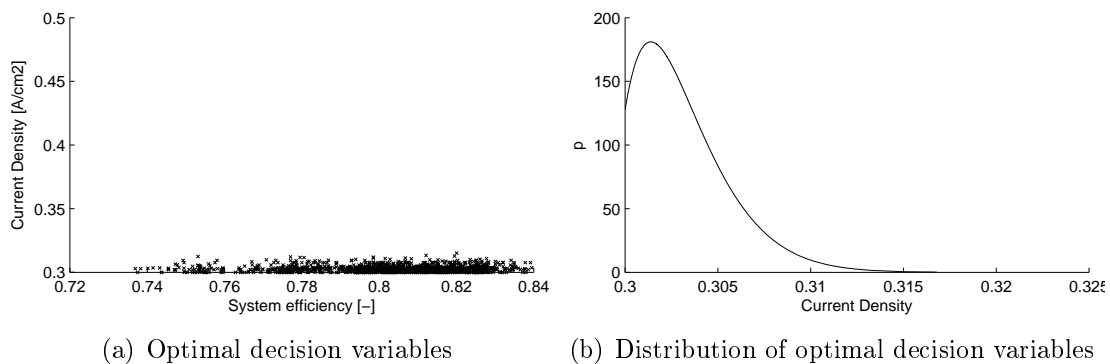


Figure 5.21: Current density statistic

Steam to carbon ratio appears to be constant at 1.48 [-]. It shows a small standard deviation (0.031). This indicates that fuel composition has a low influence on adaptation to uncertain condition.

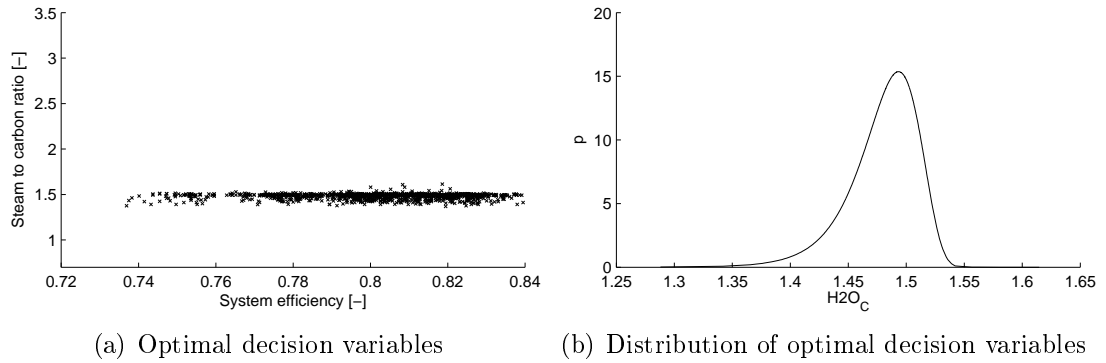


Figure 5.22: Steam to carbon ratio statistic

In opposition, the steam reforming temperature (mean at 1057 [K]) has a standard deviation of 4.1 [K]. Modeled by a Pearson IV distribution, it correspond to a maximal deviation in the order of magnitude of 15 [K]. This is due to its high temperature making it influent on pinch analysis.

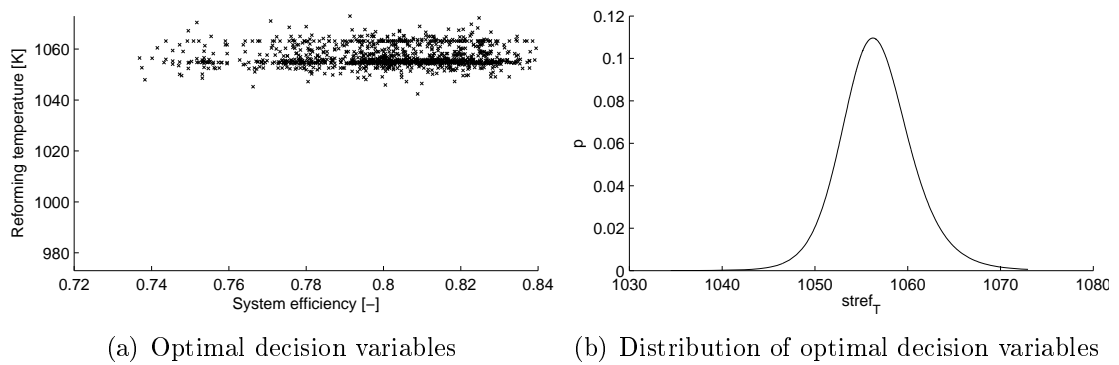


Figure 5.23: Steam reforming temperature statistic

Finally, the air factor appears constant as well with a mean value at 3.18 [-]

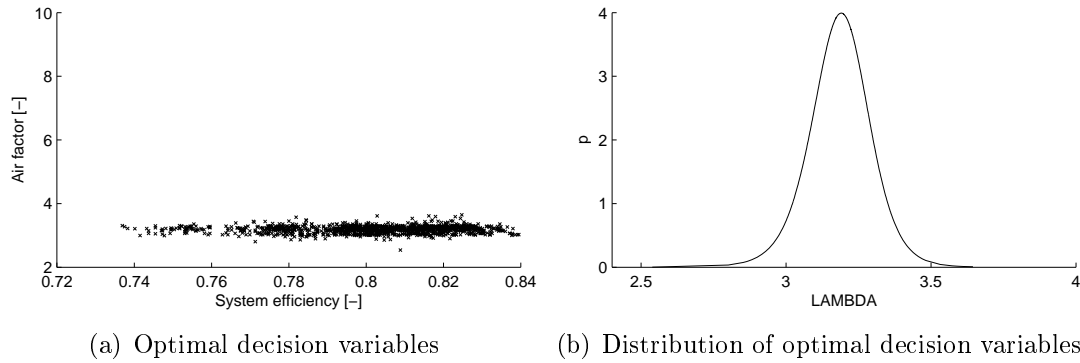


Figure 5.24: Fuel cell temperature statistic

Standard and stochastic optimization results are summarized in table 5.2. The value given for stochastic optimization is their mean value.

Variables	Standard optimization		Stochastic optimization	Unit
	Minimum	Maximum	Mean	
$\xi_{H_2O,c}$	1.29	1.34	1.4805	$[-]$
T_{ref}	1067	1073	1057	$[K]$
T_{FC}	1073		1070	$[K]$
λ	2.94	3.31	3.19	$[-]$
fu	0.8		0.798	$[-]$
i	0.3		0.303	$[A/cm^2]$
$T_{in,turb,c}$	1307	1319	1306	$[K]$
$T_{in,burner,H_2O}$	—	—	—	$[K]$
$T_{in,comp,a}$	299		307	$[K]$
$T_{in,comp,c}$	299		307	$[K]$
π_a	not reported here			$[-]$
π_c	2.97	3.13	2.84	$[-]$
$\xi_{H_2O/a,out}$	0		0	$[-]$

Table 5.2: Comparison of standard and stochastic optimization results

Since the only decision variables in stochastic optimization which is changing is π_a , a sensitivity analysis can be performed on it, considering all others decision variables at their mean value.

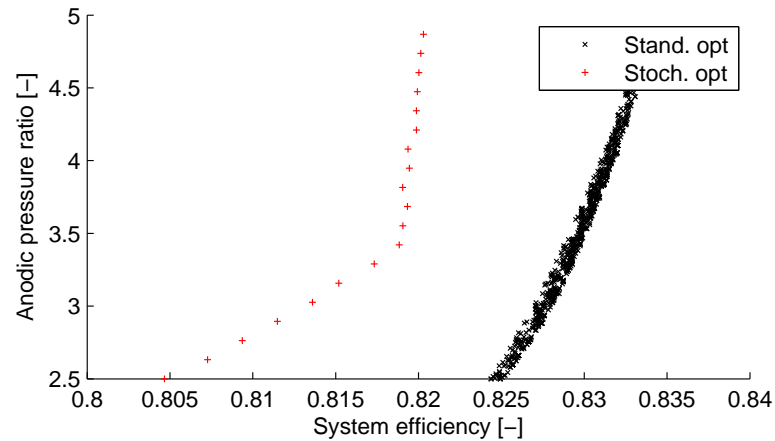


Figure 5.25: Standard Pareto curve and sensitivity analysis on stochastic results

The angle in the Pareto curves at $\pi_a = 3.42$ correspond to high temperature pinch activation. By analyzing details of figure 5.25, it can be seen that for $\pi_a > 3.42$, hot utility is necessary. It is interesting to notice influence of ΔT_{min} on the stochastic solution. In figure 5.26, the black points correspond to a fuel cell temperature of 1070 [K] as in figure 5.25. The red points have been computed with a fuel cell temperature of 1073 [K], which is the value resulting from standard optimization. The blue points have been computed at 1065 [K] for comparison. Each of this three cases have been computed with the mean ΔT_{min} and with the higher value.

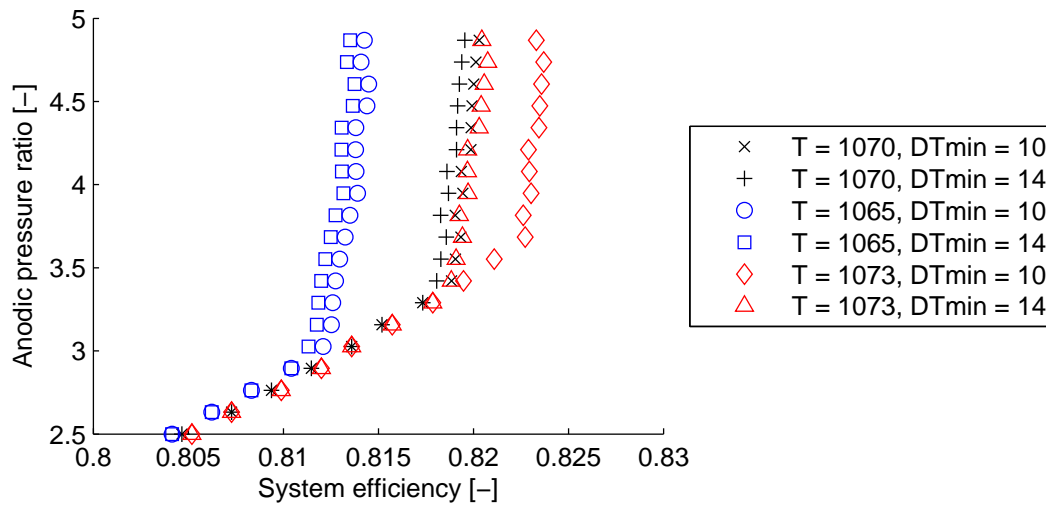


Figure 5.26: Influence of fuel cell temperature and ΔT_{min} on stochastic solution

It can be seen that standard optimization value leads to greater variation when exposed to the same ΔT_{min} variation (around 5 times bigger) than with the temperature given by stochastic optimization. Low temperature case at 1065 [K] shows a low variation as well, but with lower efficiency due a pinch point activation at lower π_a .

This could be applied by performing Monte-Carlo on the whole uncertain space for one point of each Pareto curve.

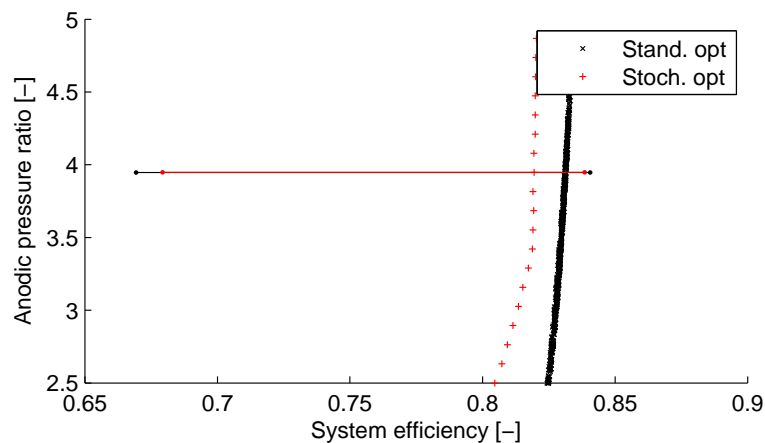


Figure 5.27: Standard Pareto curve and sensitivity analysis on stochastic results

It can be seen in figure 5.27 that stochastic optimization leads to a smaller efficiency variation range, and a lower mean. Here again, difference between mean and mode is important. This example shows that standard optimization gives optimal value with respect to the mode of uncertain variables whereas stochastic optimization is based on mean values. Table 5.3 summarize mean and standard deviation for the two points chosen in figure 5.27.

Optimization	Estimator	Value
Standard	Mean	0.805
	Standard deviation	0.0202
Stochastic	Mean	0.814
	Standard deviation	0.0177

Table 5.3: Mean and standard deviation comparison

This demonstrate the basic principle that, the mode, the mean is more representative of the a distribution due to its integer formulation. As a consequence, it shows that optimizing a system on mean values leads to better global performances than an optimization based on the mode.

It should be noticed that the variance of stochastic solutions is not necessary lower. Indeed, it has not been considered has an objective. So, this approach only guarantee a mean improvement compared to standard optimization.

Relevance of such an optimization can be discussed. Indeed insuring a gain of 1 or 2 [%] efficiency whereas it is subject to uncertain variation of 15 [%]. However, this is highly depending on the context. It can be observed that standard variation is in the order of magnitude of 2 [%] for the studied examples, meaning that tails of the performance distribution may be neglected. This introduce the issue of quantile, determining the probability to be over or below a given performances. Despite some technologies have to insure to operate respecting performances at 100 [%], some other cases may allow lowered performances for a small period if they are compensated during rest of time. The acceptable limit for the quantile depends on the decision maker choice to accept a given risk is the profit in case of success is sufficient. However, such decision is subject to financial risk analysis which are out of the framework of this study.

Despite this approach appears to be efficient and uncertain space representative, it can be seen that analyzing the results remains a difficult task. This is due to the fact that influence of each uncertain variables can not be clearly distinguished, what is increased by system complexity.

5.4 Conclusion

Pareto curve subject to uncertain variables has been described.

It has been demonstrated that evolutionist algorithm offers enough model evaluation to ensure the representativity of the uncertain variables space. Moreover, the ability of the solver to evaluate maximum deviation has been exposed. This is related to ability of the system to compensate uncertainties influence. This has led to the comparison with the two stages programming problem.

Stochastic programming optimization results have been presented and compared with standard optimization results. It has been shown that optimal temperature can adapt to ensure heat exchange in constant load conditions. Moreover, it can be observed that optimal decision variables lead to the best compromise between variation of ΔT_{min} and total efficiency.

Finally the importance of difference between mode and variance has been highlighted. Indeed, stochastic optimization leads to a higher mean performance, whereas most probable performance are better for standard optimization.

A great advantage of this approach is that continuity or differentiability of the objective function do not need to be ensured.

Chapter 6

Moments method results

Moments method will be applied to energy system design. Its computational resource consumption will be compared with stochastic programming.

Optimal decision variables will be analyzed, and the role of the two high temperature pinch points will be emphasized.

Finally, variance of the three solutions will be studied more in depth. It will be shown that a great advantage of moments method is that it allows to identify contribution of each uncertain variables in objective variance.

6.1 Optimization convergence and number of iterations

The algorithm to apply moments method in optimization is given in figure 6.1.

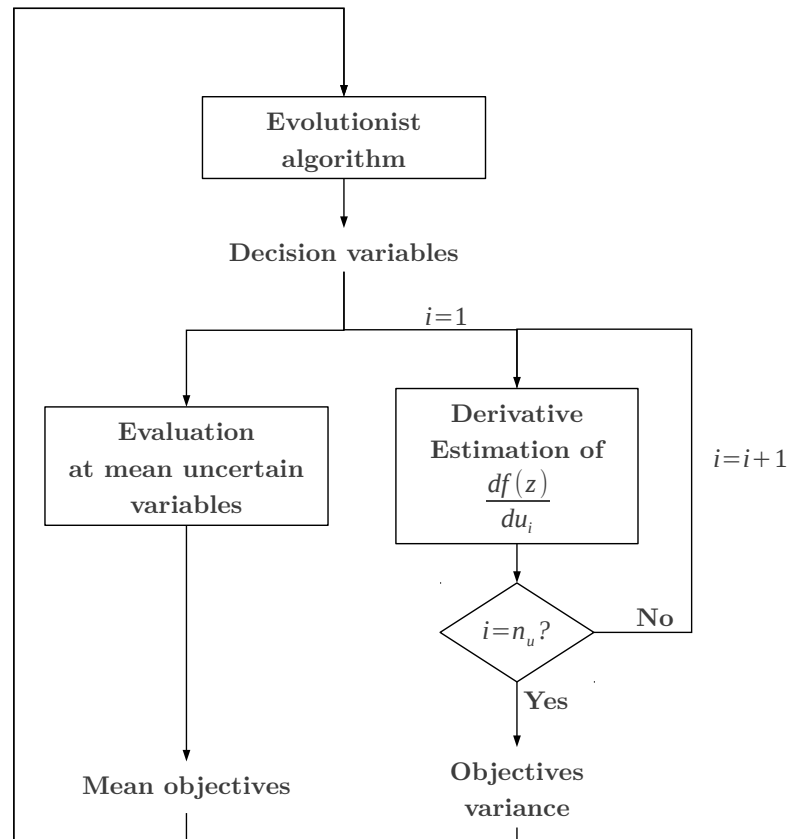


Figure 6.1: Algorithm of moments method applied to optimization

Here variance of the efficiency has been added as objectives. The second objective variance, the anodic pressure ratio, has not been considered here since it is a decision variable and is not uncertain.

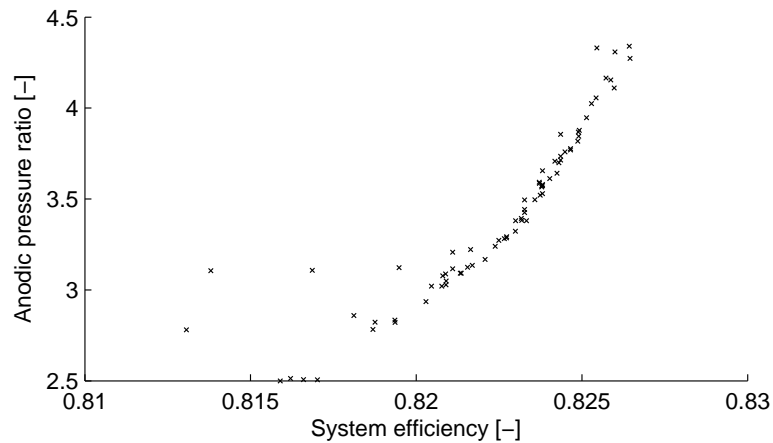


Figure 6.2: Pareto front for the optimization based on moments method

It can be seen in figure 6.3 that the optimization based on moments propagation has converged. To improve readability, the total population has not been reported. Its envelope has been computed based on Delaunay triangulation [15], the last generation being the darkest. On the right, it can be observed that the pareto front is progressing, while on the left, the space of sub-optimal solution is becoming smaller. It can be seen that the last generations do not show any progress, what means that optima has been reached.

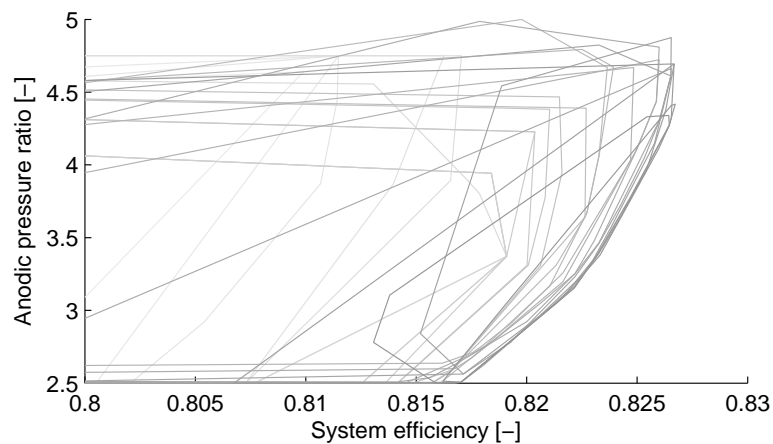


Figure 6.3: Pareto front for moments method optimization

This models is based on 13 uncertain variables. As described in section 2.3.2 a number of model evaluations per iteration to propagate uncertainties is $2n_u + 1$.

Here, the optimization necessitates $16 \cdot 10^3$ iterations, what means $16 \cdot 10^3 \cdot (2 \cdot 13 + 1) = 432 \cdot 10^3$ model evaluations. As a reminder, stochastic optimization needed $85 \cdot 10^3$ evaluations. So, moments method has consumed around 5 times more resource. However, such comparison is highly related to the model and the solver used. Indeed, for a better convergence, moments method may become competitive.

6.2 Decision variables analysis

As it can be seen in figure 6.4 steam reforming temperature increases with efficiency from 1043 to 1055 [K].

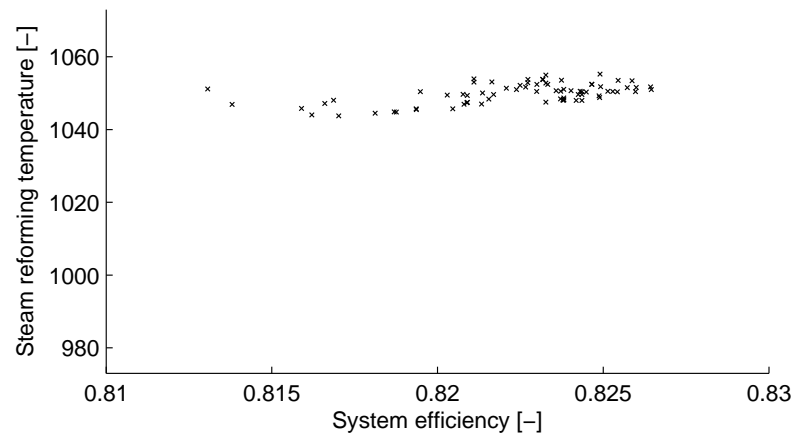


Figure 6.4: Steam reforming temperature for moments method

It is lower than standard optimization. This is due to the fact that a margin avoiding pinch activation is considered as it can be seen in figure 6.5. As it will be described further, this correspond to the fact that variance globally increases with efficiency.

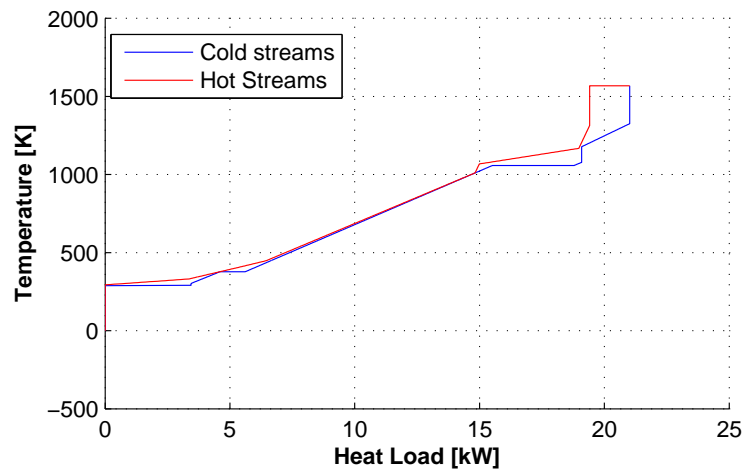


Figure 6.5: Composite curve for mid pressure of figure 6.11

In a same manner, π_c increases from 3.56 to 3.63 [-] (what is higher than standard optimization results) so that cathodic turbine outlet temperature $T_{out,turb,c}$ decrease.

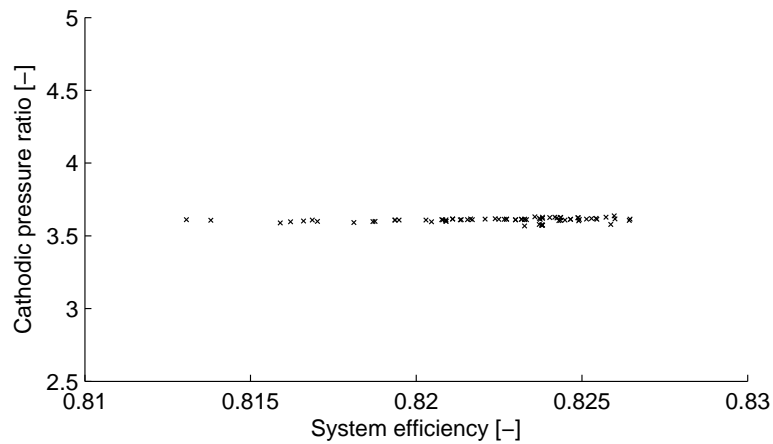


Figure 6.6: Cathodic pressure ratio for moments method

The effect of π_c is increased by decreasing cathodic turbine inlet. Indeed, it varies with efficiency from 1338 to 1318 [K]. It remains a higher temperature than in standard optimization. This is due to the fact that fuel cell is subject to higher variance (figure 6.13). Gas turbines specific power is then favored.

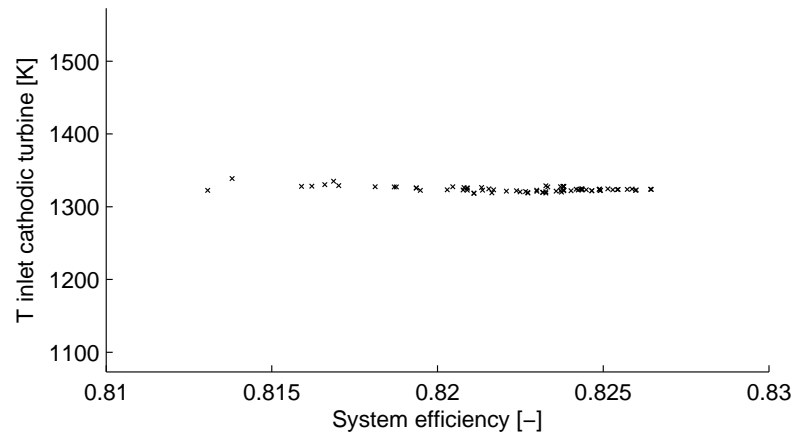


Figure 6.7: Cathodic turbine inlet temperature for moments method

From that point of view, steam to carbon ratio shows a slight tendency to decrease (from 1.61 to 1.68 [-]). However, this decrease is negligible. However, it should be noticed that here again, this results is higher than in standard case to increase power produced by the anodic gas turbine. Indeed, high $\xi_{H_2O,c}$ allows to compress less air in the anodic compressor and more water in the pump, demanding less energy to reach atmospheric pressure.

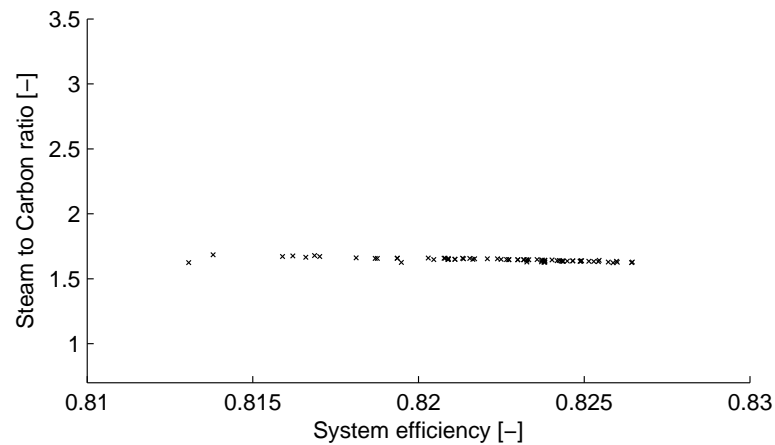


Figure 6.8: Steam to carbon ratio for moments method

This implies a slight decrease from 2.96 to 2.72 [-] in air factor since less air is necessary for the fuel cell to be operated.

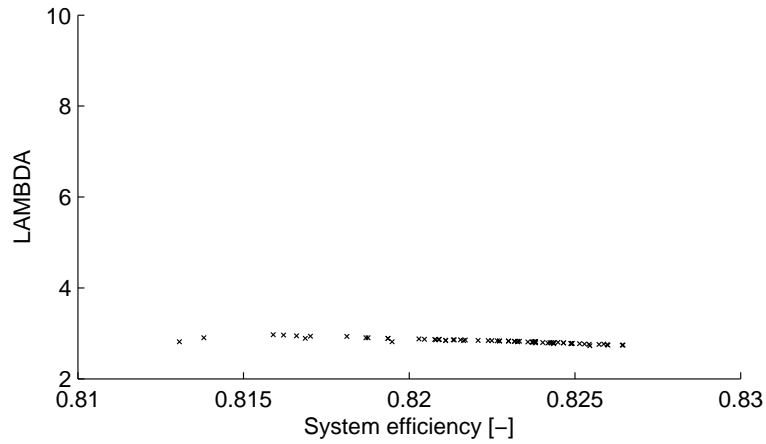


Figure 6.9: Air factor for moments method

Other decision variables are quite similar to standard optimization results and are given in appendix C. Their value are summarized in table 6.1

Variables	Stand. opt.		Stoch. opt.	Moments method		Unit
	Minimum	Maximum	Mean	Minimum	Maximum	
$\xi_{H_2O,c}$	1.29	1.34	1.4805	1.61	1.68	[-]
T_{ref}	1067	1073	1057	1043	1055	[K]
T_{FC}	1073		1070	1071	1073	[K]
λ	2.94	3.31	3.19	2.72	2.96	[-]
fu	0.8		0.798	0.794	0.8	[-]
i	0.3		0.303	0.3	0.32	[A/cm ²]
$T_{in,turb,c}$	1307	1319	1306	1318	1338	[K]
$T_{in,burner,H_2O}$	-					[K]
$\xi_{H_2O/a,out}$	0					[-]
$T_{in,comp,a}$	299		307	298	302	[K]
$T_{in,comp,c}$	299		307	298	299	[K]
π_a	not reported here					[-]
π_c	2.97	3.13	2.84	3.56	3.63	[-]

Table 6.1: Comparison of standard and stochastic optimization results

It can be first seen that $\xi_{H_2O,c}$ is higher in both stochastic and moments methods. It is due to the fact that big steam to carbon ratio imply higher mass flow rate in the pump of the anodic Brayton cycle, which is less energy consuming than the

compressor. Then, its uncertainty induce less deviation on the total performances than compressor's one.

Uncertainties on ΔT_{min} lead to supplementary firing. It allows, in the case of moments method, a higher cathodic turbine inlet temperature, so that bigger cathodic pressure ratio are optimal.

In the case of stochastic programming approach, the opposite consequence on cathodic cycle can be observed. Turbine inlet temperature is lower as well as pressure ratio. This is due to the principle of each method. In the case of moments method, moments are extrapolated based on the neighborhood of the mean value. Conflict due to impossible heat exchanges will not be detected for extreme values of uncertain variables. Since stochastic programming is based only on simulation of the deterministic model without extrapolation, such constraint will be considered as impossible, so that $T_{in,turb,c}$ will be lowered to insure that heat exchange is possible, pressure ratio being adapted.

This underlines the importance of implementing constraint verification in the moments method.

6.3 Variance analysis

First it can be observed that variance is increasing with efficiency.

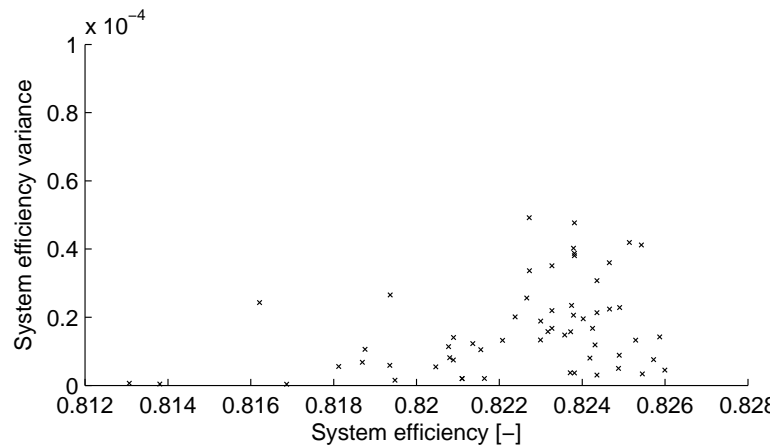


Figure 6.10: Efficiency and its variance

In conventional optimization, the variance simulated by Monte-Carlo is in the order of magnitude of 10^{-3} . It can be seen here that the maximum variance obtained by moments method is 0.6×10^{-4} . It should be noticed that variance in figure 6.10 may appear to be not converged. This is due to a scaling effect, since

results would have been merged with the abscissa axis otherwise.

As it will be described in this section this is mainly due to the fact that pinch points are activated, making the system more sensitive to uncertainty variation. In future work, decision variables space shall be separated in $n_{pinch,act}$ spaces. The variable $n_{pinch,act}$ being the number of pinch that are not activated on every solutions. This is to avoid the risk of discontinuity in derivative estimation. For example, in equation 2.36:

$$\frac{\partial y}{\partial u_i} = f'(u_i) = \lim_{h \rightarrow 0} \frac{f(u_i + h/2) - f(u_i - h/2)}{h} \quad (6.1)$$

A pinch activation between $f(u_i + h/2)$ and $f(u_i - h/2)$ would lead to wrong derivative estimation. This has not been implemented in the methods proposed here. So, Three points of figure 6.11 have been carefully chosen to ensure avoiding pinch activation and analyzed.

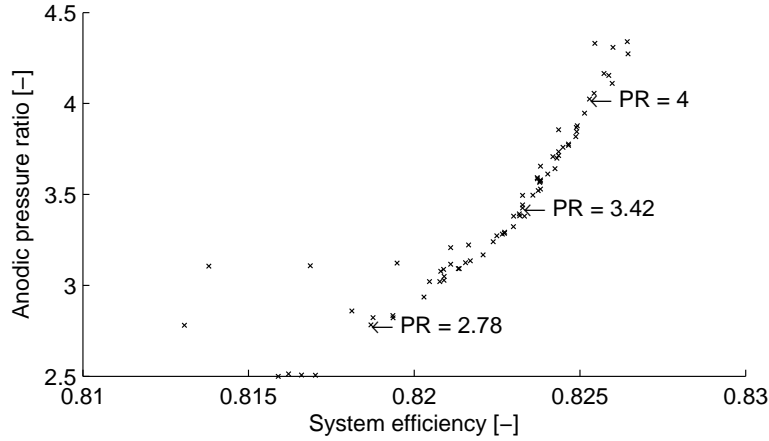


Figure 6.11: Points analyzed

The related performances are given in table 6.2.

Pressure ratio [-]	Efficiency [-]	Variance [-]
4	0.825	$1.5 \cdot 10^{-5}$
3.42	0.823	$1.4 \cdot 10^{-5}$
2.78	0.818	$1 \cdot 10^{-5}$

Table 6.2: Performances of studied points

A great advantage of moments methods is that it is based on the sum of contribution of each uncertain variables to the different moments (the variance in this case). So, by reporting this contributions, it becomes possible to study which uncertainties influence the more the chosen estimator. In figure 6.12 the variance of the three points is given with the participation of each uncertain variable.

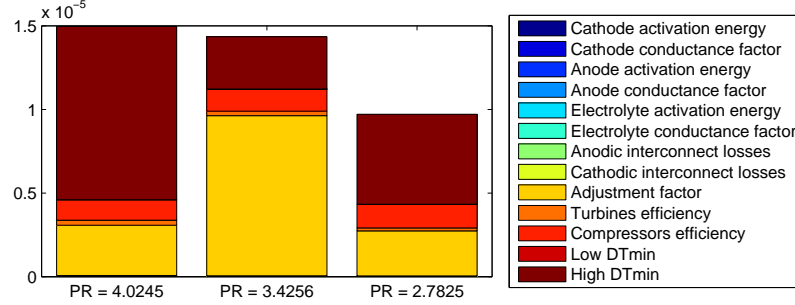


Figure 6.12: Variance of the efficiency for the selected points

It can be seen that ΔT_{min} is one of the two most influent variables. As described in previous chapter, this is due to the fact that the hot utility load is a linear function of ΔT_{min} . The other significant variable is the adjustment factor. Finally, compressors and turbines efficiencies appears to be significant.

In figure 6.13, it can be seen that the most influent uncertain variables on fuel cell electricity production is the anode activation energy. This may appear to be in contradiction with the influence of f_{CC} on total efficiency. This is due to two factors:

- Sensitivity to adjustment factor are globally bigger than variation due to anode activation energy. However, the difference of sensitivity of the fuel cell electricity production to f_{CC} and $E_{A,a}$ is smaller than the sensitivity of the total efficiency. In other words:

$$\begin{aligned}
 & \frac{\partial \varepsilon}{\partial f_{CC}} > \frac{\partial \varepsilon}{\partial E_{A,a}} \\
 \text{and: } & \frac{\partial \dot{E}_{FC}}{\partial f_{CC}} > \frac{\partial \dot{E}_{FC}}{\partial E_{A,a}} \\
 \text{but: } & \frac{\left(\frac{\partial \varepsilon}{\partial E_{A,a}} \right)}{\left(\frac{\partial \varepsilon}{\partial f_{CC}} \right)} < \frac{\left(\frac{\partial \dot{E}_{FC}}{\partial E_{A,a}} \right)}{\left(\frac{\partial \dot{E}_{FC}}{\partial f_{CC}} \right)} \tag{6.2}
 \end{aligned}$$

It can be explained by the fact that total power produced by the system is fixed at 10 [kW]. Fuel utilization and air factor are imposed for each solution as well. So, the only way to compensate fuel cell efficiency decrease is to increase air and fuel massflows, increasing by the way power produced by the gas turbines. This means that the adjustment factor variation implies bigger change in flowrates.

- As given in equation 2.33 and reported here:

$$\sigma_y^2 = \underbrace{\sum_{i=1}^{n_u} \left(\frac{\partial y}{\partial u_i} \right)^2 \cdot \sigma_{u_i}^2 + y_\mu^2}_{1^{st} \text{ order}} + \underbrace{\sum_{i=1}^{n_u} \left(y \frac{\partial^2 y}{\partial u_i^2} \right) \cdot \sigma_{u_i}^2 + \sum_{i=1}^{n_u} \left(\frac{\partial y}{\partial u_i} \cdot \frac{\partial^2 y}{\partial u_i^2} \right) \cdot \gamma_{u_i}}_{2^{nd} \text{ order}} - \mu_y^2 \quad (6.3)$$

So, objectives variance (as well as any other output of the model) depend not only on partial derivative, but on the variance of each uncertain variable. Here, $E_{A,a}$ variance is greater than f_{CC} variance.

This two points conjugated lead to a higher contribution of anode activation energy than adjustment factor to fuel cell electricity production. It should be noticed that such example demonstrate the importance of accurate input data on uncertain variables. Indeed, it can be seen here that variance, and thus the chosen distribution function, has a key role in propagation.

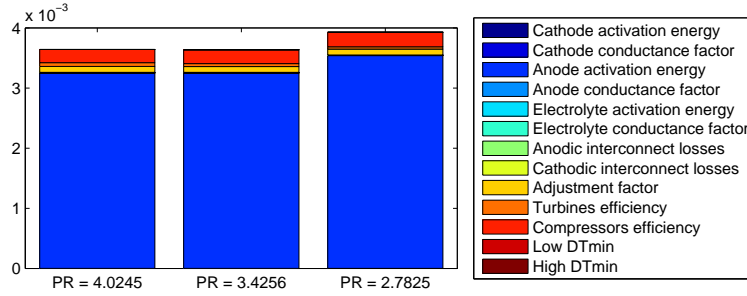


Figure 6.13: Variance of the fuel cell power produced for the selected points

It can be seen in figure 6.14 that gas turbines efficiency is the most important factor on anodic Brayton cycle electricity production. However, the adjustment factor influence is still significant for reason mentioned previously, as well as for cathodic cycle (figure 6.15).

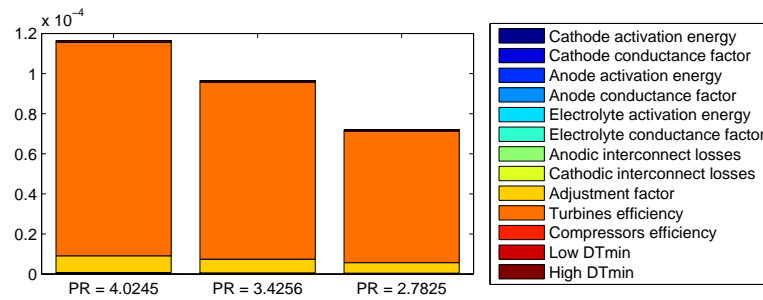


Figure 6.14: Anodic Brayton cycle power production variance

Unlike anodic cycle, most influent uncertain variable for cathodic cycle is the compressor efficiency. This is due to the fact that in previous case, the amount of steam is gas turbine outlet is condensed and pumped. It demands then less energy to pump liquid water than compressing gas.

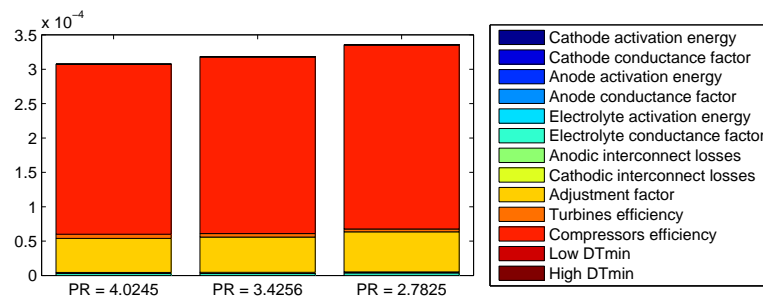


Figure 6.15: Cathodic Brayton cycle power production variance

As expected, ΔT_{min} is the most influent factor in hot utility consumption variance.

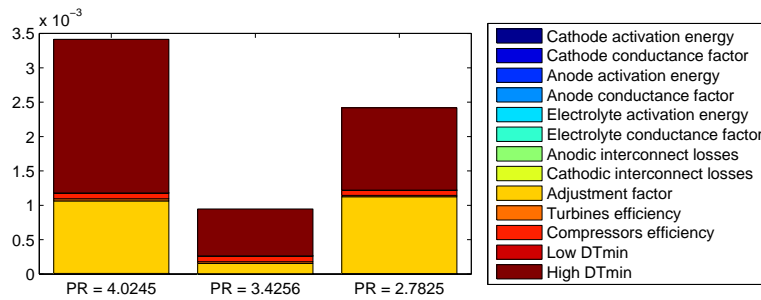


Figure 6.16: Hot utility consumption variance

Energy required for oxygen production has not been studied here, since it is not significant in the total balance, neither in its variance.

Figure 6.17 summarized the variance of each power input and output contributing to efficiency. As it can be seen, fuel cell electricity production has the greater variance of the three output. Anodic cycle has the lowest variance due to a limited influence of uncertain compressor efficiency. It can be seen that these variances are translated mainly in system fuel consumption variance, with variance of additional heat provided by hot utility depending on the pinch activated.

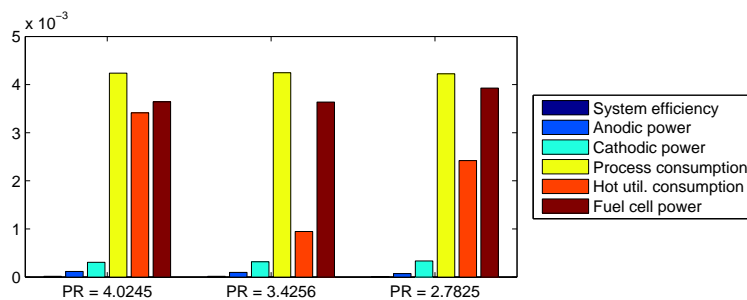


Figure 6.17: Comparison of variance for each contribution to total efficiency

6.4 Conclusion

Optimization based on moments method for uncertainties propagation has been performed. Its convergence has been verified. It has needed more model evaluations than the stochastic approach. However, moments methods can fit any solver since there is not representativity issue.

It has been shown that the two highest temperature pinch points are the more

sensitive, what confirms results of stochastic programming.

Finally variance of the efficiency and energy production and consumption has been studied. It has shown that variance of uncertain variables influences differently the fuel cell power or the total efficiency. This underlines the fact that on one hand, a relevant design under uncertainty should be based on accurate distribution of uncertain variables, and on the other hand that derivative estimation precision plays an important role as well.

Chapter 7

Conclusion and future work

Optimizing complex energy system is a difficult task. Great efforts are made to improve the research of an optimal design and the accuracy of the proposed solutions. In this context, including uncertainty in the optimization procedure is not trivial. It has been shown that uncertainty can not be considered after optimization, but should be integrated in the problem resolution. Methods already applied in continuum mechanics and finance have been investigated. The first objective of this thesis has been to compare on one hand mathematical approaches and on the other hand the specificity of energy system design. This has been done in several steps.

First, the formulation of energy system design has been presented as an optimization problem. It has underlined the fact that the solver used in this study, as well as other heuristic methods, do not allow to verify the optimality conditions since there is no derivative estimation. It means that the results shall be interpreted carefully, and that the optimization may have to be conducted several times to insure that the global optima is reached.

Variables involved in design problem have been classified. Influence of each uncertain variables with respect to decision variables has been detailed for each step between pre-design of the system to its operation. Objective function and constraints, incorporated in a numerical model in the current case, have been described. Here, a decomposition in “onion” layer [49] has been chosen. Other option would have been:

- A stages decomposition, considering a design stage and a slave problem solving the optimal control problem. Such approach would be coherent with the two stages programming problem, on which optimization of energy system under uncertainty is based. However, finding an appropriate control for each design is not possible for complex superstructure with the methods currently available.

- A physical decomposition, separating the process in several sequential part. In the example used in this study, in may have been the fuel processing, the fuel cell and the two inverted Brayton cycle.
- A time scale decomposition, similar to stages decomposition, but linking uncertainties with the operating variables able to compensate them with respect to their variation frequency.

The main goal common to these modeling approaches is to manage the trade-off between the number of sub-problems to be optimized and their size.

In the decomposition considered here, energy integration is an important issue that shall be further studied in future work. Its advantages and drawbacks have been discussed. It offers the possibility to estimate heat exchanger network performances in an efficient manner, but its results are not differentiable, and may even not be continuous. It implies that uncertainty propagation has to be applied piecewisely or in a scenario approach.

Once the model and the involved variables have been described, methods for uncertainty propagation have been listed. It has been shown that Monte-Carlo is not efficient, despite it is widely used. Moments method and orthogonal polynomials appear to be the most promising technique. It is a difficult task to compare their performances since the number of model evaluations required for the orthogonal polynomials is related to the model complexity. However, their validity domain should be further studied. Indeed, if derivatives estimation for moments method is valid in a very small neighborhood of the design point, orthogonal polynomials may allow to cover a bigger area, since they can easily consider order higher than two. This would mean that orthogonal basis do not have to be built at each model evaluation, sparing computing resource.

An innovative approach defined as stochastic programming has been described and tested. It has shown only a slight increase of the number of iterations during optimization. However, this method is only valid for solver based on a great number of iterations to ensure a complete exploration of the uncertain variables space. It should be also noticed that stochastic programming results have not been compared with a real two stages approach.

A method has been proposed for optimizing the operating variables in the same time as the design variables. It did not succeed due to convergence problem. Most of the methods proposed to optimize operating variables. However, in an energy system design procedure, an indicator of the process adaptability is needed, not necessarily a detailed control strategy. Such a value should be based on the partial derivative of the objective function and on the maximum tolerated range for operating variables.

A *SOF*C model has been used and optimized. The found results are coherent with the previous studies on such systems. The critical role of the pinch analysis

for this system has been stressed.

A stochastic optimization has been applied on this model. The representativity of the uncertain variables space has been ensured. A default of this method is that it can be verified only after optimization. It has been observed that less efficient solutions are removed based on solver parameters. However, the relation between such parameters and the acceptable deviation of objective can not be clearly defined and quantified.

Such an optimization leads to distributed optimal decision variables. The model used here presented several constant optimal values (or linear). This is practical to study their distributions. One dependent variable distribution has been studied, based on the variation around a fitted function. Another possible approach would be to use the bootstrap method [21].

The difference between mode and variance has been highlighted. Indeed, most of the design are based on most probable value, what will lead to worse results if any uncertain variables deviate from their mode.

The issue of generating random numbers has not been discussed in this study. However, “true” random numbers are not easy to produce by an algorithm, composed of deterministic operations. However, hazard is a notion difficult to characterize mathematically. Here, it has been assumed that MATLAB generates numbers “enough” random.

The moments method has been applied on *SOFCC* case as well. Its convergence has been verified and it has been seen that it leads to similar conclusions than the stochastic optimization concerning the pinch analysis. It has been shown that this approach allows to evaluate the participation of each uncertain variable to the objective variance. First, it demonstrates the importance of accurate statistic for data input. Then, it shows that the variance of the efficiency can not be deduced from the variance of the members of the energy balance. This can be extrapolated to any objectives about the dependent variables allowing to compute it.

In the case studied, the applied methods propose several action to decrease objective variance. It has been demonstrated that uncertainty on ΔT_{min} is the bottleneck of the system. It has to be compensated by an supplementary firing, allowing bigger temperature difference. Moreover, to avoid impossible heat exchange, cathodic gas turbine inlet temperature is decreased, increasing the margin on ΔT_{min} at pinch point. This can be observed in stochastic programming approach, what emphasize the importance of verifying constraint violation in energy integration with moments method. Finally, Greater steam to carbon ratio decrease the mass flow rate of anodic compressor, and then the influence of the uncertainty on its efficiency.

The model studied here is has two objectives. However, the pressure ratio serves to explore the search space, so as not to focus on higher π_a , what would be the case

if only efficiency was considered. It is then close to a mono objective optimization. It should be noticed that stochastic programming has been successfully tested on a three objectives case. It consists in a gas turbine with carbon dioxide sequestration. The objectives were the investment cost, the exergetic efficiency and the CO_2 capture rate. It has not been integrated in this study since investment cost relies on heat exchanger area estimation by energy integration. As it has been described, this is not compatible with moments method. So the fuel cell example has been chosen to compare results of both approach.

In the method presented in this study, each objectives variation is computed separately. However, uncertain variables influent on both of the objectives is intuitively more critical than a variables related to only one of them. An option would be to consider that performances can vary in an ellipse around their nominal value, and to use the area of this ellipse (given by the product of variances) as additional objectives.

It should be noticed that all methods presented in this study are valid for unimodal distribution. Kernel density function [69] allows to deal with multi-modal distribution. However, distribution in energy system are usually unimodal, and if not, can be treated in a scenario approach.

In this thesis, the mathematical base for energy systems design under uncertainty has been presented and discussed. Two methods have been compared. One or the other can be chosen depending on the type of solver, so that it is not a limiting factor any more. It has been demonstrated that purchasing the optimal performances leads to solutions only valid for the most probable case, and that no margin are left for the operating variables to balance the uncertainties influence.

Bibliography

- [1] J. Acevedo and E. N. Pistikopoulos. Stochastic optimization based algorithms for process synthesis under uncertainty. *Computers & Chemical Engineering*, 22(4-5):647–671, 1998.
- [2] J. S. Albuquerque and L. T. Biegler. Data reconciliation and gross-error detection for dynamic systems. *AIChE Journal*, 42(10):2841–2856, 1996. Cited By (since 1996): 93.
- [3] Susanna W. M. Au-Yeung. Finding probability distributions from moments. Technical report, Imperial College of Science, Technology and Medicine, 2003.
- [4] N. Autissier. *Small scale SOFC systems : design, optimization and experimental results*. PhD thesis, 2008.
- [5] Nordhal Autissier, Francesca Palazzi, Francois Marechal, Jan Van herle, and Daniel Favrat. Thermo-economic optimization of a solid oxide fuel cell, gas turbine hybrid system. *Fuel Cell Science and Technology*, 7:123–129, 2007.
- [6] V. Barthelmann, E. Novak, and K. Ritter. High dimensional polynomial interpolation on sparse grids. *Advances in Computational Mathematics*, 12(4):273–288, 2000. Cited By (since 1996): 93.
- [7] H. Becker and F. Maréchal. Energy integration of industrial sites with heat exchange restrictions. *Computers and Chemical Engineering*, 37:104–118, 2012. Cited By (since 1996): 4.
- [8] R.E. Bellman and L.A ZADEH. Decision-making in a fuzzy environment. *Management Science*, 17(4):b–141–64, 1970. Cited By (since 1996): 973.
- [9] Etienne Bernier, Francois. Maréchal, and Rejean Samson. Multi-objective design optimization of a natural gas-combined cycle with carbon dioxide capture in a life cycle perspective. *Energy*, 35(2):1121–1128, 2010. Cited By (since 1996): 1.

- [10] L. T. Biegler and I. E. Grossmann. Retrospective on optimization. *Computers & Chemical Engineering*, 28(8):1169–1192, 2004.
- [11] M. Bierlaire. *Introduction à l'optimisation différentiable*. Presse Polytechnique et Universitaire Romande, Lausanne, Switzerland, 2006.
- [12] John R. Birge and Francois Louveaux. *Introduction to Stochastic Programming*. Operations Research. Springer, 1997.
- [13] Raffaele Bolliger. *Méthodologie de la synthèse des systèmes énergétiques industriels*. PhD thesis, Lausanne, 2010.
- [14] George E.P Box, J. Stuart Hunter, and William G. Hunter. *Statistics for experimenters : design, innovation, and discovery, 2nd ed.* Wiley-Interscience, Hoboken, N.J., 2005.
- [15] B. Delaunay. Sur la sphère vide. *Izvestia Akademii Nauk SSSR, Otdelenie Matematicheskikh i Estestvennykh Nauk*, 7:793–800, 1934.
- [16] O. Ditlevsen and H.O. Madsen. *Structural Reliability Methods*. John Wiley, Chichester, 2007.
- [17] U. M. Diwekar and E. S. Rubin. Stochastic modeling of chemical processes. *Computers & Chemical Engineering*, 15(2):105–114, 1991.
- [18] M. Dubuis and F. Maréchal. *Proposition of methodology for optimization of energy system design under uncertainty*, volume 30 of *Computer Aided Chemical Engineering*. 2012.
- [19] Matthias Dubuis and Francois Maréchal. Optimal energy system design under uncertain parameters. In *PRES'09, 12th Conference on Process Integration, Modeling and Optimisation for Energy Saving and Pollution Reduction*, Rome, 2009.
- [20] Matthias Dubuis and Francois Maréchal. Methods for complex energy system design under uncertainty. In *23rd International Conference on Efficiency, Cost, Optimization, Simulation and Environmental Impact of Energy Systems*, Lausanne, Switzerland, 2010.
- [21] B. Efron. Bootstrap confidence intervals for a class of parametric problems. *Biometrika*, 72(1):45–58, 1985. Cited By (since 1996): 97.
- [22] M. Escobar, J. O. Trierweiler, and I. E. Grossmann. *SynFlex. A Computational Framework for Synthesis of Flexible Heat Exchanger Networks*, volume 29 of *Computer Aided Chemical Engineering*. 2011.

- [23] Emanuele Facchinetti. *Integrated Solid Oxide Fuel Cell : Gas Turbine Hybrid Systems with or without CO₂ Separation*. PhD thesis, Lausanne, 2012.
- [24] George S. Fishman. *Monte Carlo : concepts, algorithms, and applications*. Springer, New York, 1999.
- [25] C. A. Floudas, A. R. Ciric, and I. E. Grossmann. Automatic synthesis of optimum heat exchanger network configurations. *AIChE Journal*, 32(2):276–290, 1986. Cited By (since 1996): 123.
- [26] C. A. Floudas, Z. H. Gumus, and M. G. Ierapetritou. Global optimization in design under uncertainty: Feasibility test and flexibility index problems. *Industrial and Engineering Chemistry Research*, 40(20):4267–4282, 2001. Cited By (since 1996): 16.
- [27] C.A. Floudas and I.E. Grossmann. Synthesis of flexible heat-exchanger networks for multiperiod operation. *Computers And Chemical Engineering*, 10(2):153 – 168, 1986.
- [28] M. François and B. Irsia. Synep1 : A methodology for energy integration and optimal heat exchanger network synthesis. *Computers and Chemical Engineering*, 13(4-5):603–610, 1989. Cited By (since 1996): 7.
- [29] Y. Fu and U. M. Diwekar. An efficient sampling approach to multiobjective optimization. *Annals of Operations Research*, 132(1-4):109–134, 2004.
- [30] Martin Gassner and Francois Marechal. Methodology for the optimal thermo-economic, multi-objective design of thermochemical fuel production from biomass. *Computers and chemical engineering*, 33(3):769–781, 2009.
- [31] Luc Girardin. *A GIS-based Methodology for the Evaluation of Integrated Energy Systems in Urban Area*. PhD thesis, Lausanne, 2012.
- [32] Luc Girardin, Raffaele Bolliger, and François Maréchal. On the use of process integration techniques to generate optimal steam cycle configurations for the power plant industry. In *12th International Conference on Process Integration, Modelling and Optimisation for Energy Saving and Pollution Reduction*, Rome, Italy.
- [33] I. E. Grossmann and L. T. Biegler. Part ii. future perspective on optimization. *Computers & Chemical Engineering*, 28(8):1193–1218, 2004.
- [34] I. E. Grossmann, K. P. Halemane, and R.E. Swaney. Optimization strategies for flexible chemical process. *Computers and Chemical Engineering*, 7(4):439–462, 1983.

- [35] I. E. Grossmann, H. Yeomans, and Z. Kravanja. A rigorous disjunctive optimization model for simultaneous flowsheet optimization and heat integration. *Computers & Chemical Engineering*, 22:S157–S164, 1998.
- [36] I.E. Grossmann and R.W.H. Sargent. Optimum design of multipurpose chemical-plants. *Industrial and Engineering Chemistry Process Design and Development*, 18(2):343 – 348, 1979.
- [37] T. Gundersen and I.E. Grossmann. Improved optimization strategies for automated heat-exchanger network synthesis through physical insights. *Computers and Chemical Engineering*, 14(9):925 – 944, 1990.
- [38] V. Gupta and I. E. Grossmann. Solution strategies for multistage stochastic programming with endogenous uncertainties. *Computers and Chemical Engineering*, 35(11):2235–2247, 2011.
- [39] K. P. Halemane and I. Grossmann. A remark on the paper 'theoretical and computational aspects of the optimal design centering, tolerancing, and tuning problem'. *Circuits and Systems, IEEE Transactions on*, 28(2):163 – 164, feb 1981.
- [40] K. P. Halemane and I. E. Grossmann. Optimal process design under uncertainty. *Aiche Journal*, 29(3):425–433, 1983. Times Cited: 114 Article English Cited References Count: 11 Qt999.
- [41] C. N. Hamelinck, A. P. C. Faaij, H. den Uil, and H. Boerrigter. Production of ft transportation fuels from biomass; technical options, process analysis and optimisation, and development potential. *Energy*, 29(11):1743–1771, 2004. Cited By (since 1996): 117.
- [42] Joel Heinrich. A guide to the pearson type iv distribution. Technical report, University of Pennsylvania, 2004.
- [43] J. C. Helton and F. J. Davis. Latin hypercube sampling and the propagation of uncertainty in analyses of complex systems. *Reliability Engineering and System Safety*, 81(1):23–69, 2003. Cited By (since 1996): 300.
- [44] G. Heyen. Diagnostic des systèmes énergétiques, 2006.
- [45] C. Hirsch, G. Roge, A. Karl, V. Couailler, A. Dervieux, B. Eisfeld, A. Duftoy, A. Pasanisi, and A. Hutton. Uncertainty management and quantification in industrial analysis and design, 2011.

- [46] Y. J. Hong, J. Xing, and J. B. Wang. A second-order third-moment method for calculating the reliability of fatigue. *International Journal of Pressure Vessels and Piping*, 76(8):567–570, 1999. Cited By (since 1996): 3.
- [47] N. L. Johnson. Systems of frequency curves generated by methods of translation. *Biometrika*, 36(Pt. 1-2):149–176, 1949. Cited By (since 1996): 347.
- [48] N.L. Johnson, S. Kotz, and Balakrishnan N. *Continuous Univariate Distribution volume 1*. Wiley, New York, 1994.
- [49] Ian C. Kemp. *Pinch Analysis and Process Integration*. Butterworth-Heinemann, Oxford, UK, 2007.
- [50] Kim Kihyung and Michael von Spakovsky. *Dynamic Proton Exchange Membrane Fuel Cell System Synthesis/Design and Operation/Control Optimization under Uncertainty*. PhD thesis, Blacksburg, Virginia, 2008.
- [51] Almut Kirchner, Andreas Kemmler, Mario Keller, Martin Jakob, and Giacomo Catenazzi. Analyse des schweizerischen energieverbrauchs 2000 - 2010 nach verwendungszwecken. 2011.
- [52] M. J. Leibman, T. F. Edgar, and L. S. Lasdon. Efficient data reconciliation and estimation for dynamic processes using nonlinear programming techniques. *Computers and Chemical Engineering*, 16(10-11):963–986, 1992. Cited By (since 1996): 111.
- [53] Geoffrey B. Leyland. *Multi-Objective Optimisation Applied to Industrial Energy Problems*. PhD thesis, 2002.
- [54] B. Linnhoff and E. Hindmarsh. The pinch design method for heat exchanger networks. *Chemical Engineering Science*, 38(5):745–763, 1983. Cited By (since 1996): 303.
- [55] B. Linnhoff, D.W. Townsend, and et al. A user guide on process integration for the efficient use of energy. *The Institution of Chemical Engineers*, 1982.
- [56] Francois Marechal, Francesca Palazzi, Julien Godat, and Daniel Favrat. Thermo-economic modelling and optimisation of fuel cell systems. *Fuel Cells*, 5(1):5–24, 2005.
- [57] S. Mekid and D. Vaja. Propagation of uncertainty: Expressions of second and third order uncertainty with third and fourth moments. *Measurement: Journal of the International Measurement Confederation*, 41(6):600–609, 2008. Cited By (since 1996): 3.

- [58] Adam Molyneaux. *A Practical Evolutionary Method for the Multi-Objective Optimisation of Complex Energy Systems, including Vehicle Drivetrains*. PhD thesis, 2002.
- [59] J. Moon, S. Kim, and A. A. Linninger. Integrated design and control under uncertainty: Embedded control optimization for plantwide processes. *Computers and Chemical Engineering*, 35(9):1718–1724, 2011. Cited By (since 1996): 1.
- [60] Nebojsa Nakicenovic and Rob Swart. Summary for policymakers, emissions scenarios. Technical report, 2000.
- [61] K. P. Papalexandri and E. N. Pistikopoulos. A multiperiod minlp model for the synthesis of flexible heat and mass exchange networks. *Computers and Chemical Engineering*, 18(11-12):1125–1139, 1994. Cited By (since 1996): 56.
- [62] Soterios A. Papoulias and I. E. Grossmann. Structural optimization approach in process synthesis - i. *Computers And Chemical Engineering*, 7(6):695–706, 1983.
- [63] Soterios A. Papoulias and I. E. Grossmann. Structural optimization approach in process synthesis - ii. *Computers And Chemical Engineering*, 7(6):707–721, 1983.
- [64] Soterios A. Papoulias and I. E. Grossmann. Structural optimization approach in process synthesis - iii. *Computers And Chemical Engineering*, 7(6):723–734, 1983.
- [65] Karl Pearson. Contributions to the mathematical theory of evolution.-ii. skew variation in homogeneous material. *Philosophical Transactions of the Royal Society of London A*, 186:343, 1895.
- [66] Zoé Périn-Levasseur. *Energy efficiency and conversion in complex integrated industrial sites: Application to a sulfite pulping facility*. PhD thesis, Lausanne, 2009.
- [67] E. N. Pistikopoulos and M. G. Ierapetritou. Novel-approach for optimal process design under uncertainty. *Computers & Chemical Engineering*, 19(10):1089–1110, 1995.
- [68] M. Rosenblatt. Remarks on a multivariate transformation. *The Annals of Mathematical Statistics*, 23(3):470–472, 1952.

- [69] K. H. Sahin and U. M. Diwekar. Better optimization of nonlinear uncertain systems (bonus): A new algorithm for stochastic programming using reweighting through kernel density estimation. *Annals of Operations Research*, 132(1-4):47–68, 2004. Cited By (since 1996): 14.
- [70] N. V. Sahinidis. Optimization under uncertainty: State-of-the-art and opportunities. *Computers and Chemical Engineering*, 28(6-7):971–983, 2004. Cited By (since 1996): 170.
- [71] Anna Sciazko and Matthias Dubuis. Surrogate modeling techniques applied to energy system. Technical report, 2011.
- [72] Y. Shastri and U. M. Diwekar. An efficient algorithm for large scale stochastic nonlinear programming problems. *Computers & Chemical Engineering*, 30(5):864–877, 2006.
- [73] S.A. Smolyak. Quadrature and interpolation formulas for tensor products of certain classes of functions. *Doklady Akademii nauk SSSR*, 4:240–243, 1963.
- [74] Bassel Solaiman. *Processus stochastiques pour l'ingénieur*. PPUR, Lausanne, Switzerland, 2006.
- [75] S. Stavroyiannis, I. Makris, V. Nikolaidis, and L. Zangaris. Econometric modeling and value-at-risk using the pearson type-iv distribution. *International Review of Financial Analysis*, 22(5):10–17, 2012. Article in Press.
- [76] Karthik Subramanian, U. M. Diwekar, and Amit Goyalb. Multi-objective optimization for hybrid fuel cells power system under uncertainty. *Journal of Power Sources*, 132:99–112, 2004.
- [77] Bruno Sudret. Uncertainty propagation and sensitivity analysis in mechanical models contributions to structural reliability and stochastic spectral method. Technical Report Rapport d'activité scientifique présenté en vue de l'obtention de l'Habilitation à Diriger des Recherche, 2007.
- [78] Bruno Sudret, Marc Berveiller, and Maurice Lemaire. A stochastic finite element procedure for moment and reliability analysis. *European Journal of Computational Mechanics*, 15(7-8):825–866, 2006.
- [79] L. Tantimuratha, G. Asteris, D. K. Antonopoulos, and A. C. Kokossis. *A conceptual programming approach for the design of flexible HENs*, volume 8 of *Computer Aided Chemical Engineering*. 2000.

- [80] Laurence Tock and Francois Maréchal. Process design optimization strategy to develop energy and cost correlations of co2 capture processes. In *22 European Symposium on Computer Aided Process Engineering*, London, UK, 2012.
- [81] Y. Tsujikawa, K. Kaneko, and J. Suzuki. Proposal of the atmospheric pressure turbine (apt) and high temperature fuel cell hybrid system. *JSME International Journal, Series B: Fluids and Thermal Engineering*, 47(2):256–260, 2004. Cited By (since 1996): 6.
- [82] J. Van Herle, F. Maréchal, S. Leuenberger, and D. Favrat. Energy balance model of a sofc cogenerator operated with biogas. *Journal of Power Sources*, 118(1-2):375–383, 2003. Cited By (since 1996): 46.
- [83] T. Watanabe, T. Yamamoto, K. Yasumoto, H. Morita, Y. Mugikura, A. Yamashita, K. Tomida, H. Yokokawa, N. Sakai, T. Horita, and K. Yamaji. Development of performance analysis method on sofc - long time operation of tubular sofc and comparison to post test analysys. In *Proceedings of the 6th International Conference on Fuel Cell Science, Engineering, and Technology*, pages 925–928, 2008.
- [84] D. Xiu. Efficient collocational approach for parametric uncertainty analysis. *Communications in Computational Physics*, 2(2):293–309, 2007. Cited By (since 1996): 81.
- [85] Dongbin Xiu and George Em Karniadakis. The wiener-askey polynomial chaos for stochastic differential equations. *Journal of Scientific Computing*, 24(2):619–644, 2002.
- [86] Cong Xu, Peter M. Follmann, L. T. Biegler, and M. S. Jhon. Numerical simulation and optimization of a direct methanol fuel cell. 2005.
- [87] W. Xu and U. M. Diwekar. Improved genetic algorithms for deterministic optimization and optimization under uncertainty. part ii. solvent selection under uncertainty. *Industrial & Engineering Chemistry Research*, 44(18):7138–7146, 2005.
- [88] Yi-min ZHANG, Li-sha ZHU, and Xin-gang WANG. Advanced method to estimate reliability-based sensitivity of mechanical components with strongly nonlinear performance function. *Applied Mathematics and Mechanics (English Edition)*, 31(10):1325–1336, 2010.

Appendix A

Probability distribution function

A.1 Pearson IV

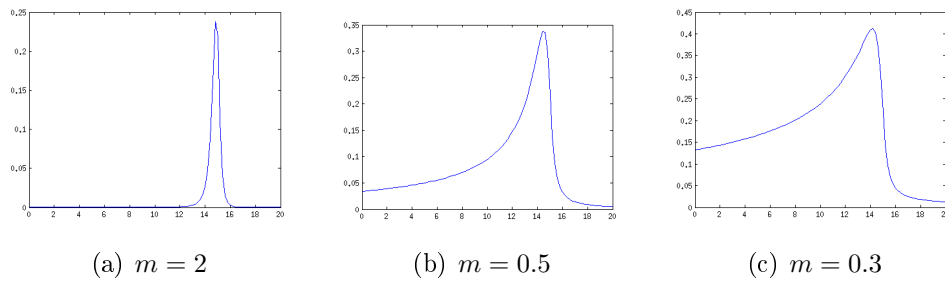
Pearson type IV is the hardest type to model. Its probability density function is given by [42]:

$$p(x) = k \left(1 + \left(\frac{x - \lambda}{a} \right)^2 \right)^{-m} \cdot \exp \left(-\nu \cdot \arctan \left(\frac{x - \lambda}{a} \right) \right) \quad (\text{A.1})$$

Where parameters m , ν , λ and a are given by [48]:

$$\begin{aligned} m &= \frac{1}{2c_2} \\ \nu &= \frac{2c_1(1 - m)}{\sqrt{4c_0c_2 - c_1^2}} \\ b &= 2(m - 1) \\ a &= \sqrt{\frac{b^2(b - 1)}{(b^2 + \nu^2)}} \\ \lambda &= \frac{a\nu}{b} \end{aligned} \quad (\text{A.2})$$

It should be noticed that this is valid for $m > 1/2$. If it is not the case, one or both of tails of the density function may have an asymptotic behaviour as shown in figure A.1.

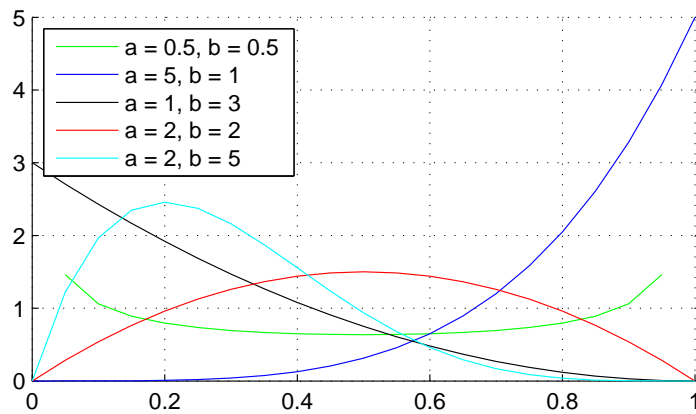
Figure A.1: Different m parameter for Pearson IV distribution

The normalisation constant k can be computed based on gamma distribution (real and complex) [75]:

$$k(m, \nu, \lambda, a) = \frac{2^{m-2} \left| \Gamma \left(m + \frac{i\nu}{2} \right) \right|^2}{\pi a |\Gamma(2m - 1)|^2} \quad (\text{A.3})$$

A.2 Beta distribution

Beta distribution is very useful since it is based on a finite range and may represent symmetric distribution as well as asymmetric (figure A.2).

Figure A.2: Beta *pdf* for several values for a and b

Its probability density function is given by:

$$\begin{aligned}
 p(x, a, b) &= \frac{x^{a-1}(1-x)^{b-1}}{\int_0^1 t^{a-1}(1-t)^{b-1} dt} \\
 &= \frac{\Gamma(a+b)}{\Gamma(a)\Gamma(b)} x^{a-1}(1-x)^{b-1}
 \end{aligned}
 \tag{A.4}$$

Where $0 \leq x \leq 1$, $a > 0$, $b > 0$ and $\Gamma(c)$ is the gamma function given by (for $c > 0$):

$$\Gamma(c) = \int_0^\infty e^{-t} t^{c-1} dt
 \tag{A.5}$$

Its mean, mode and variance are given in table A.1.

Parameters	Analytical expression
Mean	$\mu = \frac{a}{a+b}$
Mode	$mode = \frac{a-1}{a+b-2}$ for $a > 1$ and $b > 1$
Variance	$\sigma^2 = \frac{ab}{(a+b)^2(a+b+1)}$

Table A.1: Parameters as a function of a and b

For a variables out of the range $[0, 1]$, location and and scale can be change by variable substitution, what leads to the four parameters beta distribution function.:

$$\begin{aligned}
 x' &= x(r-q) + q \\
 x &= \frac{x' - q}{r - q} \\
 p(x', a, b, q, r) &= \frac{p(x, a, b)}{r - q}
 \end{aligned}
 \tag{A.6}$$

Its influence on the different parameters is given in table A.2, where index $2p$ refers to the two parameters distribution:

Parameters	Analytical expression
Mean	$\mu = \mu_{2p}(r-q) + q$
Mode	$mode = mode_{2p}(r-q) + q$
Variance	$\sigma^2 = \sigma_{2p}^2(r-q)^2$

Table A.2: Parameters as a function of a and b for a four parameters distribution

A.3 Normal distribution

Normal probability density function is an infinite distribution. It is shown in figure A.3 for different means and standard deviations.

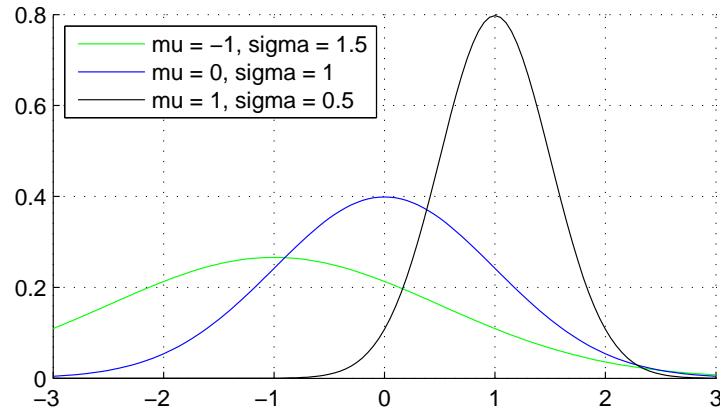


Figure A.3: Normal *pdf* for different mean and variance

Its distribution function is given by:

$$p(x, \mu, \sigma) = \frac{1}{\sqrt{2\pi\sigma^2}} e^{-\frac{(x - \mu)^2}{2\sigma^2}} \quad (\text{A.7})$$

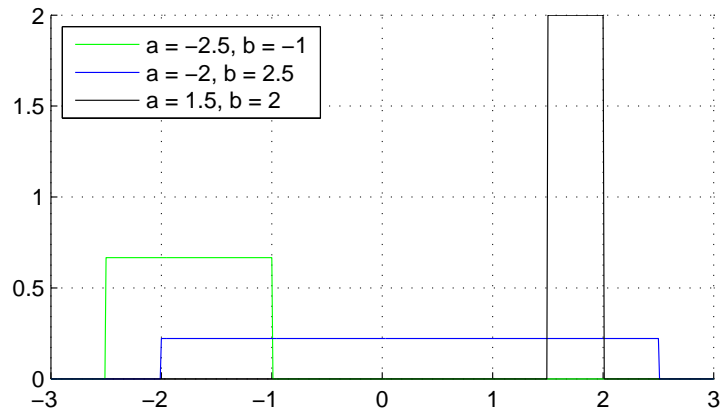
It can be observed that $[-n_{sd}\sigma, n_{sd}\sigma]$ correspond to P_n % of the set with the following value:

n_{sd}	Tolerance interval [%]
1	68
2	95
3	99.7

Table A.3: Standard deviation and tolerance interval

A.4 Uniform distribution

As represented in figure A.4, it is only defined by its range.

Figure A.4: Uniform *pdf* for different ranges

Its probability distribution function is given by:

$$p(x, a, b) = \begin{cases} \frac{1}{b-a} & \text{for } a \leq x \leq b \\ 0 & \text{for } x < a \text{ or } x > b \end{cases} \quad (\text{A.8})$$

Its mean and variance are given in table A.4.

Parameters	Analytical expression
Mean	$\mu = \frac{a+b}{2}$
Variance	$\sigma^2 = \frac{(b-a)^2}{12}$

Table A.4: Mean and variance of the uniform distribution

Appendix B

Stochastic programming: complementary results

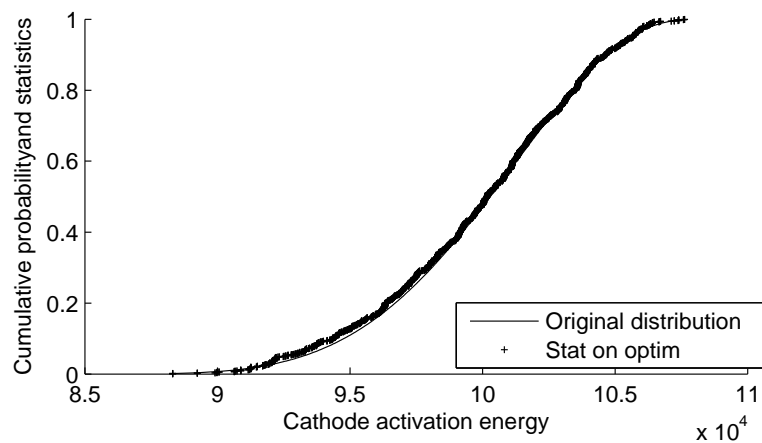


Figure B.1: Cathodic activation energy *cdf* and statistics

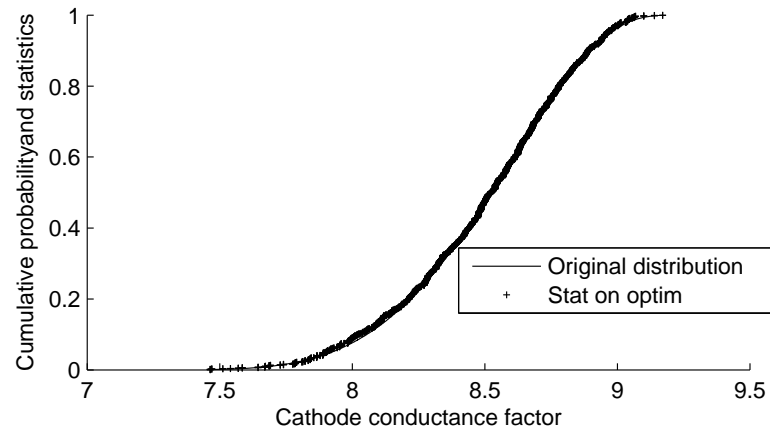


Figure B.2: Cathodic conductance factor *cdf* and statistics

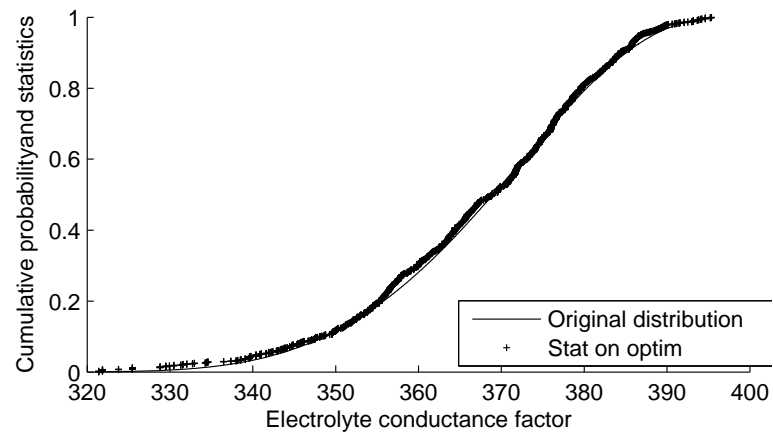
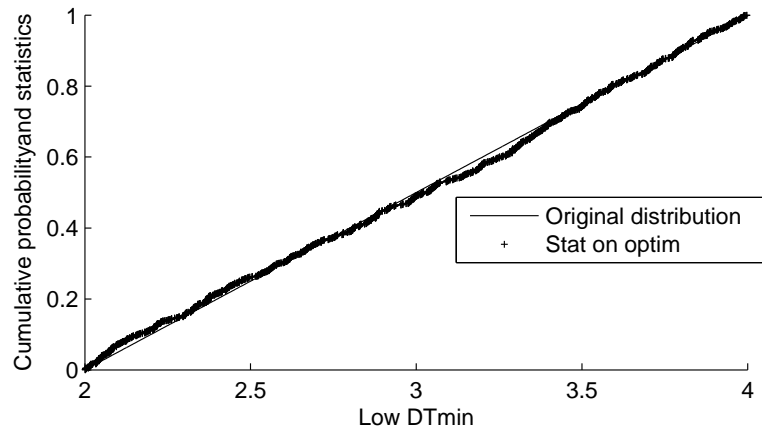
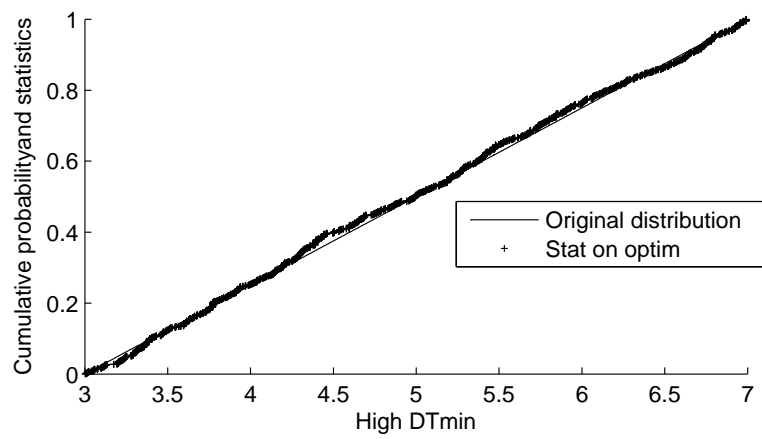


Figure B.3: Electrolyte conductance factor *cdf* and statistics

Figure B.4: Low $DTmin$ cdf and statisticsFigure B.5: High $DTmin$ cdf and statistics

Appendix C

Moments method: complementary results

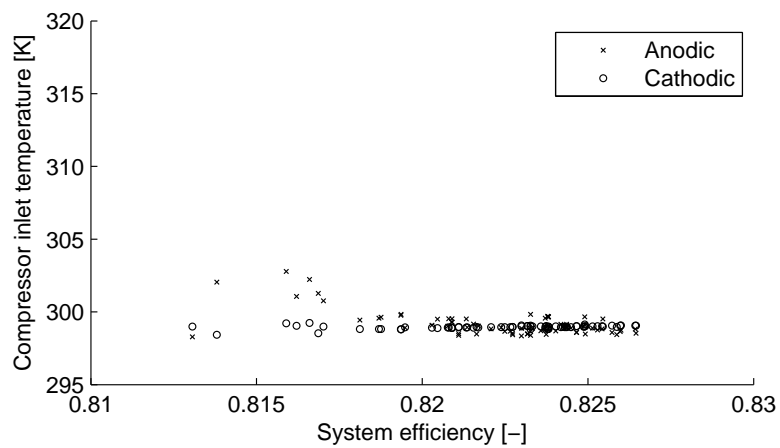


Figure C.1: Anodic and cathodic compressor inlet temperature for moments method

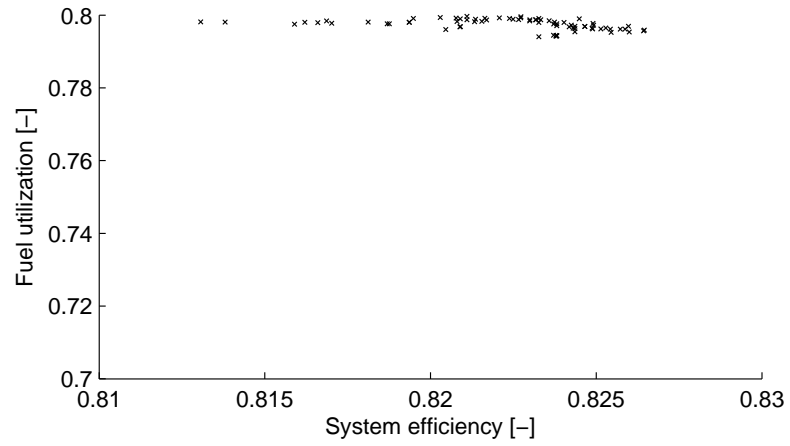


Figure C.2: Fuel utilization for moments method

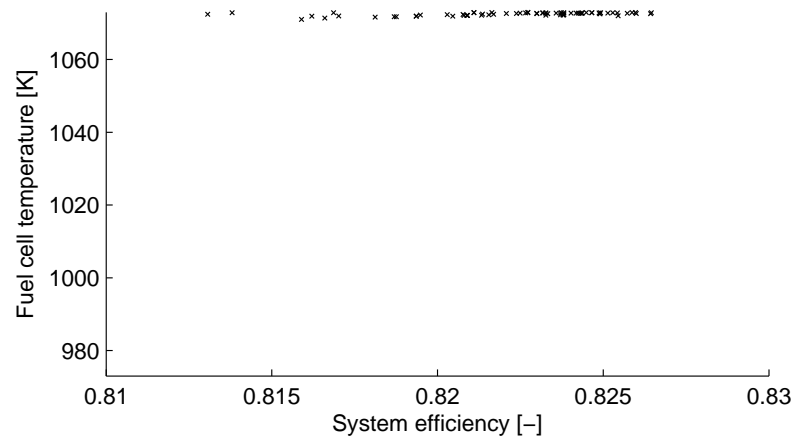


Figure C.3: Fuel cell temperature for moments method

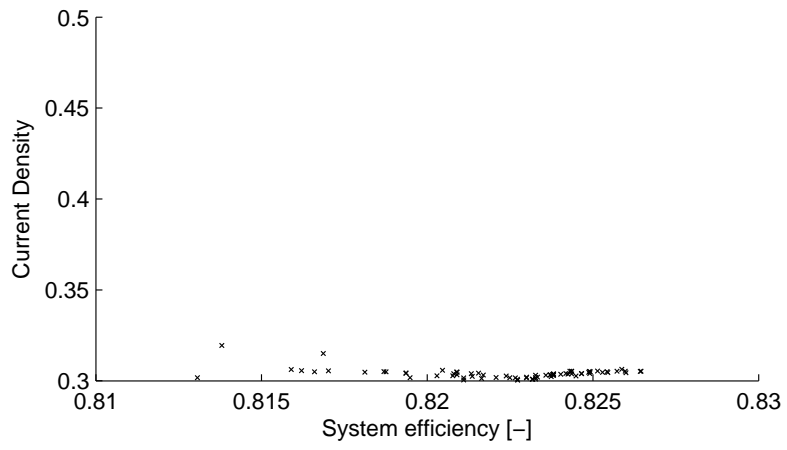


Figure C.4: Current density for moments method

List of Tables

1.1	IPCC scenarios classification in 4 families	2
2.1	Distribution and related orthogonal polynomials	34
2.2	Propagation methods results	36
2.3	Uncertainty propagation methods	47
3.1	$\Delta T_{min}/2$ distribution and parameters	56
3.2	Fuel cell decision variables	60
3.3	Fuel cell test conditions	61
3.4	Statistics comparison	63
3.5	Fuel cell uncertain variables (beta distribution, a and b parameters)	63
3.6	Fuel cell uncertain variable (uniform distribution)	63
3.7	Anodic and cathodic gas turbine	64
3.8	Gas turbines uncertain variables (beta distribution, a and b parameters)	65
4.1	Fuel cell decision variables for point A in figure 4.8	72
5.1	Boundaries of drawn uncertain variables	83
5.2	Comparison of standard and stochastic optimization results	93
5.3	Mean and standard deviation comparison	96
6.1	Comparison of standard and stochastic optimization results	105
6.2	Performances of studied points	107
A.1	Parameters as a function of a and b	127
A.2	Parameters as a function of a and b for a four parameters distribution	127
A.3	Standard deviation and tolerance interval	128
A.4	Mean and variance of the uniform distribution	129

List of Figures

1.1	IPCC scenarios for CO_2 emissions from energy and industry area [60]	3
1.2	End-use energy consumption statistics for Switzerland (2010) [51]	3
1.3	Energy sources for space heating of private households (2010) [51]	4
1.4	Binomial distribution for the district heating example	5
1.5	Scheme of the notion of precise/accurate measurement [44]	7
2.1	Linear problem	13
2.2	Resolution sequence	15
2.3	Onion representation	16
2.4	Variables classification	19
2.5	Influence of decision variables and uncertainties in time	22
2.6	Monotonicity issue	26
2.7	Uncertainty propagation output	29
2.8	Non-injectivity problem representation	30
2.9	Convergence of Monte-Carlo simulation	31
2.10	Pearson system	37
2.11	Propagation by moments method	38
2.12	Normal distribution and potential compensated area	39
2.13	Variance decrease effect	39
2.14	Propagation by moments method including flexibility	40
2.15	Stochastic programming optimization	41
2.16	Stochastic optimization results	42
2.17	Difference between mean and mode	43
2.18	FORM principle	44
2.19	Reliability defined by quantile	45
3.1	Heat exchange definition	51
3.2	Composite curves construction	52
3.3	Composite curve under uncertain temperature	54
3.4	Influence of pinch	54
3.5	Global superstructure	55

3.6	Fuel cell scheme	58
3.7	Statistics on <i>SOFC</i> characterization	62
3.8	Current-Tension statistics for 60 % fuel utilization	62
3.9	$T - s$ diagram of an inverted Brayton cycle	64
4.1	Optimal Pareto front for <i>SOFC</i> model	68
4.2	Steam to carbon ratio	68
4.3	Air factor λ	69
4.4	Optimal cathodic pressure ratio	70
4.5	Cathodic turbine inlet temperature	70
4.6	Gas turbines and compressors specific power	71
4.7	Anodic and cathodic compressors inlet temperature	71
4.8	Sankey diagram	72
4.9	Sankey diagram	73
4.10	Composite curve (corrected temperatures)	73
4.11	Hot utilities specific power for the whole Pareto front	74
5.1	Pareto for standard, stochastic with uncertain variables and stochastic with uncertainties at the mode	78
5.2	Adjustment factor <i>cdf</i> and statistics	79
5.3	Anodic conductance factor <i>cdf</i> and statistics	80
5.4	Anodic activation energy theoretical <i>cdf</i> and statistics on alive population	81
5.5	Maximum and minimum drawn and alive values	81
5.6	Sensitivity analysis on anode activation energy	82
5.7	Electrolyte activation energy	83
5.8	Anodic interconnect losses	84
5.9	Cathodic interconnect losses	84
5.10	Anodic and cathodic gas turbines efficiency	84
5.11	Anodic and cathodic gas compressors efficiency	85
5.12	Uncertainties on streams involved in high temperature pinch	86
5.13	Cathodic turbine inlet temperature statistic	87
5.14	Anodic turbine outlet temperature variation	87
5.15	Anodic compressor outlet temperature variation: Stochastic/standard optimization results	88
5.16	Anodic compressor inlet temperature statistic	89
5.17	Fuel cell temperature statistic	89
5.18	Cathodic compressor inlet temperature statistic	90
5.19	Cathodic pressure ratio statistic	90
5.20	Fuel utilization statistic	91
5.21	Current density statistic	91

5.22	Steam to carbon ratio statistic	92
5.23	Steam reforming temperature statistic	92
5.24	Fuel cell temperature statistic	93
5.25	Standard Pareto curve and sensitivity analysis on stochastic results	94
5.26	Influence of fuel cell temperature and ΔT_{min} on stochastic solution .	95
5.27	Standard Pareto curve and sensitivity analysis on stochastic results	95
6.1	Algorithm of moments method applied to optimization	100
6.2	Pareto front for the optimization based on moments method	101
6.3	Pareto front for moments method optimization	101
6.4	Steam reforming temperature for moments method	102
6.5	Composite curve for mid pressure of figure 6.11	103
6.6	Cathodic pressure ratio for moments method	103
6.7	Cathodic turbine inlet temperature for moments method	104
6.8	Steam to carbon ratio for moments method	104
6.9	Air factor for moments method	105
6.10	Efficiency and its variance	106
6.11	Points analyzed	107
6.12	Variance of the efficiency for the selected points	108
6.13	Variance of the fuel cell power produced for the selected points . . .	109
6.14	Anodic Brayton cycle power production variance	110
6.15	Cathodic Brayton cycle power production variance	110
6.16	Hot utility consumption variance	111
6.17	Comparison of variance for each contribution to total efficiency . . .	111
A.1	Different m parameter for Pearson IV distribution	126
A.2	Beta <i>pdf</i> for several values for a and b	126
A.3	Normal <i>pdf</i> for different mean and variance	128
A.4	Uniform <i>pdf</i> for different ranges	129
B.1	Cathodic activation energy <i>cdf</i> and statistics	131
B.2	Cathodic conductance factor <i>cdf</i> and statistics	132
B.3	Electrolyte conductance factor <i>cdf</i> and statistics	132
B.4	Low DT_{min} <i>cdf</i> and statistics	133
B.5	High DT_{min} <i>cdf</i> and statistics	133
C.1	Anodic and cathodic compressor inlet temperature for moments method	135
C.2	Fuel utilization for moments method	136
C.3	Fuel cell temperature for moments method	136
C.4	Current density for moments method	137

Curriculum Vitae

Matthias Dubuis

Tel. : +41 (0)21 693 35 50

E-mail : matthias.dubuis@epfl.ch

Citizenship : Swiss

Date of birth : 05.01.1983

Scientific experience

2008-2012 : PhD Student (subject : *Energy system design under uncertainty*), Laboratory for Industrial Energy Systems, Ecole Polytechnique Fédérale de Lausanne (EPFL), Switzerland

2007-2008 : Internship (subject : *A Geographical information based system for the evaluation of integrated energy conversion systems in urban areas*) on urban energy system in Laboratory for Industrial Energy Systems, Ecole Polytechnique Fédérale de Lausanne (EPFL), Switzerland on

2006-2007 : Internship at EDF in Research and Development on *Thermo-economic study on industrial heat pump integration*

Education

2001-2007 : MSc in mechanical engineering, EPFL, Switzerland.

Languages

French, Native

English, Oral and written good skills

German, Oral and written good skills